

Session 8

REPROCESSING OFFGAS CLEANING

TUESDAY: October 21, 1980  
CHAIRMAN: J.G. Wilhelm  
Kernforschungszentrum  
Karlsruhe

TRIBUTYL PHOSPHATE REMOVAL FROM REPROCESSING OFF-GAS  
STREAMS USING A SELECTED SORBENT  
G.B. Parker

IODINE TRAPPING AND CONDITIONING IN THE MERCUREX SYSTEM  
G.E.R. Collard, D. Hennart, J. Van Dooren, W.R.A.  
Goossens

RESULTS OF CLEANING OF THE DISSOLVER OFF-GAS IN THE  
PASSAT PROTOTYPE DISSOLVER OFF-GAS FILTER SYSTEM  
J. Furrer, R. Kaempffer, A. Linek, A. Merz

CONDITIONING OF REPROCESSING DISSOLVER OFF-GAS PRIOR TO  
Kr-RETENTION BY CRYOGENIC DISTILLATION  
H.D. Ringel, H. Barnert-Wiemer, H. Hackfort, M. Heidendael

I-129, Kr-85, C-14 and NO<sub>x</sub> REMOVAL FROM SPENT FUEL  
DISSOLVER OFF-GAS AT ATMOSPHERIC PRESSURE AND AT REDUCED  
OFF-GAS FLOW  
E. Henrich, R. Hufner

IMPROVED IODINE AND TRITIUM CONTROL IN REPROCESSING  
PLANTS  
E. Henrich, H. Schmieder, W. Roesch, F. Weirich

SOME ASPECTS OF AEROSOL PRODUCTION AND REMOVAL DURING  
SPENT FUEL PROCESSING STEPS  
F.J. Herrmann, E. Lang, E. Henrich, J. Furrer

OPENING REMARKS OF SESSION CHAIRMAN:

Reprocessing Offgas Cleaning is the title of this session. I do not want to say too much about its importance because on one hand there is a lot of research work going on, but on the other hand I miss the plants which will use the results of the research work. Moreover, the need for offgas cleaning inside reprocessing plants is well known. The reprocessing plant is the place where all volatile isotopes are released from the fuel, mainly with the offgas of the dissolver. This may be known by everybody here in the audience, and so I would like to get on with the papers.

TRIBUTYL PHOSPHATE REMOVAL FROM REPROCESSING  
OFF-GAS STREAMS USING A SELECTED SORBENT

G. B. Parker  
Pacific Northwest Laboratory  
Richland, Washington\*

Abstract

Laboratory experiments have been conducted to determine the effectiveness of inorganic sorbent materials to remove tributyl phosphate ( $C_4H_9O_3$ )  $PO_4$  (TBP) vapors from fuel reprocessing off-gas streams. These experiments used small laboratory-scale columns packed with selected sorbent materials to remove TBP and iodine at conditions approaching those in actual reprocessing off-gas streams. The sorbent materials for TBP removal were placed upstream of iodine sorbent materials to protect the iodine sorbent from the deleterious effects of TBP. Methyl iodide in an airstream containing 30% TBP in normal paraffin hydrocarbons (NPH) and water vapor was metered to two packed columns of sorbents simultaneously (in parallel). One column contained a segment of 8-in. x 14-in. mesh alumina sorbent for TBP removal, the other did not. The measure of the effectiveness of TBP sorbent materials for TBP removal was determined by comparing the iodine retention of the iodine sorbent materials in the two parallel columns.

Experiments using a 18 wt% Ag substituted mordenite iodine sorbent were conducted. Results indicated that the iodine retention capacity of the sorbent was reduced 60% by the TBP and that the column containing iodine sorbent material protected by the alumina TBP sorbent retained 30 times more iodine than the column without TBP sorbent. TBP concentration was up to 500 mg/m<sup>3</sup>. Similar experiments using a 7 wt% Ag impregnated silica gel indicated that the TBP vapor had little effect on the iodine retention of the silica gel material. The stoichiometric maximum amount of iodine was retained by the silica gel material.

Further experiments were conducted assessing the effects of  $NO_2$  on iodine retention of this 7 wt% Ag sorbent. After the two columns were loaded with iodine in the presence of TBP (in NPH), one column was subjected to 2 vol%  $NO_2$  in air. From visual comparison of the two columns, it appeared that the  $NO_2$  regenerated the silica gel iodine sorbent and that iodine was washed off the silica gel iodine sorbent leaving the sorbent in the original state.

I. Introduction

Tributyl phosphate ( $C_4H_9O$ )<sub>3</sub>  $PO_4$  (TBP) diluted with dodecane (or normal paraffin hydrocarbon, NPH) is the solvent extractant commonly used in the PUREX process to separate uranium and plutonium

\* Pacific Northwest Laboratory is operated by Battelle Memorial Institute for the U.S. Department of Energy under contract DE-AC06-76RLO-1830.

from fission products in spent light water reactor (LWR) fuel during the dissolution process. When recycled acid is used in the dissolution process, small amounts of NPH and TBP vapor are released to the off-gas streams, both from the dissolver and the vessel vent. These gas streams contain other airborne fission products released during the reprocessing steps. These airborne fission products need to be removed. Iodine and organic iodides are major radioactive constituents of these airborne products.

Current proposed treatment methods for iodine removal involve the use of silver-loaded inorganic sorbents. European laboratory and pilot-plant studies have shown that the presence of TBP vapor in these gas streams reduce the capacity of the silver beds to remove iodine resulting in more frequent replacement of the silver beds.<sup>(1)</sup> Studies at the Karlsruhe Reprocessing Pilot Plant (WAK) have shown that airborne TBP in concentrations of approximately 6 mg/l significantly reduced the iodine sorption capacity of AC6120 material. Removal efficiency of AC6120, however, could be restored by introducing NO<sub>2</sub> into the air stream. Dodecane was found to have no deleterious effects.

Very little work has been done in the United States on the problems associated with the TBP contamination of the silver beds. Previous work was reported at the 15th DOE Nuclear Air Cleaning Conference.<sup>(2)</sup> This work reported on the screening experiments to select candidate sorbents for TBP removal. Continued work in this area involved demonstrating the effectiveness of the TBP sorbents in a simulated off-gas stream. The investigation into air-cleaning processes to remove TBP vapors from fuel reprocessing off-gas streams is described more fully in PNL-2080-18.<sup>(3)</sup>

This paper focuses on the experiments using a selected solid sorbent to remove TBP upstream of commercial sorbents used to remove iodine from off-gas streams. It also describes the results of an experiment to assess the effects of NO<sub>2</sub> on iodine retention of silver sorbent, which was first loaded with iodine in the presence of TBP.

## II. Experiments and Results

A bench-scale demonstration unit was constructed to evaluate the effectiveness of the selected sorbent to remove TBP under conditions approaching those in actual reprocessing off-gas streams (see Figure 1). During experimentation, dry-cylinder air was fed to two, jacketed, gas-washing bottles maintained at 50°C. The constant temperature was maintained by water circulated around the reservoirs of the bottles. The bottles each contained a mixture of water plus 30% TBP in NPH. The stainless-steel lines leaving the bottles were heated to 100°C. Methyl iodide vapor in N<sub>2</sub> was fed to the air stream by a Matheson mass-flow controller, and the entire stream was metered to two columns through Matheson rotameters. The two columns were 2.5 cm in diameter and made of stainless steel. One segmented column was packed with a commercially available iodine sorbent, the other column with two sections of the selected TBP sorbent material followed by two or three segments of the same iodine sorbent as in the other column. The column segments were held together by gaskets and snap joint couplings (see Figure 2 for an example of a column

segment). The entire column assemblies were placed in an oven and maintained at 130 to 135°C for all experiments.

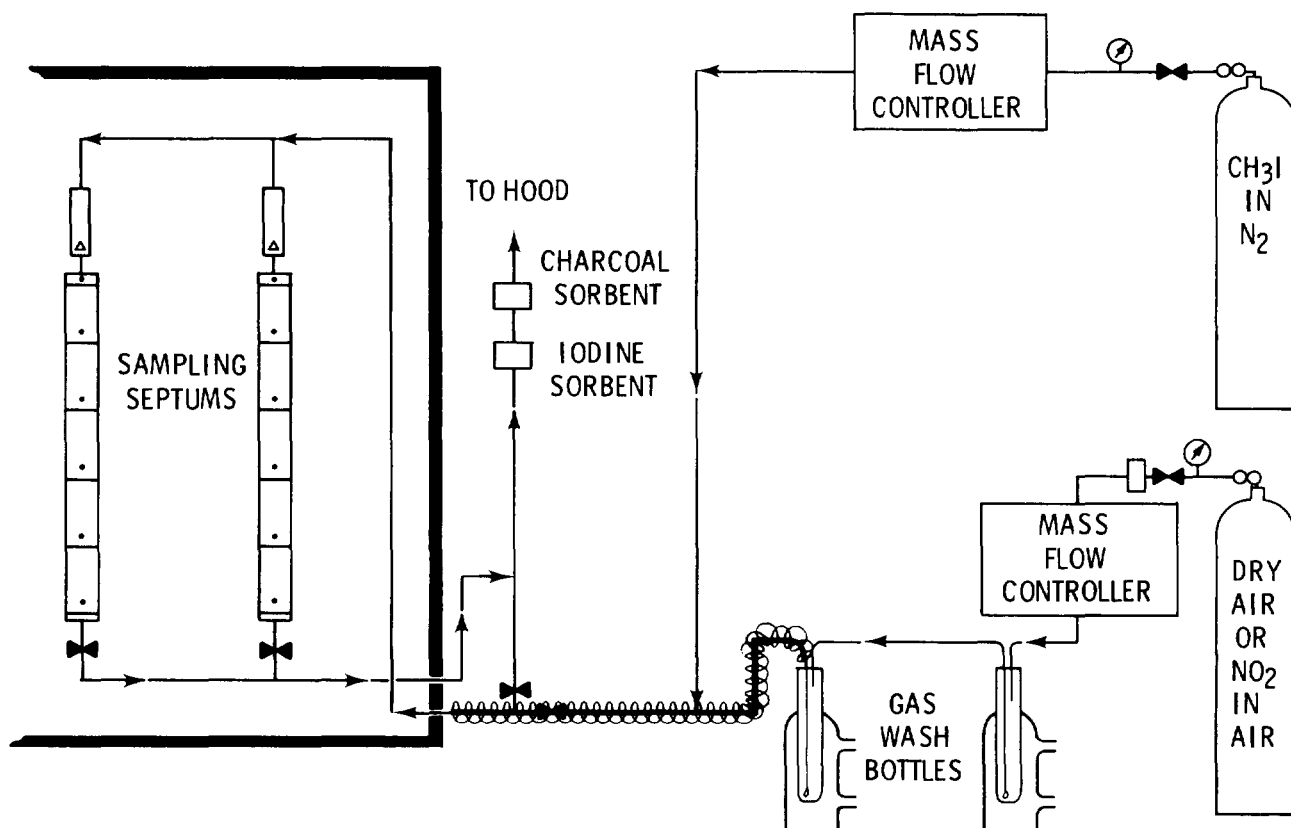


Figure 1. Diagram of apparatus for loading iodine onto selected sorbents.

During an experiment, the breakthrough of methyl iodide, measured by electron capture gas chromatography, was followed in each column segment throughout both columns. Methyl iodide analysis was performed by periodically sampling the feed streams to the columns and downstream of each packed bed segment with a gas-tight syringe through septum sealed sampling ports. The effectiveness of the TBP sorbent materials for TBP removal was determined by measuring the iodine retention of iodine sorbent material. Provisions were made to feed other vapors or gases into the main feed stream.

#### Evaluation of TBP Sorbent A

An experiment was conducted using the bench-scale demonstration unit to evaluate TBP sorbent A as a sorbent to remove TBP and protect the iodine sorbent beds. Sorbent A is an 8 x 14 mesh granular activated alumina that showed the highest TBP retention of any material examined.<sup>(3)</sup>

In this experiment, Column I contained two 5-cm segments of material A followed by three 5-cm segments of a commercially available 18 wt% Ag substituted mordenite iodine sorbent. Column II contained four 5-cm segments of the 18% Ag mordenite sorbent. The columns were conditioned with air at 2% relative humidity for 20 hr followed by 1 hr of conditioning with air plus TBP/NPH vapor

prior to metering methyl iodide into the air stream. During the experiment, average airflow was 2 l/min, and average methyl iodide concentration was 160 mg/m<sup>3</sup>. TBP vapor concentration was about 500 mg/m<sup>3</sup>.

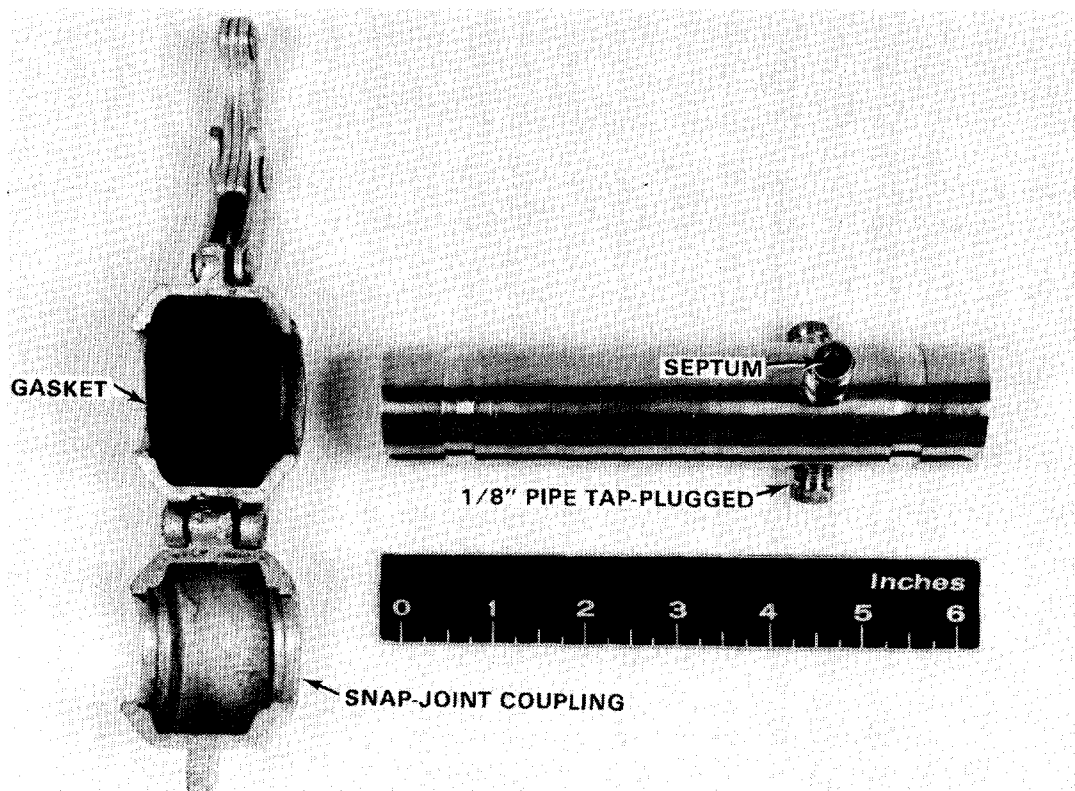


Figure 2. Typical stainless-steel column segment for retaining sorbent materials.

During the experiment, the breakthrough progression of methyl iodide was followed through each segment of the iodine sorbent. This breakthrough is represented as a graph of  $C/C_0$  versus grams methyl iodide metered, where  $C$  = concentration of methyl iodide leaving a 5-cm column segment of sorbent and  $C_0$  = concentration of methyl iodide in the feed stream to the column.

Total methyl iodide metered to Column I was 6.75 g and to Column II 6.11 g. Figure 3 is the breakthrough for sections A, B, C, and D of Column I. Figure 4 is the breakthrough curve for sections A and C of Column II, and Figure 5 is the breakthrough curve for sections B and D of Column II.

To determine the effectiveness of material A to protect the silver mordenite, a comparison of breakthrough curves was made between section C in Column I and section A in Column II and between section D in Column I and section B in Column II. Table I summarizes the breakthrough data.

The iodine retention at a 1% breakthrough in 10 cm of Column I (sections C and D) was 30 times greater than the iodine retention in 10 cm of Column II (sections A and B). Material A protected the sorbent increasing the iodine retention. The iodine retention of the material was also significantly less than theoretical. The breakthrough for the unprotected Column I, extrapolated to  $C/C_0 = 100\%$ , was  $\sim 0.7$  g, which is 60% of the theoretical maximum.

It should also be noted that a small amount of iodine was retained by the TBP sorbent in sections A and B of Column I. This was unexpected and is assumed to be adsorption of the iodine onto the TBP sorbent material. This same phenomenon was noted in other experiments.

A second experiment was completed to evaluate material A as a sorbent to remove TBP and protect iodine sorbent beds. Two 2.5-cm dia stainless-steel columns were prepared. Column I contained five 5-cm segments of a 7% Ag impregnated silica gel iodine sorbent, and Column II contained two 5-cm segments of material A followed by three 5-cm segments of the 7% Ag impregnated silica gel iodine sorbent. The columns were preconditioned with air at 2% relative humidity for 20 hr, and air and TBP/NPH vapor for 1.5 hr prior to metering methyl iodide. Conditions for this experiment were air flowing at 1.9 l/min to each column and average methyl iodide concentration of 160 mg/m<sup>3</sup>. TBP concentration was about 10 mg/m<sup>3</sup>.

At the end of the experiment 8.5 g of methyl iodide had been metered to each column. The breakthrough curves for Column I are given in Figure 6 and Column II are given in Figure 7.

To determine the effectiveness of the TBP sorbent (material A) to protect the iodine sorbent, a comparison of breakthrough curves was made between section A in Column I and section C in Column II, between section B in Column I and section D in Column II and between section C in Column I and section E in Column II. Table II summarizes the breakthrough data.

The iodine retention of the iodine sorbent in sections A and B of Column I and sections C and D of Column II was nearly the same. This indicated that material A contained in sections A and B of Column II had little effect on the iodine retention of the iodine sorbent located downstream. More importantly, however, the data also indicated that iodine retention was near the stoichiometric maximum (within the uncertainty) and therefore the presence of the generated airborne TBP concentration of 10 mg/m<sup>3</sup> did not have a deleterious effect on the iodine sorbent.

#### Effect of NO<sub>2</sub> on Iodine Sorbent

The final experiment was altered slightly from the previous studies using the bench-scale demonstration unit. In this experiment, the effects of NO<sub>2</sub> on iodine retention were assessed. No protective sorbent for TBP removal was used in this experiment. The protective sorbent was to be included in future studies using NO<sub>2</sub> in the feed stream; however, the project was terminated before additional experiments were started.

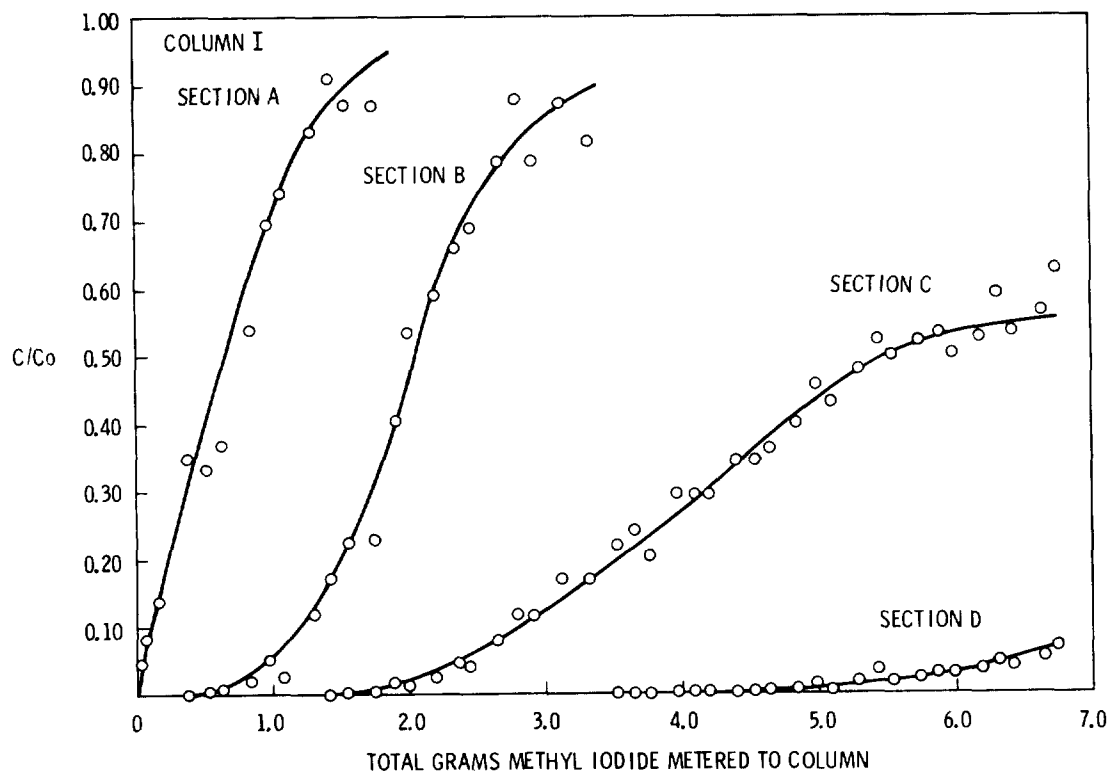


Figure 3. Breakthrough history for methyl iodide loading onto Column I.

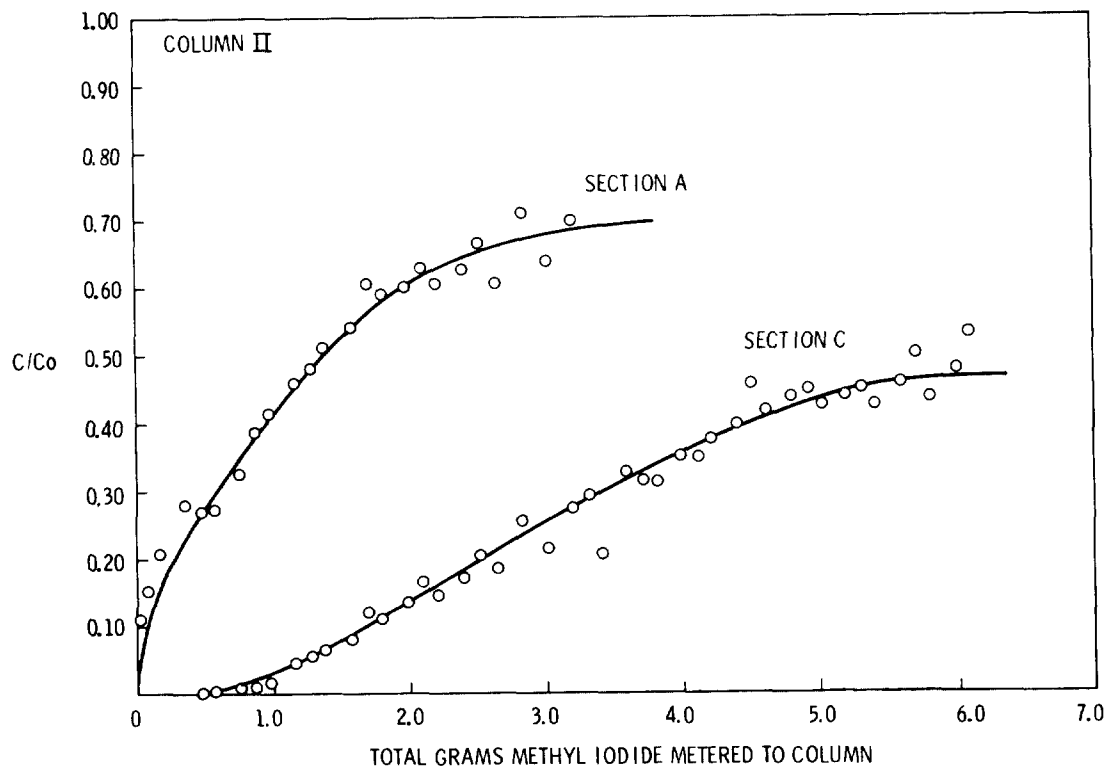


Figure 4. Breakthrough history for methyl iodide loading onto 18 wt% Ag substituted mordenite, Column II, sections A and C.

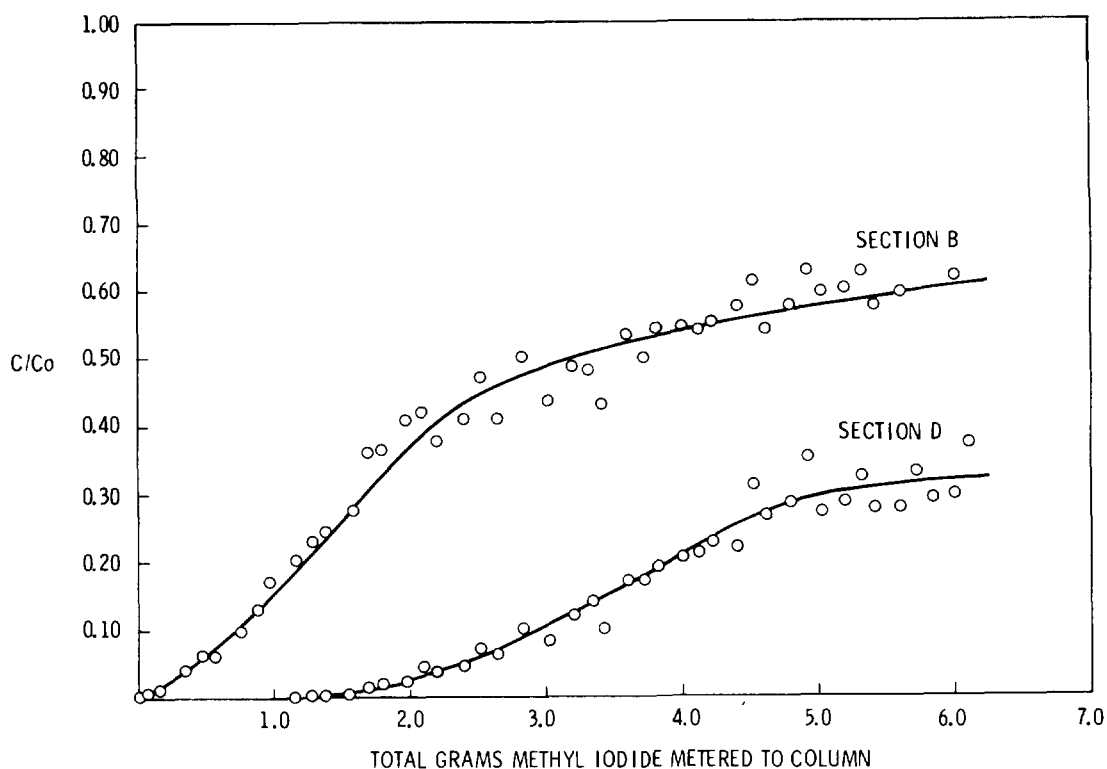


Figure 5. Breakthrough history for methyl iodide loading onto 18 wt% Ag substituted mordenite, Column II, sections B and D.

Table I. Iodine retention of 18% Ag substituted mordenite iodine sorbent.

Sample	Measured % CH <sub>3</sub> I Breakthrough (C/C <sub>0</sub> × 100)	Calculations From Breakthrough Curves* gI/g Ag	Theoretical Maximum** gI/g Ag
Column I			
Section A	90	(1.3) <sup>†</sup>	
Section B	82	(1.25) <sup>†</sup>	
Section C	55	0.4	1.2
Section D	7	0.2	
Section E	None	<0.1	
Column II			
Section A	65	0.4	1.2
Section B	60	0.2	
Section C	45	0.2	
Section D	30	0.1	

\* Calculated iodine retention at 1% breakthrough in two sections of silver sorbent (from raw data) with uncertainty +25% at a 95% confidence level: Column I (protection) 4.4 g, Column II (no protection) 0.14 g.

\*\* Based on reaction Ag+I=AgI.

† Grams of Iodine.



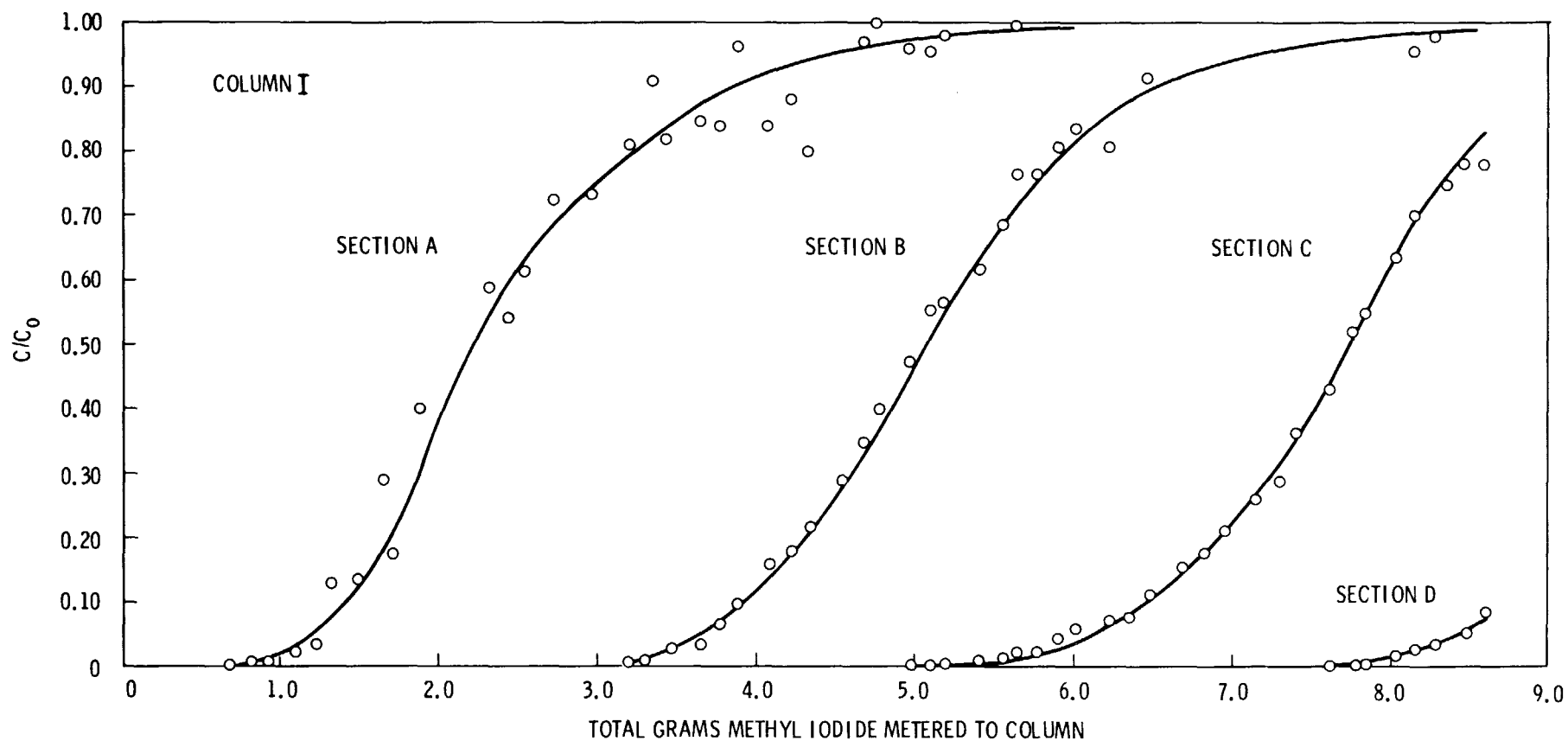


Figure 6. Breakthrough history for methyl iodide loading onto 7 wt% AgI impregnated silica gel sorbent, Column I.

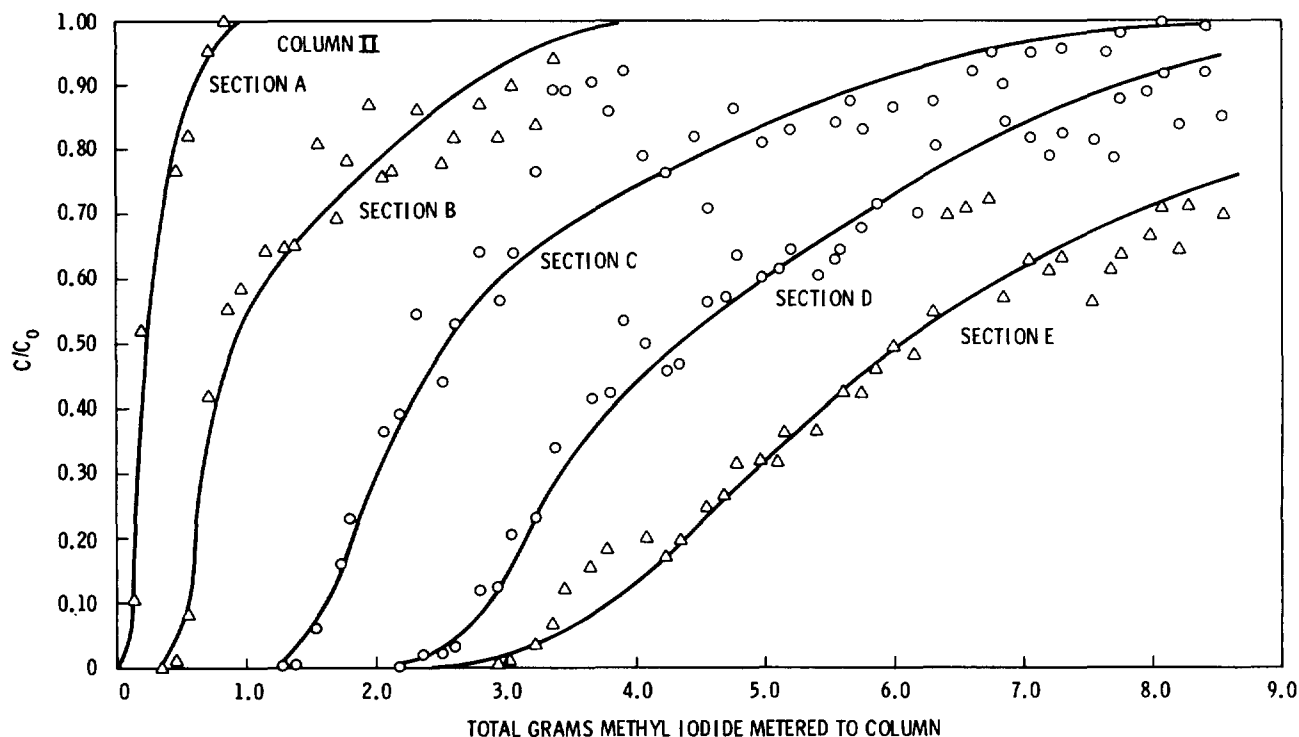


Figure 7. Breakthrough history for methyl iodide loading onto Column II.

Table II. Iodine retention of 7% Ag impregnated iodine sorbent.

Sample	Measured % CH <sub>3</sub> I Breakthrough (C/Co x 100)	Calculated CH <sub>3</sub> I Retention From Breakthrough Curves* gI/g Ag†	Theoretical Maximum** gI/g Ag
Column I			1.2
Section A	100	1.5	
Section B	98	1.4	
Section C	83	1.3	
Section D	7	0.9	
Column II			1.2
Section A	100 (material H)	(<0.3)‡	
Section B	100 (material H)	(<0.5)	
Section C	100	1.5	
Section D	95	0.97	
Section E	76	0.77	

\* Uncertainty is  $\pm 25\%$  at the 95% confidence level.

\*\* Based on the reaction  $\text{Ag} + \text{I} = \text{AgI}$ .

† Based on 7 wt% Ag.

‡ Grams of iodine.

Two stainless-steel columns were prepared. Both columns contained 5 cm of 7 wt% Ag silica gel iodine sorbent in five segments. The columns were placed in the oven and preconditioned for 24 hr with air at 2% relative humidity and with TBP/NPH vapor for 1 hr prior to metering methyl iodide. The columns were kept at 130° to 135°C throughout the experiment.

Methyl iodide was metered along with TBP/NPH vapor-laden air flowing at 1.95 l/min until a total of 6.66 g was loaded onto each column. The approximate methyl iodide concentration was 200 mg/m<sup>3</sup>, and the approximate TBP vapor concentration was 500 mg/m<sup>3</sup>.

Breakthrough curves for each column were constructed from the data. Figure 8 is the breakthrough for Column I and Figure 9 is the breakthrough curve for Column II. Iodine retention calculations are given in Table III. As in a previous experiment, the TBP had no effect on the total loading of iodine on the 7% Ag silica gel sorbent even though the TBP vapor concentration was increased from 10 mg/m<sup>3</sup> to 500 mg/m<sup>3</sup>. Calculated loading was greater than the stoichiometric maximum in both columns.

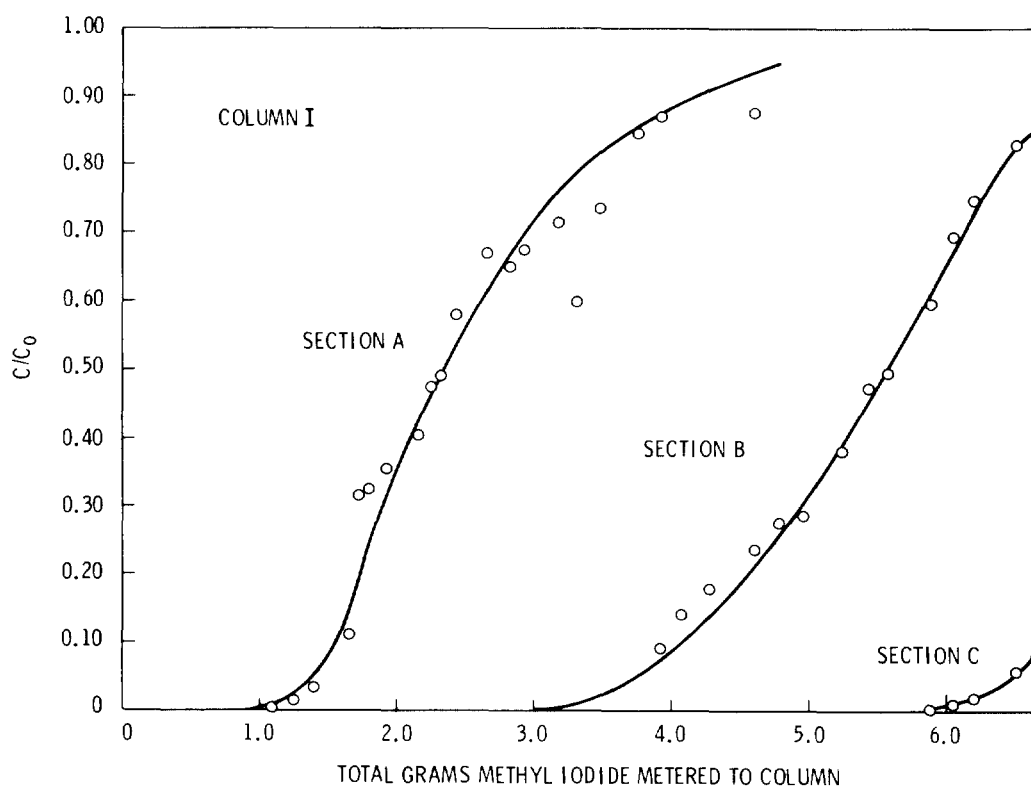


Figure 8. Breakthrough history for methyl iodide loading onto 7 wt% Ag impregnated silica gel sorbent, Column I.

The material from Column I was removed, examined and photographed to note the changes that occurred. The original material was white and beaded. At the end of the iodine loading, the material in the first two 5-cm sections of Column I was a light yellow mixed with a few black beads; the third 5-cm section was about an equal mixture of yellow and grey-black beads; the last two sections were entirely black. This was expected since the first two sections were saturated with iodine and yellow is a characteristic color of AgI. The middle section was only partially loaded with iodine, confirmed by the mix of yellow- and black-colored beads. The last two sections had not "seen" any iodine and were black. The black color is a characteristic of silver oxide formed by reaction of the sorbent with the air or TBP/NPH vapor. The material in all segments was

# 16th DOE NUCLEAR AIR CLEANING CONFERENCE

free-flowing and no organic residue could be visually detected, although the odor of TBP was noticeable in all segments.

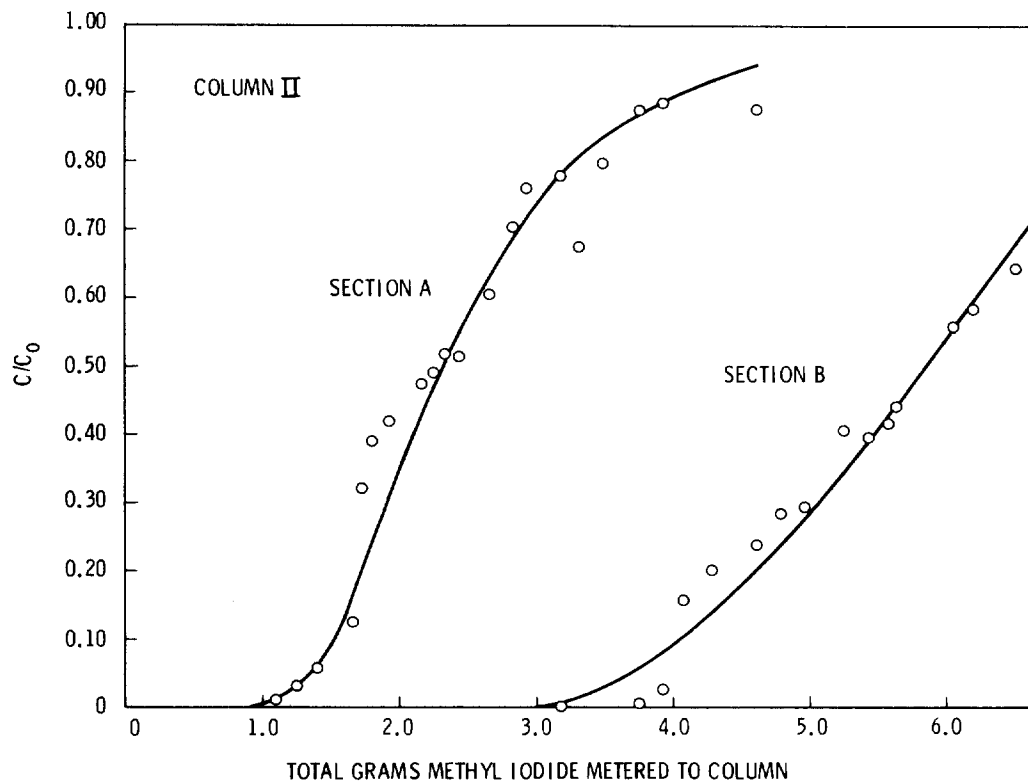


Figure 9. Breakthrough history for methyl iodide loading onto 7 wt% Ag impregnated silica gel sorbent, Column II.

Table III. Iodine retention of 7% Ag iodine sorbent prior to introducing  $\text{NO}_2$ .

Sample	Measured % $\text{CH}_3\text{I}$ Breakthrough ( $C/C_0 \times 100$ )	Calculated $\text{CH}_3\text{I}$ Retention From Breakthrough Curves* $\text{gI/g Ag}^\dagger$	Theoretical Maximum** $\text{gI/g Ag}$
Column I			1.2
Section A	100	1.8	
Section B	100	1.8	
Section C		0.7	
Section D	0	---	
Section E	0	---	
Column II			1.2
Section A	100	1.8	
Section B	100	1.8	
Section C		1.2	
Section D	0	---	
Section E	0	---	

\* Uncertainty is  $\pm 25\%$  at the 95% confidence level.

\*\* Based on the reaction  $\text{Ag} + \text{I} = \text{AgI}$ .

† Based on 7 wt% Ag.

Column II was left in the oven at 130 to 135°C. Dry air containing ~2% NO<sub>2</sub> only was then metered to the column at 1.9 l/min for 45 hr. This concentration of NO<sub>2</sub> was in the range expected in actual reprocessing off-gas streams.<sup>(4)</sup> This process was done to determine the effect NO<sub>2</sub> had on the iodine sorbent after being loaded with iodine in the presence of TBP/NPH. It has been postulated that NO<sub>2</sub> in an air stream containing TBP/NPH will counter-act the deleterious effects of the TBP on the 7% Ag silica gel sorbent by some uncertain mechanism.<sup>(1)</sup> It was assumed that Column II looked the same as Column I (which was removed) before introducing the NO<sub>2</sub>.

At the end of 45 hr the material in Column II was examined and photographed. The first two 5-cm segments were all white and resembled the virgin material. The third 5-cm segment was nearly all white with a thin layer of yellow near the bottom (downstream) of the segment. The last two segments were a pure light yellow; this as noted earlier is characteristic of silver iodide. It appears that the iodine loaded onto the first two segments of Column II was "washed" onto the last two segments of the column by the NO<sub>2</sub>, leaving the iodine sorbent in the original white state (regenerated). This was not expected. Rather, it was assumed that the first two segments of Column II would remain loaded with iodine and be the characteristic yellow color. It was also expected that any of the material not loaded with iodine (the material that was dark) would be regenerated to the white color of the virgin material. The silver on the silica gel would be reduced to the ionic (original) AgNO<sub>3</sub> state from the oxide (black) state by the NO<sub>2</sub>.

### III. Conclusions

The following conclusions were drawn from the work reported in this paper.

- The presence of airborne TBP vapor at a concentration of 500 mg/m<sup>3</sup> reduced the capacity of a commercially available 18 wt% Ag substituted mordenite iodine sorbent to retain iodine by 60% (compared to stoichiometric retention). This material could not be used efficiently in actual process off-gas streams without pretreatment to remove TBP. Furthermore, material A was demonstrated to be an effective sorbent for TBP and protect the 18 wt% Ag mordenite iodine sorbent downstream. Protected columns were able to retain 30 times more iodine than unprotected columns.
- A 7 wt% Ag commercial silica gel iodine sorbent was not affected by airborne TBP at ~10 mg/m<sup>3</sup> concentration. The stoichiometric maximum amount of iodine at saturation (100% breakthrough) was retained by columns of the material kept at 130 to 135°C. In some cases greater than the stoichiometric amount of iodine calculated from breakthrough data was retained by the silica gel sorbent at saturation. Because of this, the iodine sorbent material may be able to be used in actual process streams containing low concentrations (~10 mg/m<sup>3</sup>) TBP without treating the off-gas to remove the TBP.

- Visual examination of 7 wt% Ag sorbent loaded with iodine in presence of TBP/NPH and then subjected to 2 volume %  $\text{NO}_2$  in air indicated that the  $\text{NO}_2$  will regenerate the sorbent. The iodine appeared to wash off the material and leave the material in the original state. This would be undesirable in an actual process stream containing  $\text{NO}_2$ . It is necessary to irreversibly trap the iodine in a stable matrix. Additional analytical work is needed to confirm this conclusion.

### III. References

1. Wilhelm, J. G. and J. Furrer, "Head-end iodine removal from a reprocessing plant with a solid sorbent." In Proceedings of the 14th ERDA Air Cleaning Conference. National Technical Information Service, Springfield, Virginia (1976).
2. Parker, G. B. and L. C. Schwendiman, "Investigation of air cleaning processes for removing tributyl phosphate vapors from fuel reprocessing off-gas streams." In Proceedings of the 15th DOE Nuclear Air Cleaning Conference, CONF-780819 National Technical Information Service, Springfield, Virginia (1978).
3. Parker, G. B, Investigation of Air Cleaning Processes For Removing Tributyl Phosphate Vapors From Commercial Fuel Reprocessing Off-Gas Streams, Project Termination Report. PNL-2080-18, Pacific Northwest Laboratory, Richland, Washington (September 1979).
4. Thomas, T. R., L. P. Murphy, B. A. Staples and J. T. Nichols. Airborne Iodine Loading Capacities of Metal Zeolites and a Method for Recycling Silver Zeolite, ICP-1119, ERDA, Idaho Operations Office, Idaho Falls, Idaho (1977).

## DISCUSSION

SRIDHAR: On the desorbed iodine, what is the chemical species? Is it retained as  $\text{CH}_3\text{I}$  as it comes out of the beds, or is it in some other form or variety?

PARKER: I really don't know. I could not measure any iodine while running the  $\text{NO}_2$  through the columns. I was doing some gas chromatographic analysis, but only for methyl iodide, and I could not pick any up. So, the species must not be methyl iodide. But what form of iodine it is in, I don't really know. Has anybody got any ideas?

WILHELM: You may know that we have AC 6120, an amorphous silicious acid, which is impregnated with silver nitrate. It has a very special porosity and other properties. We found the same change in color from gray or dark brown to nearly white or yellow when sweeping the material with  $\text{NO}_2$ . The reason is very simple. Silver nitrate is reduced to silver, part of which is oxidized to silver oxide, and silver oxide has a dark brown color. If you run  $\text{NO}_2$  through the trap, the silver and silver oxide are converted again to silver nitrate, so the color changes to white. What we did not find, was movement of

the chemisorbed radioactive iodine along the filter bed or desorption. The movement of iodine may be special to the conditions you had, or to the material you used for the sorption process.

EVONIUK: In the experiment where you ran  $\text{NO}_2$  on a material balance, was there enough  $\text{NO}_2$  to completely react with the loaded methyl iodide that was at the front part, or did  $\text{NO}_2$  get carried further down to the upper part of the column, i.e., to the end part of the column?

PARKER: That's a good question. I will tell you why I chose 45 hours and 2 percent  $\text{NO}_2$ . First of all, 2 percent  $\text{NO}_2$  is somewhere in the range of what you would like to see in a typical commercial reprocessing offgas stream. Forty-five hours was about how much time I had until the end of the year. I really don't know whether there was a sufficient amount of  $\text{NO}_2$  in there to achieve a material balance, or any kind of complete reaction. It was a guess, more or less, and this concentration was run until I ran out of time. Obviously, it shows that what is needed is a little more detailed type of experiment to see whether, on a stoichiometric basis, there is a sufficient amount of  $\text{NO}_2$  to do the washing off, or if there is enough for all the material that is in there. Is that what you are asking?

EVONIUK: I was wondering if the  $\text{NO}_2$  did not replace the adsorbed species at the beginning part of the bed.

PARKER: I doubt if it stayed on the material in any way. I think it was like a catalyst, or like a reactant, to return the bed to its virgin form. This means, to move it back into the silver nitrate form from the silver oxide form.

HERRMANN: How did you analyze the residual tributyl phosphate after your adsorbent?

PARKER: You want to know how I knew what was depositing on to the material? I did it in two ways, one as a backup to the other. First of all, I measured the volume loss in the amount of tributyl phosphate that I had to start out with. That is a pretty rough way to estimate. The other way was to use a phosphorous analyzer which I connected to the entering stream containing the TBP. I used the phosphorous analyzer to give me an estimate of how much TBP was in the stream. With that concentration number, it was just a matter of monitoring total time to give the total amount. It was not really accurate, maybe  $\pm 25\%$ .

IODINE TRAPPING AND CONDITIONING IN THE MERCUREX SYSTEM

G.E.R. Collard, D. Hennart, J. Van Dooren, W.R.A. Goossens  
C.E.N./S.C.K., Mol, Belgium

Abstract

The Mercurex process, followed by adsorption on silvered products, has been retained by the S.C.K./C.E.N. for further investigation of a retention method for both inorganic and organic iodine compounds in reprocessing plant off-gases.

A parametric study applied to different iodine compounds has led to a design equation describing the influence of the gas and liquid flow rates and of the nitric acid and mercuric nitrate concentration on the scrubber efficiency. Mass transfer restriction in the liquid phase limits the process rate for  $\text{CH}_3\text{I}$ , while gas phase resistance to mass transfer is determinant for iodine removal.

Evolution of the iodine release from a batch-type dissolver during simulated fuel dissolution was studied. The efficiency of the process is influenced mainly by the dissolution grade of the fuel, since it depends on the form of iodine released from the dissolver and from the  $\text{NO}_x$  scrubber installed upstream the Mercurex scrubber.

A iodine-mercury separation process is proposed for treatment of the spent Mercurex solution. The process consists of the following steps :

- electrolytic precipitation of mercury after complexation with hydrazonium chloride ;
- elimination of iodine by precipitation on a fixed bed of  $\text{Cu}_2\text{O}$  put on a solid support ;
- recycling of mercuric nitrate after dissolution of mercury in nitric acid ;
- recovery of the hydrazonium chloride.

The process as proposed, is the result of a laboratory study of the different steps. Its major advantage is that the amount of waste generated is limited to a minimum. However, experiments in a larger scale equipment indicate that some modifications might be necessary.

Introduction

One of the problems in the removal of radioactive airborne isotopes from gaseous effluents of reprocessing LMFBR fuels involves iodine compounds retention, particularly the retention of the organic iodine compounds. Several advanced methods have been proposed for removing gaseous iodine species from dissolver off-gases. The most important are the Iodox process<sup>(1)</sup>, the Mercurex process<sup>(2)</sup> and the adsorption on silver exchanged<sup>(3)</sup> or impregnated<sup>(4)</sup> inorganic products. Amongst these, the Mercurex process has been chosen by the C.E.N./S.C.K. for further investigation.

The most important aspects of this investigation are presented in this paper in the sequence of three partial studies :



- the parametric evaluation of the Mercurex process according to experimental results obtained in packed-bed scrubbers ;
- the observation of the iodine behaviour in the gaseous effluents leaving a simulated dissolution vessel and passing successively through a nitrogen oxides scrubber and a Mercurex scrubber ;
- the development of a treatment process for the saturated Mercurex solutions resulting in a separation of iodine and mercury

### Engineering evaluation of the process

#### Equipment

The experiments were carried out in the gas purification mock-up GAS-TON described elsewhere<sup>(5,6)</sup>. Acid mercuric solutions are used to scrub iodine-contaminated air with recycling of the solution. The main flow of nitrogen or air is mixed with a secondary gas flow artificially loaded with molecular iodine or methyl iodide generated at a constant rate and traced with  $^{131}\text{I}$ . The characteristics of the two different packed-bed scrubbers used for the countercurrent gas-liquid contact are described in table I.

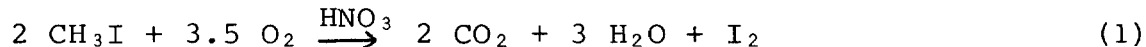
Table I. Description of the packed-bed scrubbers

Column	Column 1	Column 2
material	glass	polypropylene
diameter (m)	0.15	0.29
Packing		
material	glass	steel
type	Rashig Rings	Pall Rings
dimensions (mm)	15 × 15 × 1	25 × 25 × 0.5
specific area (m <sup>2</sup> /m <sup>3</sup> )	292	210
void fraction	0.74	0.95
height of packing (m)	1.7	1.7

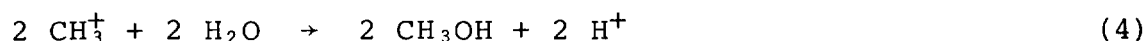
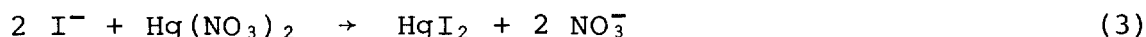
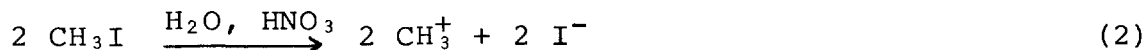
The loop is fitted with gas sampling devices before and after each column.

#### Theory

Since the reaction between methyl iodide and mercuric nitrate is not well known, it is assumed that the following reaction occurs in concentrated nitric acid solutions in the presence of air<sup>(1)</sup> :



In more diluted nitric acid solutions, the oxidation is not complete and the following reactions are supposed to be possible :



Moreover, complexes between  $\text{HgI}_2$ ,  $\text{I}^-$  and  $\text{NO}_3^-$  would be formed. Whichever of these reactions takes place, it seems that the global reaction is of pseudo first order with regard to  $\text{CH}_3\text{I}$  and would be rather rapid.

It is likely that in the Mercurex process these liquid phase reactions are combined with an absorption step of methyl iodide from the gas in the liquid phase. Thus the mathematical model of the absorption process can rely on the following assumptions :

1. flow rates are constant with time and position ;
2. resistances to mass transfer are both in the gas and liquid phases;
3. Henry's law is applicable, that is : the gas-liquid equilibrium distribution ratio of methyl iodide is independent of  $\text{CH}_3\text{I}$  concentration in the gas and depends only of the  $\text{HNO}_3$  and  $\text{Hg}(\text{NO}_3)_2$  concentrations in the solution ;
4. the reactions are sufficiently slow to be absent in the liquid film, but rapid enough to occur in the bulk of the liquid ;
5. the mass transfer coefficients are constant throughout the packed column.

The general relationships resulting from application of the two-film theory<sup>(7)</sup>, subject to the above conditions, have been applied in order to describe the absorption of methyl iodide and of elemental iodine in a packed scrubber. In this way the following equation has been found :

$$\ln DF = \frac{Z}{\frac{G}{\rho_g} \left[ \frac{A}{G^{0.8}} + \frac{B}{\gamma \cdot L^{0.8}} \right]} \quad (5)$$

where : A is a constant depending on the packing ;

B is a constant independent of the packing ;

DF is the decontamination factor for iodine ;

G is the gas load per cross sectional area ( $\text{kg} \cdot \text{m}^{-2} \cdot \text{s}^{-1}$ ) ;

L is the liquid load per cross sectional area ( $\text{kg} \cdot \text{m}^{-2} \cdot \text{s}^{-1}$ ) ;

Z is the height of the packing (m) ;

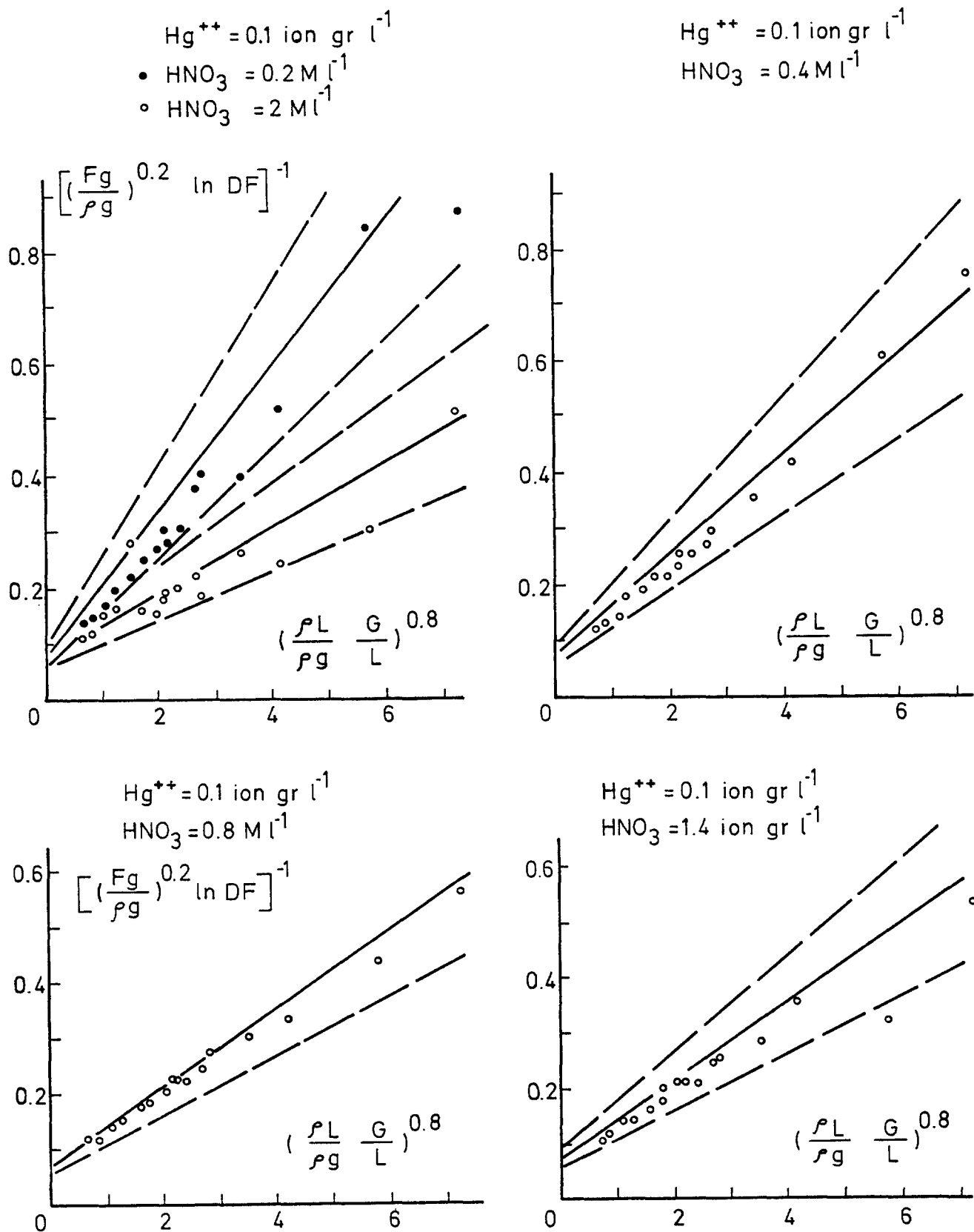
$\gamma$  is the solubility according to Oswald ;

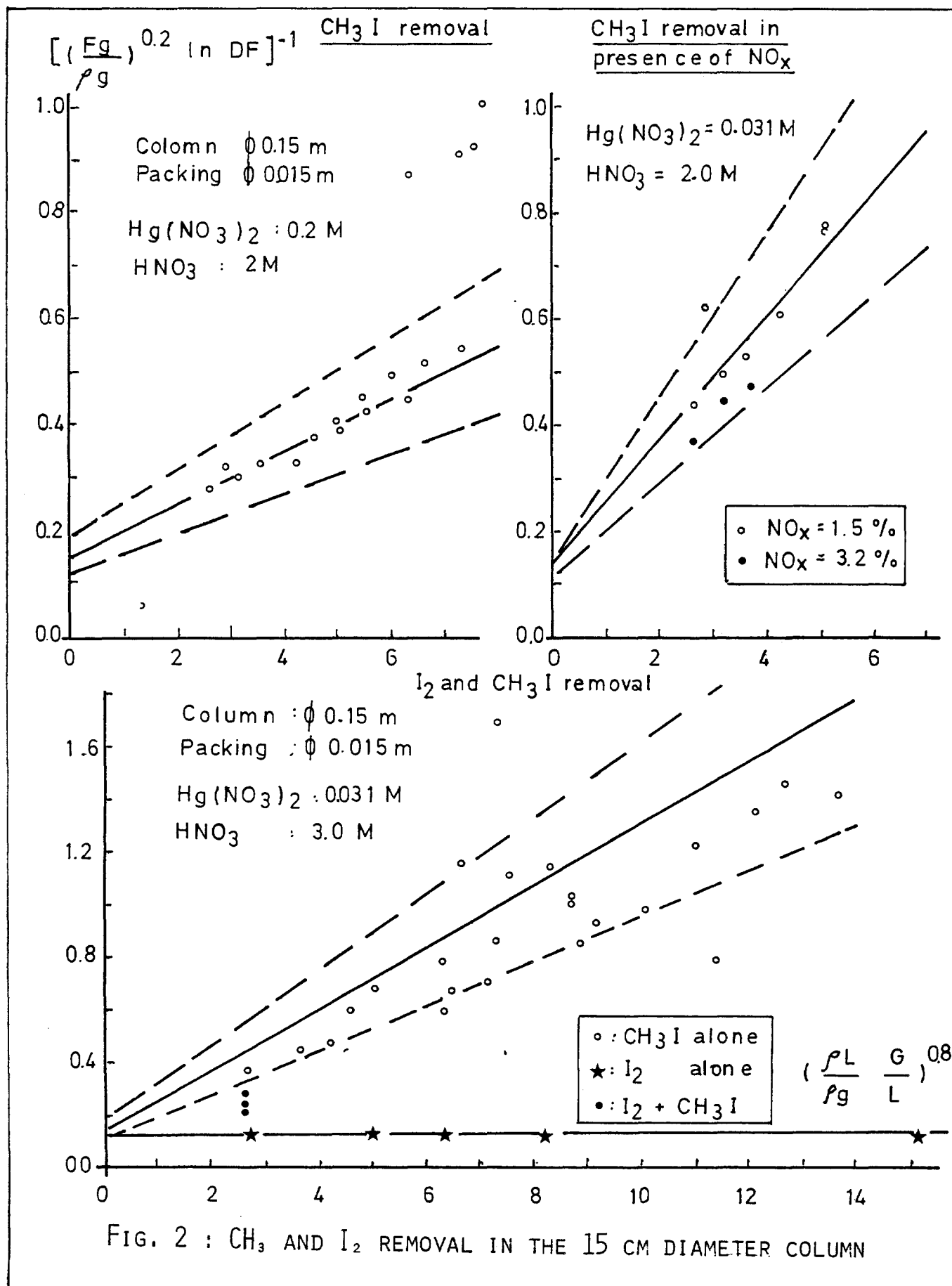
$\rho_g$  is the specific mass of the gas ( $\text{kg} \cdot \text{m}^{-3}$ ).

#### Treatment of the experimental data

This equation is used here to correlate the experimental data obtained with both columns. In the fig. 1 and 2 the gas and liquid flow rates  $F_g$  and  $F_l$  are given in cubic meters per hour, the flowmeters being calibrated in this unit. Are also given the acid and mercuric nitrate concentrations in the solution passing through the column.

The parameters in this equation are determined by rearranging the equation to the following relationship :

FIG. 1 :  $\text{CH}_3\text{I}$  SCRUBBING IN THE 29 CM DIAMETER TOWER



$$\left[G^{0.2} \ln DF\right]^{-1} = \frac{1}{Z} \left[A' + B' \frac{G^{0.8}}{\gamma \cdot L^{0.8}}\right] \quad (6)$$

where :  $A' = \frac{A}{\rho_g} \quad (7)$

$$B' = \frac{B}{\rho_g} \quad (8)$$

This form clearly indicates that a plot of  $[G^{0.2} \cdot \ln DF]^{-1}$  vs  $\left[\frac{G}{L}\right]^{0.8}$  yields a straight line with  $\frac{A'}{Z}$  as intercept of the ordinate and  $\frac{B'}{\gamma \cdot Z}$  as slope.

For each set of data obtained at a definite composition of the scrub solution, both line parameters have been calculated according to the least square method. A trial and error adjustment of the relative influence of each  $\text{HNO}_3$  and  $\text{Hg}(\text{NO}_3)_2$  concentration on the  $\frac{B'}{\gamma}$  values ended the mathematical fitting, where

$$\frac{B'}{\gamma} \propto \frac{1}{[\text{HNO}_3]} + \frac{1}{\sqrt{[\text{Hg}(\text{NO}_3)_2]}} \quad (9)$$

or 
$$\gamma = \frac{[\text{HNO}_3] \cdot \sqrt{[\text{Hg}(\text{NO}_3)_2]}}{[\text{HNO}_3] + \sqrt{[\text{Hg}(\text{NO}_3)_2]}} \times \text{constant}. \quad (10)$$

No further study was performed in order to interpret this last equation. It must be considered as valuable within the experimental concentration range. The value of the constant has been found to be equal to 8.1 for methyl iodide.

When the solubility of the absorbed compound is large, the resistance in the gas film becomes limitative and the equation (6) can be rewritten as follows :

$$[G^{0.2} \cdot \ln DF]^{-1} = \frac{A}{\rho_g Z} \quad (11)$$

as can be verified on the third part of fig. 2.

Consequently, design equations are got available which describe the removal of iodine and methyl iodide from a gas stream by means of an acid solution of mercuric nitrate in a packed column.

### Iodine behaviour during simulated dissolution

#### Equipment

The behaviour of iodine during the dissolution of non-irradiated fuel has been observed using the following equipment line : a dissolution vessel, a first washing column for  $\text{NO}_x$  removal, a second washing column for iodine compounds retention, a demister and two fixed beds for the adsorption of the remaining iodine compounds<sup>(4)</sup>. Uranium oxide (3.5 to 4.5 kg) and sodium iodide (3.5 g) traced with  $^{131}\text{I}$  (100-

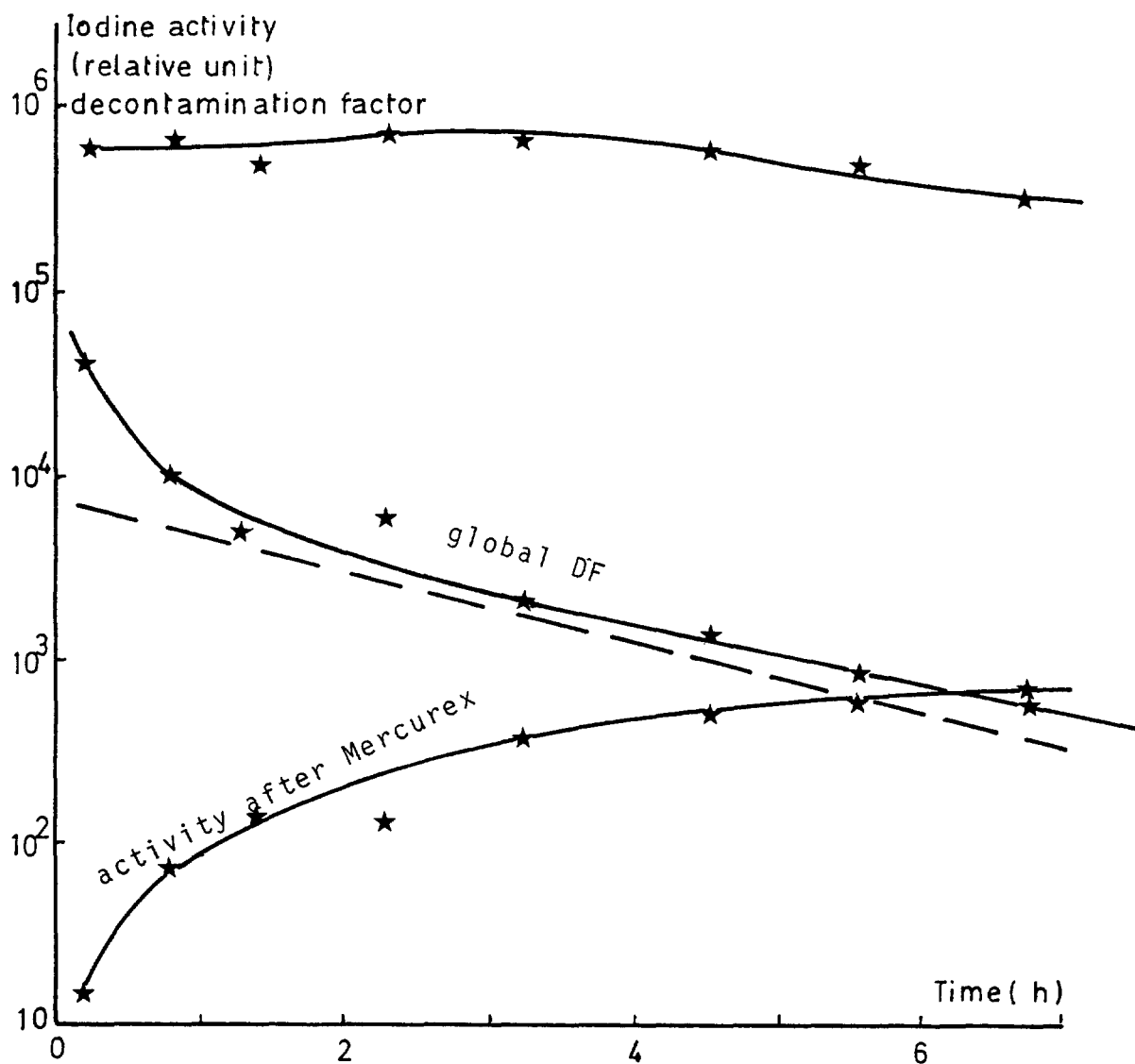


FIG. 3 : WET SECTION  
IODINE BEHAVIOUR IN THE CASES

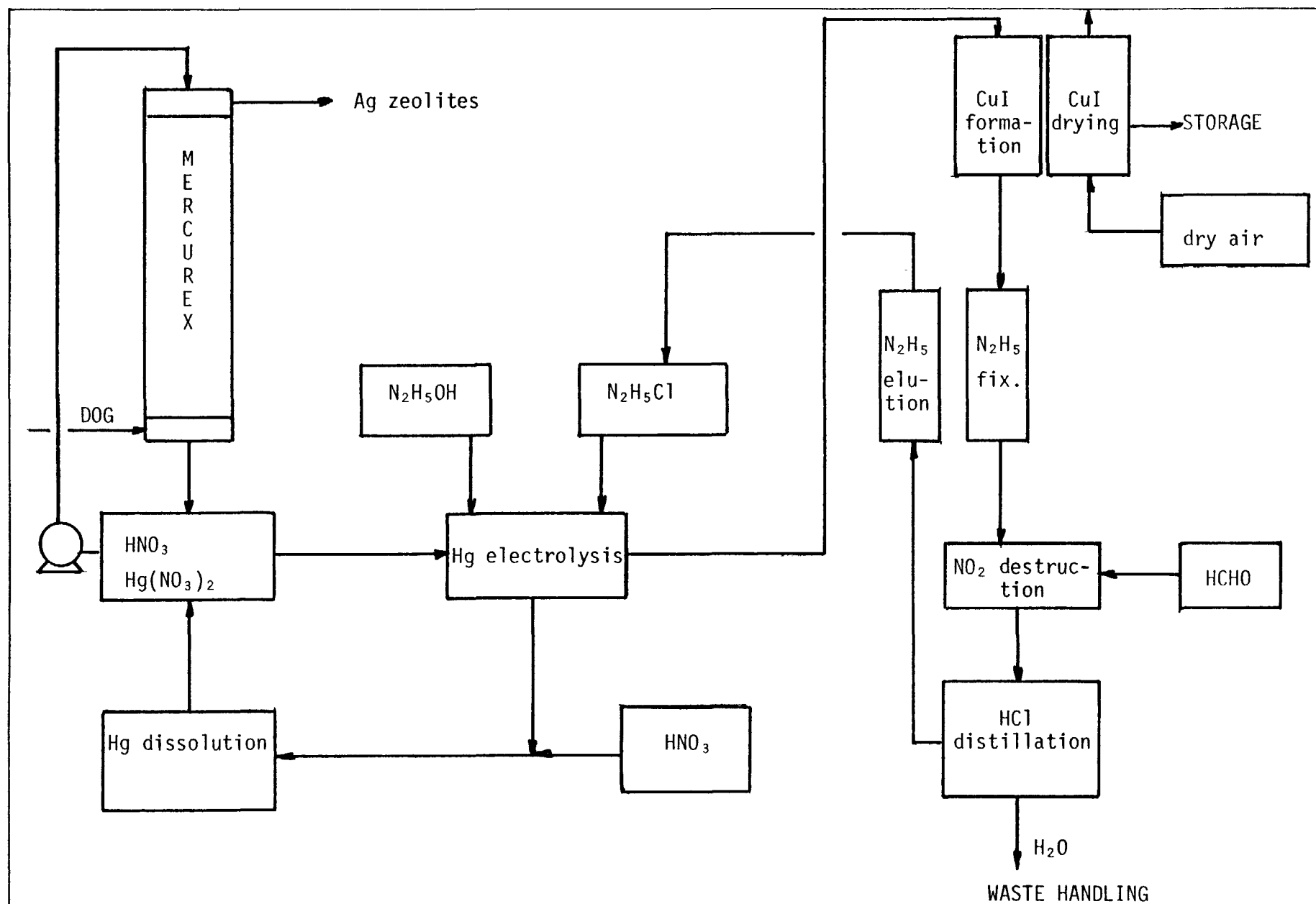


FIG. 4 : FLOW SHEET OF THE IODINE MERCURY SEPARATION PROCESS

150 mCi) were added in nitric acid (23-25 dm<sup>3</sup>) and the iodine concentration was followed in the dissolver and in the gas stream.

#### Iodine release from the dissolver

In the dissolver iodine concentration rapidly decreases during the first four hours and then tails off very slowly to the end of the runs. After eight hours, 0.5 to 3 % of the total iodine remain in the dissolver and 0.5 to 1.5 % after 100 hours.

It seems likely that the elution of iodine is accelerated by the emission of NO<sub>2</sub> due to the UO<sub>2</sub> dissolution. Afterwards, the iodine concentration decreases more slowly and finally remains constant in the solution.

#### Absorption of iodine in the NO<sub>x</sub> washing column

The NO<sub>x</sub> washing column is operated with recycled water which becomes enriched in HNO<sub>3</sub>. During the first hour of the dissolution, the activity increases in the washing solution because of the large amounts of iodine in the gas phase. Afterwards, iodine is eluted but the desorption is not yet completed after more than 100 hours. At this time, the iodine concentration in the washing solution is larger than in the dissolver.

#### Absorption of iodine in the Mercurex column (fig. 3)

The Mercurex washing column is operated with a recycled acid solution of mercuric nitrate (1 M HNO<sub>3</sub>, 0.1 M Hg(NO<sub>3</sub>)<sub>2</sub>). Due to the performance of the NO<sub>x</sub> scrubber, the iodine activity in the gas between the two columns decreases slowly, although the iodine leaving the dissolver is decreasing rapidly during the first hours of a run. During this period, the decontamination factor obtained in the Mercurex column decreases rapidly first and then more slowly. This observation permits us to suppose the chemical form of the iodine leaving the NO<sub>x</sub> scrubber to be more difficultly washed out by the mercuric solution than elemental iodine.

#### Over-all decontamination factor

During all the runs covering a period of three months, the activity measured in the gas downstream the silvered products has not been higher than the background. This fact reflects that over-all iodine decontamination factors of 10<sup>3</sup> to 10<sup>5</sup> are achieved using a Mercurex scrubber followed by a bed of silver sorbents.

#### Treatment of spent Mercurex solutions

##### Process description

The spent Mercurex solution, loaded with iodine (table II), is treated in a subsequent process, in which iodine and mercury are separated. After separation, the mercury can be recycled to the Mercurex process, while the iodine is precipitated and conditioned for storage. In order to produce a minimal amount of waste, recycling of the reagents needed is applied as far as possible. The flow-sheet of this treatment process is given in fig. 4.



Table II. Chemical composition of a spent Mercurex solution

Compound	Concentration
$\text{Hg}^{2+}$	0.2 M
$\text{H}^+$	1 M
$\text{NO}_3^-$	1.4 M
$\text{I}^-$	0.03 M

The mercury is removed from the spent Mercurex solution by electrolytic precipitation, after complexation of the mercuric ions with hydrazonium chloride. This precipitated mercury is recycled to the Mercurex scrubber by redissolution in nitric acid. The iodine in the spent solution, free of mercury, reacts with  $\text{Cu}_2\text{O}$  to  $\text{CuI}$ . Therefore the spent solution percolates a fixed bed of  $\text{Cu}_2\text{O}$  put on a solid support. Once saturated with iodide, the bed load is conditioned for final storage.

Three more steps are added to the process in order to recover the hydrazonium chloride for recycling into the mercury complexation step, namely the fixation of hydrazonium cations on an ion-exchanger which is regenerated with hydrochloric acid to give recyclable hydrazonium chloride, the destruction of nitrate by reaction with formaldehyde and the distillation of the remaining dilute hydrochloric acid to get hydrochloric acid for the regeneration of the ion-exchanger.

A major advantage of this treatment process is that the amount of waste produced is limited to a minimum. No other solid waste than  $\text{CuI}$  is regularly formed. Of course, after some time the ion-exchangers will have to be renewed. The liquid waste generated, i.e. the effluent of the distillation step, consists of water that is only slightly contaminated. No gaseous compounds other than compounds already present in reprocessing effluents are formed ( $\text{N}_2$ ,  $\text{NO}_x$ ,  $\text{CO}_2$ ).

#### Discussion of the results obtained on laboratory scale

The treatment process, as described above, is the result of a development study of the different steps on laboratory scale, which will be discussed here.

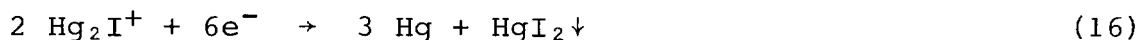
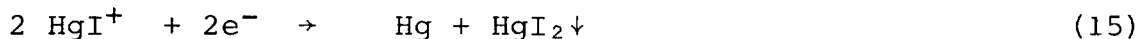
The electrolysis of the spent Mercurex solution started with a mercury cathode, which has a high overvoltage for hydrogen formation, and a platinum anode. Mercury was expected to precipitate at the cathode in this direct electrolysis.

However, direct electrolysis could not be applied for two reasons. On one hand, at the cathode the mercury present as  $\text{Hg}^{2+}$ ,  $\text{HgI}^+$  and  $\text{Hg}_2\text{I}^{3+}$  (9), did not follow the expected electrochemical reactions (13) and (14)

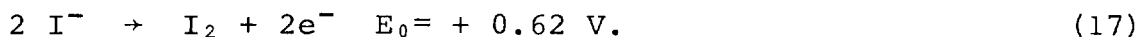




but instead  $\text{HgI}_2$  precipitated according to the following reactions :



On the other hand, at the anode iodide oxidation occurred and molecular iodine was formed :



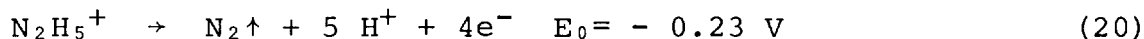
In practice, the precipitation of  $\text{HgI}_2$  was overcome by complexation of the mercuric ion with chlorides :



The formation of iodine was prevented by taking  $\text{N}_2\text{H}_5\text{Cl}$  as chloride salt for complexation. As a result, the following reactions occurred :  
-at the cathode :

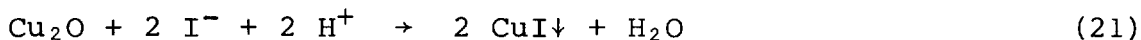


-at the anode :



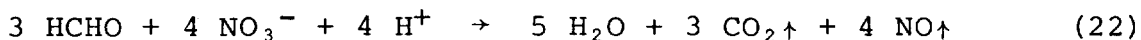
In order to avoid formation of iodine completely, the pH had to be kept higher than 1 during the electrolysis. Since the anodic reaction increases the acidity of the solution, hydrazine has to be added permanently during the electrolysis. Taking these precautions, mercury can be removed from a Mercurex solution by electrolysis upto at least 99.9 %.

The iodine present in the remaining solution as iodide, is precipitated as  $\text{CuI}$  on a fixed bed of  $\text{Cu}_2\text{O}$  on a solid support according to the following reaction :



The fixed bed option is retained because no excess of copper will appear in the effluent with this method. However, since  $\text{Cu}_2\text{O}$  is only available as a fine powder, a solid support is necessary. For this reason  $\text{Cu}_2\text{O}$  has been put as a coat on porous alumina pellets. Working at an inlet pH of 1.5, the iodide can be entirely fixed on such a  $\text{Cu}_2\text{O}$  material. Once saturated with iodide, the bed is purged with dry air as conditioning before final storage.

The effluent of the precipitation step still contains an amount of  $\text{N}_2\text{H}_5\text{Cl}$  and  $\text{N}_2\text{H}_5\text{NO}_3$ . In order to get able to recycle the hydrazonium chloride to the complexation step, a sequence of three steps has to be added. Firstly, the  $\text{N}_2\text{H}_5^+$ -cations are fixed by ion-exchange on styrene sulfonate. Secondly, the nitric acid is destroyed by reaction with formaldehyde at 100 °C according to the scheme :



It is clear that the reaction products of this destruction are common compounds in reprocessing plant effluents. Thirdly, the dilute hydrochloric acid solution left is concentrated in a distillation step and is used for the regeneration of the ion-exchanger where recyclable  $\text{N}_2\text{H}_5\text{Cl}$  is obtained. The distillation effluent consists of water, which is only slightly contaminated, and is sent to the waste treatment plant. These three steps have been tested on a laboratory scale giving complete satisfaction.

### Larger scale experiments

Recently, experiments on a larger scale have been started. A 10 l batch-electrolyser has been installed, in which a few preliminary experiments have been performed to demonstrate the soundness of the electrolysis. A mercury cathode and a platinized titanium anode were used. Again more than 99.9 % of the mercury was recovered. However, technological development work is still needed to determine optimal geometry, mixing system and working parameters of this electrolyser.

A second unit, that has been tested on a larger scale, is the fixed bed precipitation unit. Experiments were carried out with the same filling material, as previously described. Here some problems showed up, which did not in the experiments on laboratory scale. The effectiveness of the precipitation appeared to be poor : only 50 % of the  $\text{Cu}_2\text{O}$  was converted to  $\text{CuI}$  at the moment that iodide was detected at the outlet of the bed. Further, the  $\text{CuI}$  precipitate came free from the solid support. This phenomenon caused bed plugging, when the pellet size was diminished. These problems are hoped to be overcome during future research, directed to the application of other support material and to the improvement of the coating with  $\text{Cu}_2\text{O}$ .

### Conclusion

This engineering study of the Mercurex process has shown the feasibility of the process for the primary removal of iodine compounds from dissolver off-gases. Consequently, a Mercurex scrubber will be built in, in the off-gas purification loop of the HERMES installation (Head End Research Mock-up on an Engineering Scale), under construction at S.C.K./C.E.N. where batches of 10 kg irradiated fuel will be dissolved.

The laboratory study has indicated that it is possible to transform the iodine species trapped in the Mercurex solution into a iodine compound suitable for final storage. In this transformation process mercury is recycled and a minimum of common waste is formed. Larger scale experiments are needed to test the technological feasibility of this treatment process for Mercurex solutions.

### References

- (1) Groenier, W.S., An engineering evaluation of the iodex process : removal of iodine from air using a nitric acid scrub in a packed column, ORNL-TM-4125, 1973.
- (2) Stromatt, R.W., Removal of radio-iodine from Purex off-gas with nitric acid and with nitric acid-mercuric nitrate solutions, GHW-55735, 1958.

## 16th DOE NUCLEAR AIR CLEANING CONFERENCE

- (3) Pence, D.J., Duce, F.A., Maeck, Q.J., Adsorption properties of metal zeolites for airborne iodine species, Conf. 70081, 1970.
- (4) Wilhelm, J.G., Furrer, J., Head-end iodine removal from a reprocessing plant with a solid sorbent, 14th ERDA Air Cleaning Conference, 1976.
- (5) Collard, G., Broothaerts, J. et al., Technologie de la purification des gaz pour les mini-rejets dans le retraitement des combustibles des réacteurs surrégénérateurs, Conférence Nucléaire Européenne, 1975.
- (6) Broothaerts, J., Collard, G. et al., Treatment and control of gaseous effluents from light water reactors and reprocessing plants, IAEA-SM-207/8, 1976.
- (7) Nonhebel, Gas purification processes for air pollution control, Edition : Newnes-Butterworths, 1972.
- (8) Goossens, W.R.A., et al., Experience with pilot scale iodine and krypton retention facilities under simulated conditions, Seminar on radioactive effluents from nuclear reprocessing plants, Karlsruhe, Proc., pp. 567-581, Nov. 1977.
- (9) Pascal, P., Nouveau traité de chimie minérale, Tôme V, Masson et Cie, Paris, 1967.

## DISCUSSION

HENRICH: Do you expect to have some trouble because of an occasional carryover of a small fraction of the mercury to the dissolver? Afterwards, it would be very much more difficult to remove the iodine. Even small amounts of the original solution would be sufficient to cause trouble.

COLLARD: I think the answer has two aspects. As a matter of fact, mercury would be disturbing in the dissolver, but, theoretically, you have silver, mercury, and other metals in the dissolver to catch all the iodine. Nevertheless, you find iodine in the offgases. That is the first aspect of the answer. The second aspect is the precautions you have to take to avoid mercury in the dissolver. In fact, if precipitation of mercury is done in-line, you will get a regeneration of mercury and the only liquid waste you get is water. This water is sent with the low-level waste straight to the waste treatment. So, there is no recycling of this liquid. Now you can say you can have entrainment during incidents. You can also have entrainment of solution to a storage tank. Indeed, it can be a problem. If you plan to reuse the waste solution, you may have incidents in the next dissolution steps. It can be a problem. I think it is just a question of design.

EVONIUK: A couple of questions. On this pilot plant, what was your gas feed rate and your concentration going into your mercuric scrub column? I missed it on the graph. And what is your projected cost for a unit?

COLLARD: The experiment was done with a dissolver of 30 liters wherein about 12 kilos of uranium were dissolved. Iodine was added to the uranium, traced with active iodine, and we followed the iodine during the dissolution of the uranium. So we simulated the dissolution but not with fissioned uranium.

EVONIUK: What about the costs for a unit?

COLLARD: The unit is only a scrubber. The costly product is hydrazine. Hydrazine is a very expensive product, but the quantity we use is not very large. As an example, for a little reprocessing plant of 60 tons thermal fuel per year, you have to regenerate about 200 liters of solution per year. So I don't think the costs are very important.

EVONIUK: You are talking about processing how many liters of gas per year?

COLLARD: It is a liquid and not gas treatment in this case. For a thermal reactor in Belgium we did some calculations for 60 tons of fuel per year. You would have about 200 liters of solution to be treated and you would need about 50 liters of hydrazine. This is expensive, but it is not a very large amount.

RESULTS OF CLEANING DISSOLVER OFF-GAS IN THE PASSAT  
PROTOTYPE DISSOLVER OFF-GAS FILTER SYSTEM

J. Furrer, R. Kaempffer, A. Linek<sup>+</sup>), A. Merz<sup>++</sup>)

<sup>+</sup>) Laboratorium für Aerosolphysik und Filtertechnik

<sup>++</sup>) Laboratorium für Isotopentechnik  
Kernforschungszentrum Karlsruhe GmbH  
Postfach 3640, D-7500 Karlsruhe 1,  
Federal Republic of Germany

Abstract

For demonstration of an advanced dissolver off-gas cleaning system the new PASSAT 1) filter system has been developed, set up under licensing conditions pertinent to industrial scale reprocessing facilities 2) and commissioned for trial operation. Major components of the PASSAT off-gas cleaning system are the packed fiber mist eliminator with flushing capability (Brink filter) for initial removal of droplet and solid aerosols, which has been installed to extend the service life of HEPA filters, and the series connected iodine adsorption filters for optimum utilization of the iodine adsorption material, AC 6120.

The tests performed so far and the experience accumulated in testing these remotely operated filter components under simulated dissolver off-gas conditions, are described and discussed.

I. Introduction

In reprocessing spent fuel elements, the dissolver constitutes a major source of airborne particles as a result of the intensive agitation of liquids due to the generation of gas bubbles, the high temperature of the liquid and the injection of sparging air. These particles are made up of droplets of the fuel element solution and dust produced in cutting the fuel elements and carried from the shear sweep gas into the dissolver. The dissolver off-gas is first run past condenser and NO<sub>2</sub> absorption columns in which these primary aerosols can be absorbed and dissolved. However, these components in turn give rise to secondary aerosols which re-enter the off-gas stream.

The development of components for aerosol and iodine removal in PASSAT aims at obtaining data on the optimum design of a dissolver off-gas filter train as well as at reducing the radioactive waste by the use of high efficiency prefilters which allow to return into the dissolver solution the aerosols removed. The key part of the train is the recleanable mist eliminator 3) connected in series with the coarse droplet separator. This mist eliminator has been so designed that also in the range of critical aerosol sizes high retention factors are attained for airborne droplets and solid particles (DF for droplets 1 - 5  $\mu\text{m}$  > 1000; DF for solid particles 0.09 - 0.12  $\mu\text{m}$  > 1000). Thus, the prefilter permits to extend the service life of the successive HEPA filters and the iodine filters connected in series,

since droplet storage can be excluded and loading by  $\gamma$ -emitters is largely reduced.

Before the individual filter components can be installed in the new dissolver off-gas section of the Karlsruhe Reprocessing Plant, the safety relevant performance had to be proved in compliance with the requirements by the licensing authorities.

This required simulation of a dissolver off-gas whose composition was determined by the specified data of the Reprocessing Plant. The previous studies first concentrated on the verification of the behavior of solid and droplet aerosols at recleanable, packed fiber mist eliminators and their optimization. Moreover, the tests with radioactive and inactive aerosols served to determine the following filter characteristics of the packed fiber mist eliminator; loading time, distribution and liquid storage as a function of the gas flow and the aerosol concentration; pressure drops occurring at different flows; drying periods of the fiber package; optimization of the amount of liquid for cleaning the filter element, and detection of the removal efficiency as a function of the droplet and solid aerosol sizes.

The second central point of activities concerned the investigation of the iodine behavior at high iodine concentrations at the individual filter components and the verification of loading and capacity of the iodine filter drums. About 11.45 kg of elemental iodine with a radioactive tracer added were produced and fed into the system while the distribution of the iodine and the decontamination factors were evaluated.

## II. Removal of Droplets and Particles in the Packed Fiber Mist Eliminator (PFME)

### II. 1. Generation of Airborne Droplets

To examine the removal performance of different droplet separators in PASSAT, defined droplet spectra must be generated. Very small droplets can be generated by means of ultrasonic spray systems, high frequency atomizers, impact and centrifugal force separators and single and dual feed nozzles. Since the single and dual feed nozzle technique is very simple in design and likely to have high availability, this system was installed in PASSAT for airborne droplet generation.

To determine the retention factors in packed fiber mist eliminators, a dual feed nozzle with a maximum of the droplet frequency around  $< 10 \mu\text{m}$  was selected, which provides a distribution of droplet sizes in the range between 1 and  $35 \mu\text{m}$  (Fig. 1).

One particular difficulty in measuring droplet removal lies in the fact that small droplets can evaporate very quickly and then can no longer be measured. If this occurs, e.g., on the clean air side of a droplet eliminator, it would simulate high retention factors. For this reason, saline solutions were sprayed in various experiments. The salt core remaining after evaporation allows quantitative conclusions to be drawn with respect to the mass of droplets originally available and can be precipitated on nucle pore filters.

II. 2. Droplet Measurement

For rapid determination of particle size distributions in aerosol flows, scattered light measurements <sup>4)</sup> are applied preferably. The aerosol spectrometer, an optical particle counter summing up scattered light pulses, uses the light scattering effect to determine grain sizes and concentrations of flowing aerosol particles moving through a small measuring volume of the flow to be examined. The optical limitation of the measuring volume makes it possible to measure the local size distribution of the particles directly in the given flow without upsetting this pattern and changing the distribution of particles and their dispersed condition, respectively. By selecting an optically limited, very small measuring volume (100  $\mu\text{m}$  length of the edges) the fraction of coincident signals brought about by the simultaneous presence of several particles in the measuring volume becomes negligible even in the presence of relatively high particle concentrations. Thus, the scattered light is measured in the individual particle, not in the group of particles; this makes it a direct distribution measurement. The values assessed by the measuring equipment are directly passed to the computer by means of an on-line data line, are processed in an existing program and evaluated under the following aspects: In the filter drums the removal efficiency for special drop sizes as a function of diameter and the bulk removal efficiency as a function of temperature and volume flow were determined.

II. 3. Remotely Operated Packed Fiber Mist Eliminator (PFME)

The mist eliminator (Fig. 2) consists of a fiber packing designed like a filter cartridge installed in a housing with thermal insulation and additional trace heating. Two condensate discharge outlets connected to the untreated and clean air sides of the filter housing discharge all contaminated liquids accumulating in the housing via intermediate storage tanks and also remove the flushing liquids collected in cleaning the filter systems of solid deposits. For flushing the filter systems the housing is equipped with six flushing nozzles attached to the support flange, which spray coarse droplets  $> 50 \mu\text{m}$ . For decontamination of the whole housing there is a ring conduit equipped with bores installed in the upper part of the housing. The bottom part of the housing carries the sealing flange for the filter cartridge which, when the movable lid of the housing is closed, evenly presses the cartridge against the sealing flange by means of spring washers and a gasket attached to the cartridge. The gasket separates the chambers carrying untreated gas from those carrying clean gas and from the upper, clean part of the housing. The gasket material must be resistant against the chemicals and radiation doses to be expected. An annular test groove allows continuous monitoring of the tight fit of the filter cartridge during operation. For this purpose, air at a slight overpressure is fed to the test groove, escaping air indicates leakages. To avoid contamination of the upper part of the housing, the filter cartridge, which is closed at the top, is exposed to a sealing gas flow. To bring the cartridge into the optimum position, webs and a guiding lance are provided for centering relative to be fixed spray nozzles.



The filter cartridge proper consists of a bottom plate to which a hollow cylinder holding the fiber packing is attached. The hollow cylinder is welded closed at the top. The fiber packing is arranged concentrically in the cylinder, equipped with support screens and sealed at the top and the bottom to prevent short circuits between the untreated and the clean gases. For remote handling the cartridge has a holding cone for the crane attached to the upper plate. The cartridge is filled with fiber glass packings of specific packing densities and thicknesses. In order to achieve a larger outer surface for solid off-gas constituents to deposit on, and also for improved drainage in flushing, the flow was directed from the outside to the inside.

#### II. 4. Operating Principle of Droplet Retention

Larger droplets ( $d > 10 \mu\text{m}$ ) are mainly separated as a result of sealing and inertia effects. The droplets impinge upon the fiber and, under the influence of the carrier gas pressure and of gravity, penetrate through the fiber packing into the precipitator, where they are discharged to the bottom. The retention of very small droplets is controlled mainly by diffusion effects, which become the more pronounced the longer the stay time of the droplets in the fiber packing and the larger the volume and the area of the filter packing.

#### II. 5. Setup for Droplet Retention Tests

Fig. 3 is a schematic diagram of the analytical system required for testing the droplet separators.

The test setup consists of three main components:

- (1) Sample input for droplet and particle aerosols followed by a downstream homogenization section,
- (2) filter housing and filter cartridge,
- (3) sample withdrawal, measurement and evaluation.

#### II. 6. Operating Parameters and Measuring Techniques Employed

The plant parameters set for the experiments are as follows:

Gas temperature	: $30^{\circ}\text{C}$ , $50^{\circ}\text{C}$ at the filter
Relative humidity of the air:	98 - 100 % r.h. (with solid aerosols only 5 % r.h.)
Flow rate	: 75, 100, 125, 150 std. $\text{m}^3 \times \text{h}^{-1}$
Systems pressure	: 0.96 - 0.98 bar.

The droplet aerosols are generated by spraying demineralized water, in the plant upstream of the filter component and by addition of compressed air.

Upstream and downstream of the packed fiber mist eliminator a sample is taken isokinetically during operation, from which removal efficiencies of the filter components are determined as a function of

mass and diameter by means of a converted scattered light measuring system.

To verify the results, an alternative technique using a 5 % sodium nitrate solution is applied. The solution is also sprayed by the dual feed nozzle, but the aerosol samples extracted at the untreated and the clean gas sides are dried in a pipeline and moved onto nucle pore filters. The mass of  $\text{NaNO}_3$  precipitated on the filter platelets is determined by means of an electrode selective to sodium ions or by neutron activation analysis. Measuring time and the mass of  $\text{NaNO}_3$  furnish the  $\text{NaNO}_3$  bulk concentration. The droplet concentration can be calculated from the amount of solution fed and the spectrum of droplets.

The removal behavior of fiber mats with respect to solid aerosols is determined by spraying an aqueous solution of sodium fluorescein <sup>5)</sup>. Samples of the salt crystallized in the gas stream are put on nucle pore filters on the untreated and clean air sides. The filter platelets are evaluated by means of scanning electron microscopy and fluorescence spectroscopy.

## II. 7. Salt Loading Tests and Cleaning Behavior

The salt loading was provided by soluble sodium nitrate. The pre-ground salt (grain size: 2 - 5  $\mu\text{m}$ ) was sprayed into the off-gas stream by means of a salt gun, which made for almost uniform loading of the filtering area in the fiber packings. To verify the loading distribution on the filter packing, radioactively labeled salt droplet aerosols were sprayed and the radioactivity was subsequently measured at various points of the fiber packing. Short spraying of flushing water through the nozzles installed in the filter housing (flow 400  $\text{l} \times \text{h}^{-1}$ , pre-pressure 3.5 bar) will dissolve the salts from the filter mat.

## III. Results

### III. 1. Removal of Droplets and Particles by the Packed Fiber Mist Eliminator

The dual feed nozzle for droplet generation was operated in all these tests at 1  $\text{l} \text{ H}_2\text{O}/\text{h}$  and 1  $\text{l}$  of solution/h, respectively. In the measurements on the untreated and clean air sides of the packed fiber mist eliminator, droplet spectra were obtained in the ranges shown in Fig. 4. The removal efficiencies were determined at 30°C and 50°C and 100 % r.h. at different flows of 75 - 150  $\text{m}^3/\text{h}$ . No dependence on temperature was found. All bulk removal efficiencies exceeded 99.99 %. However, this value is only conditionally true, because large droplets are removed much more easily than small ones and a small number of big ones combine practically all the mass and are therefore bound to result in high removal efficiencies. For this reason, also the frequencies of identical drop sizes on the untreated and clean air sides are intercompared.

For small droplets (1 - 10  $\mu\text{m}$ ) the removal efficiency as a function of diameter was mostly between 99.8 and 99.99995 %, which corresponds to decontamination factors of 500 to  $2 \times 10^6$ .

No dependency on the volume flow of the retention factors for droplets was found. With increasing droplet diameter the removal efficiency rose steeply (Fig. 5).

Since evaporation will have to be taken into account especially in the small droplets encountered mainly on the clean air side, a 5 % sodium nitrate solution was sprayed. The mass of dried  $\text{NaNO}_3$  particles put onto nucle pore filters was determined by electrodes selective to sodium ions.

This resulted in a bulk removal efficiency of  $> 99.9\%$  for the same aerosol spectrum in a packed fiber mist eliminator (packing density  $300 \text{ kg/m}^3$ , fiber diameter  $10 - 20 \mu\text{m}$ ) with 50 mm thickness of the layers and a gas flow of  $75 \text{ std. m}^3 \times \text{h}^{-1}$ . Comparison of this result with the better result obtained from scattered light measurements indicates that some evaporation of small water droplets on the clean air side cannot be excluded. The packed fiber mist eliminator was exposed to sodium fluorescein particles of an average particle diameter of  $0.12 \mu\text{m}$  (Fig. 6). Tab. I lists the decontamination factors found as a function of the volume flow and the average velocity in the fiber packing, respectively. The decontamination factor is in excess of 1000. Moreover, it is seen from Fig. 7 that removal decreases with increasing velocity  $\bar{v}$  in the filter packing.

Tab. I. Dependence on volume flow and mean velocity  $\bar{v}$ , respectively, in the packing of the decontamination factors of packed fiber mist eliminators (thickness of layer: 50 mm, test aerosol: airborne sodium fluorescein particles)

$V / \text{m}_N^3 \times \text{h}^{-1}$	75	100	125	150
$\bar{v} \text{ cm} \times \text{s}^{-1}$	2.9	3.9	4.8	5.8
DF	$4.5 \times 10^3$	$1.9 \times 10^3$	$1.4 \times 10^3$	$1.2 \times 10^3$

### III. 2. Salt Loading, Cleaning and Drying

In addition to recycling of the radioactive substances into the process solutions, the amounts of flushing agent used to clean the fiber packing are of major importance because, should they be collected in temporary or final storage tanks, they would have to be considered as low or medium level wastes. Flushing serves to

- (1) reduce the radioactivity accumulating on the fiber packing,
- (2) dissolve the salts crystallized on the fiber packing and, in this way, nearly restore the original differential pressure over the fiber layer.

For test purposes, the fiber packing in the mist eliminator is loaded with aerosols through an annular cylindrical space from the

outside. The larger outer surface of the cylinder is useful as an impact area only if all of this area is used for loading with aerosols. Radioactively labeled aerosols make it possible, on the basis of the radioactivity distribution on the surface of the fiber packing, to obtain information about the distribution of the off-gas stream permeating it.

To determine the aerosol distribution on the fiber packing, a 5 % Mn-56 (NO<sub>3</sub>)<sub>2</sub> solution was sprayed into the gas stream and subsequently the radioactivity was measured at specific points on the filter housing by means of a dose rate meter. A relatively constant load on the whole circumference of the filter was measured at the respective levels.

For simulation of salt loading in PASSAT, 130 g of sodium<sup>-3</sup> nitrate ( $\dot{V} = 75 \text{ m}_N^3 \times \text{h}^{-1}$ ,  $t = 50^\circ\text{C}$ , r.h. = 100 %,  $\dot{m} = 4 \text{ g} \times \text{m}_N^{-3}$ ) were sprayed onto the fiber glass packing. This quantity roughly corresponds to a salt loading of the filter in a reprocessing plant under a volume flow of  $130 \text{ m}_N^3 \times \text{h}^{-1}$  and a loading with an assumed  $10 \text{ mg} \times \text{m}^{-3}$  of solid particles within four days and without interim self-cleaning as a result of high air humidity and impinging droplets. Short spraying of flushing water (approx. 30 l) onto the filter packing dissolved most of the salts and, after a drainage period of three hours, the original differential pressure was restored.

To quantify this recleaning and study the behavior of the droplet aerosols embedded in the fiber packing during flushing and their removal, a Ba-139 (NO<sub>3</sub>)<sub>2</sub> solution was sprayed into the gas stream. After loading different rinses were carried out and the behavior of the radioactivities discharged as a function of time was measured in the condensate pipes (Fig. 8). The radioactivity was measured by collimated scintillation detectors shielded with lead (NaI).

Fig. 9 shows 15 minutes flushing with a total of 75 l of H<sub>2</sub>O. This amount is sufficient to flush out of the fiber packing embedded radioactivity (within the limits of detection). Fig. 10 shows several recleaning steps with periodic flushing and drainage times, respectively. Comparison with once-through flushing indicates that, although the cleanup effect is the same, the water consumption is higher in periodic flushing (105 : 75 l). Periodic flushing however, offers the advantage that the pressure drop associated with recleaning is about 20 % lower. Moreover, this diagram shows that radioactivity is removed on the untreated gas side only at the beginning (for approx. 5 minutes) of the first flushing step. This is largely due to the radioactivity washed out adhering to the caisson of the filter cartridge. In subsequent flushing steps no further radioactivity was detected in the untreated gas condensate.

It will be necessary in the dissolver off-gas filter line to rinse the filter element of the mist separator through the fiber packing as soon as a higher differential pressure has been reached, or to replace it by a new element. If even flushing cannot reduce the differential pressure from 4000 Pa at 150 std. m<sup>3</sup>/h flow, the filter cartridge must be replaced remotely. In order to avoid contamination of the cell by spilling solution in this process, the fiber packing is dried in a preheated air stream before replacement.

(Tests of direct replacement after operation in a simulated off-gas stream indicated between two and four drops of liquid spilled when the filters were transported through the cell.)

The drying time of the filter element was determined by measuring the relative humidity of the off-gas on the untreated and the clean gas sides of the filter; if the humidity values agreed, the filter was considered to be dry. The values found are listed in Tab. II.

Tab. II. Drying times of the packed fiber mist eliminator at different test parameters ( $\phi_u$  = relative humidity upstream,  $\phi_d$  = relative humidity downstream)

Inlet temperature of gas used for drying	Relative humidity of gas used for drying	Gas flow	Drying time at $\phi_u = \phi_d$
70°C	5 %	150 std.m <sup>3</sup> /h	approx. 10 h
90°C	2 %	50 std.m <sup>3</sup> /h	approx. 6 h

After six hours of drying time at a temperature of the gas used for drying of 90°C the filter system can be bagged out into a 200 l waste drum for final storage.

#### IV. Behavior of Iodine and Iodine Removal in PASSAT

In the iodine removal technique <sup>6)</sup> applied in the Karlsruhe Reprocessing Plant in the Federal Republic of Germany as early as in 1975 a concept was implemented in which the iodine from the dissolver off-gases is precipitated almost quantitatively in fixed bed filters. The same technique is planned for use in future reprocessing plants. Iodine is removed in a reaction of the iodine compounds with silver nitrate impregnated iodine adsorption material, AC 6120 <sup>7)</sup>, in a two-stage iodine filter, whose first stage must be loaded as completely as possible, in order to save silver, while the second stage acts as a safety filter ensuring that the necessary decontamination factor is maintained.

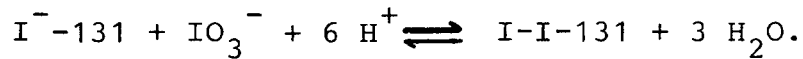
The iodine concentrations so far encountered in the dissolver off-gas of the Karlsruhe Reprocessing Plant amounted to 40 - 70 mg x m<sup>-3</sup>, while future reprocessing plants will probably show markedly higher iodine concentrations of 1 - 2 g x m<sup>-3</sup>, due to larger dissolver batches and minimization of the off-gas volume flow.

In order to verify the plate-out behavior of iodine in an off-gas system under simulated dissolver off-gas conditions and also test iodine removal in the iodine filters of PASSAT, tests were run by adding elemental iodine to the off-gas.

IV. 1. Preparation and Introduction of Elemental Tracer Iodine

The iodine generator consists of a reaction vessel holding a potassium iodate solution acidified with nitric acid, into which a metering pump feeds NaI with tracer I-131. The reaction occurs at 98°C, air being used for sparging and the elemental iodine being air lifted into the gas stream from the reaction vessel through a heated pipeline with sparging air from the PASSAT system (Fig. 11).

The preparation reaction follows this equation:



The reaction occurs quantitatively.

The concentration of iodine in the off-gas during this introduction was  $1.1 \text{ g} \times \text{m}^{-3}$ . 500 g of elemental I-127 with I-131 as a tracer were introduced per experiment. A total of 11.45 kg of iodine with 39 mCi I-131 were generated.

IV. 2. Behavior of Iodine and Precipitation on AC 6120

During transport of the iodine in that part of the system in which liquid gas components deposit as a result of condensate and drop separation, an absorption-desorption equilibrium is established by dissolution of a small fraction of the gasborne iodine in the liquid residues. Desorption of the iodine precipitated in the wet part of PASSAT occurs after the end of the test within approximately five hours. If the drop separator is fully loaded with the sprayed droplets ( $1 \text{ l} \times \text{h}^{-1}$ ), 0.035 % of the iodine (measured through the I-131 radioactivity) from the liquid precipitated on the fiber packing at an absorption capacity of approx. 8 l of water is moved through the condensate pipelines into the temporary storage vessels. This is 50 % of the calculated value.

Difficulties due to corrosion of some stainless steel grades occur in the  $\text{H}_2\text{O}/\text{NO}_2$  and the  $\text{HNO}_3$  and  $\text{HNO}_2$  systems with elemental iodine in the condensate carrying parts of the plant. Although pickling and passivation of the stainless steel was carried out as a pre-treatment, corrosion produced surface abrasion. Iodine was not detected in the corrosion products. This corrosion can be excluded by choosing special steel grades or titanium. After having passed through the packed fiber mist eliminator, the off-gas is heated to 90°C in PASSAT. After this heating no more corrosion was detected in downstream plant components.

On opening of the filter units (packed fiber mist eliminator, HEPA filter and iodine filter) no airborne contamination was found in the iodine monitor <sup>8)</sup> with a limit of detection of  $2 \times 10^{-9} \text{ Ci I-131/m}^3$ . The intake pipeline was located directly in the opened housing. Also wipe tests on the insides of the housing lids did not indicate any iodine deposits in the dry part of the system (r.h. < 10 %). When elemental tracer iodine was fed to the first iodine filter drum of the two-stage iodine filter, uniform loading of the first filter drum was found qualitatively. Fig. 12 shows the removal efficiency of the first iodine filter drum as a function of loading.

# 16th DOE NUCLEAR AIR CLEANING CONFERENCE

The iodine is removed in a direct reaction between silver nitrate and elemental tracer iodine and by isotope exchange with I-131 of any AgI-127 present.

The iodine quantity fed to PASSAT was 11.45 kg with a total amount of tracer of 39 mCi of I-131. One iodine filter drum contains 85.5 kg of AC 6120 with 12 wt.% of silver; this corresponds to a quantity of 10.3 kg of silver. A maximum of 12.1 kg of iodine can be adsorbed chemically. During normal operation of the iodine filters, off-gas samples are taken upstream in and downstream of the filter housings to determine the load factor and the removal efficiencies. The I-131 radioactivity serves to determine mass balances.

Taking into account the iodine quantities of approx. 30 g of I<sub>2</sub> in the intake air of the first iodine filter, which were extracted for sampling purposes, this results in a load factor of the iodine sorption material of 95 %, up to a penetration of approx. 16 g I<sub>2</sub> and a remaining removal efficiency of the first iodine filter of approx. 97 %. The penetration of 16 g of elemental iodine corresponds to the chemical adsorption of iodine found in the first few millimeters of the second iodine filter cartridge. Tab. III indicates the removal efficiencies detected as a function of the amounts of iodine fed to iodine filter I.

Tab. III. Removal efficiencies at the first iodine sorption filter as a function of loading and gas composition (Fig. 12)

Test number	Iodine (kg)	I-131 (mCi)	Removal efficiency (%)	Carrier gas
T 1	1.08	4	≥ 99.99	Luft
T 2	1.45	4	≥ 99.99	"
T 3	6.45	4	≥ 99.99	"
T 4	7.45	7	≥ 99.99	"
T 5	8.45	4	-	"
T 6	9.45	4	≥ 99.99	"
T 7	9.95	6	99.95	"
T 8	10.45	2	99.76	"
T 9	10.95	2	99.98	" + 6 % NO <sub>2</sub>
T10	11.45	2	96.97	" + 4 % NO <sub>2</sub>

When 500 g of iodine with radioactive tracers was introduced following the uptake of approx. 10.5 kg in the iodine filter, this was done in an air/NO<sub>2</sub> mixture at 6 vol.% NO<sub>2</sub>. This showed the regeneration process<sup>9)</sup>, which had been observed earlier, in slightly aged AC 6120 iodine sorption material caused by an increase in capacity as a result of the conversion of reduced silver into reactive silver nitrate.

### V. Conclusion

Design, testing and optimization of a mist eliminator designed as a remotely handled packed fiber filter fitting into a waste drum constitutes a major step forward in implementing the head end off-gas cleaning concept. The objective of developing and testing a functioning prefilter for droplet and solid aerosols with flushing capability to protect the downstream HEPA filter has been attained and even exceeded in a few requirements, such as removal of solid aerosols. The retention factors attained of > 1000 for airborne droplets and solid particles, the slight differential pressures (10 - 15 mbar)<sub>3</sub> encountered in this operation (at a maximum volume flow of 150 m<sub>N</sub><sup>3</sup> x h<sup>-1</sup>), the good flushing capability and the short drying times allow these filters to be installed in a dissolver off-gas line.

With 95 % of the silver content of the first iodine filter used to retain elemental iodine, a residual removal efficiency of 97 % was found. Contamination of cell air by I-131 during replacement of an iodine filter cartridge and of upstream filter elements, such as packed fiber mist eliminators and HEPA filters, was not detected. The iodine concentration set in this case was 1.1 g x m<sub>N</sub><sup>-3</sup> (loading of the cartridge: 39 mCi of I-131/cartridge).

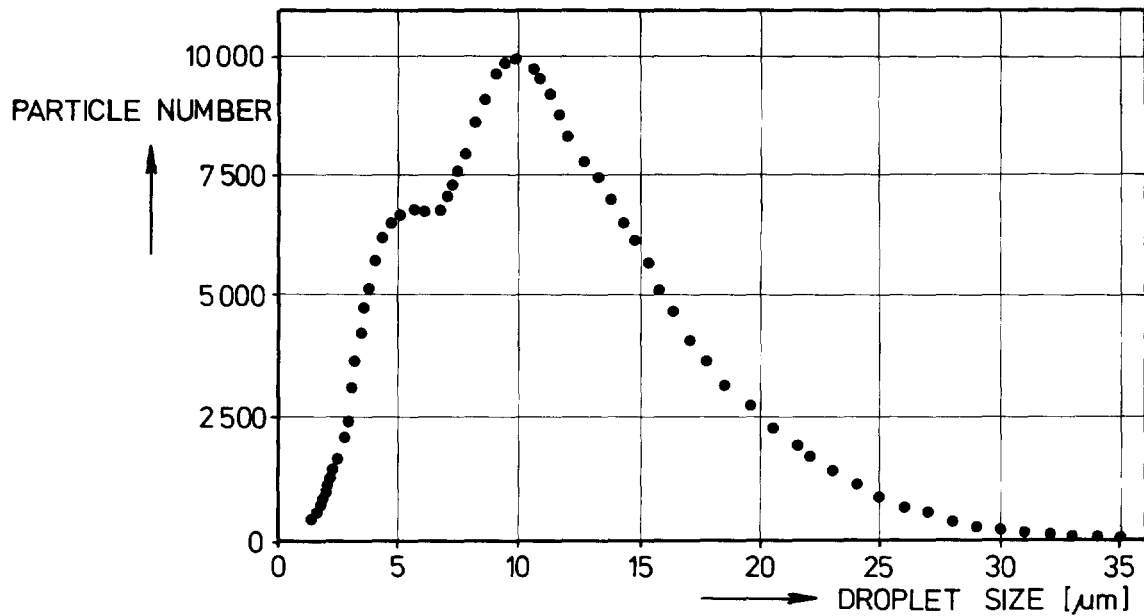
### VI. References

- 1) J. Furrer, J.G. Wilhelm, K. Jannakos: "Aerosol and Iodine Removal System for the Dissolver Off-Gas in a Large Fuel Reprocessing Plant". CONF-780 819, p. 494 (1978).
- 2) K. Jannakos, W. Lange, G. Potgeter, J. Furrer, J.G. Wilhelm: "Selected Solutions and Design Features from the Design of Remotely Handled Filters and the Technology of Remote Filter Handling". 16th DOE Air Cleaning Conference, San Diego (1980)
- 3) J.A. Brink: "Removal of Phosphoric Acid Mists", Chap. 5 in Gas Purification Process, George Newnes, Ltd. London 1964, Part B.
- 4) H. Umhauer: "Ermittlung von Partikelgrößenverteilungen in Aerosolströmen hoher Konzentrationen mit Hilfe einer Streulichtmeßeinrichtung", Chem.Ing.Techn. 47(1975),7.
- 5) J. Dupoux, A. Briand: "Air Filter Efficiency as a Function of Particle Size and Velocity". Water, Air and Soil Pollution, 3, p. 537 (1974).



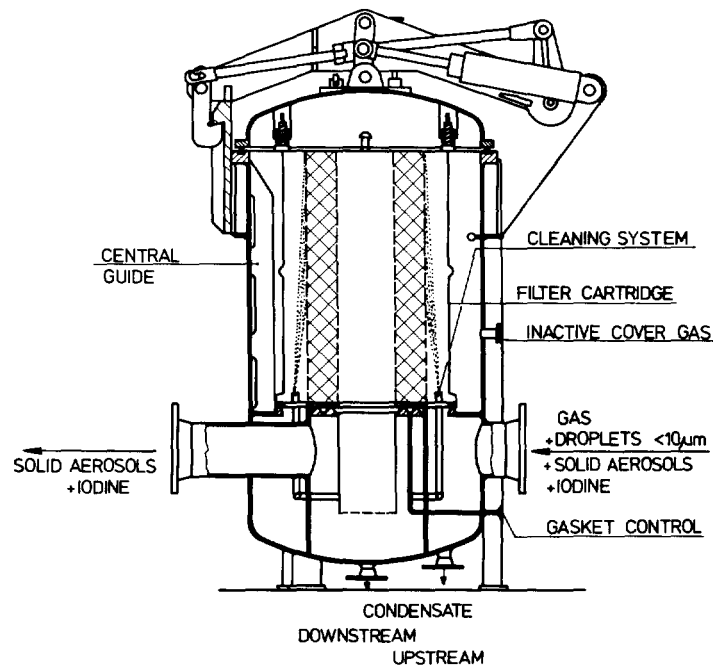
# 16th DOE NUCLEAR AIR CLEANING CONFERENCE

- 6) J.G. Wilhelm, J. Furrer, E. Schultes: "Head-End Iodine Removal from a Reprocessing Plant with a Solid Sorbent". CONF-760 822, p. 447 (1976).
- 7) J.G. Wilhelm, H. Schüttelkopf: "An Inorganic Adsorber Material for Off-Gas Cleaning in Fuel Reprocessing Plants". CONF-720 823, p. 540 (1972).
- 8) J.G. Wilhelm, H. Mahnau: "Continuous Monitoring of Radioactive Iodine Emissions". CONF-740 807, p. 863 (1974).
- 9) J. Furrer, J.G. Wilhelm: "Iodine Trapping from the Exhaust Air of Reprocessing Plants". Seminar on Iodine Filter Testing. Doc. V/559/74, p. 185.



KfK LAF/80

FIG.1 Droplet spectrum of the jet (SCHLICK 970/0)



KfK LAF/80

FIG.2 PASSAT packed fiber mist eliminator (PFME) for droplet removal  $< 10\mu\text{m}$

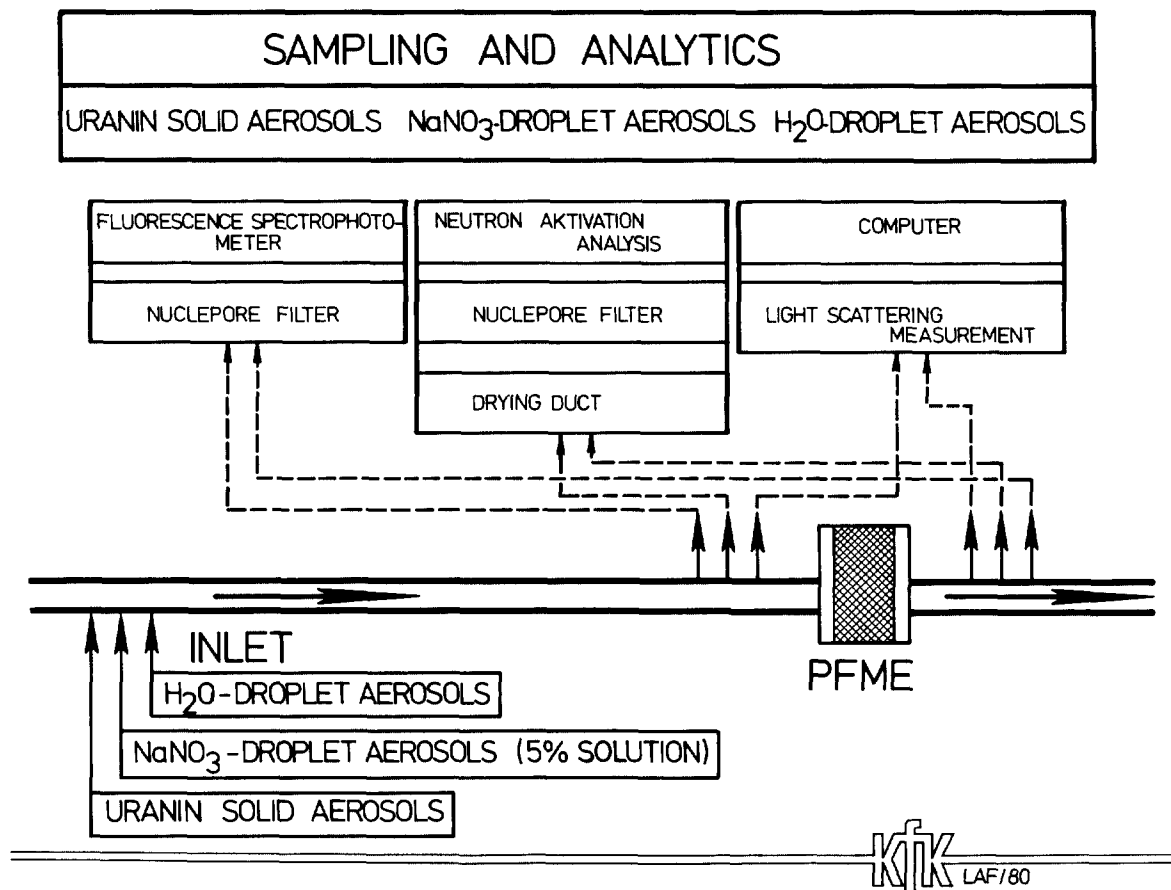


FIG.3 Test methods for the packed fiber mist eliminator (PFME)

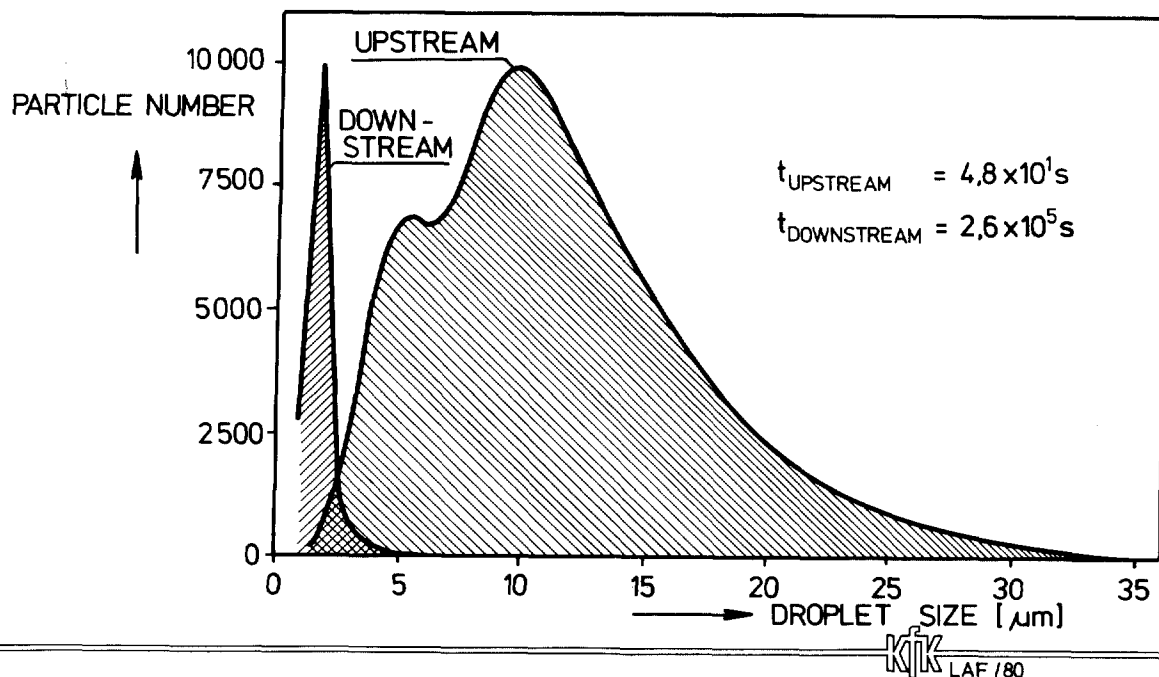
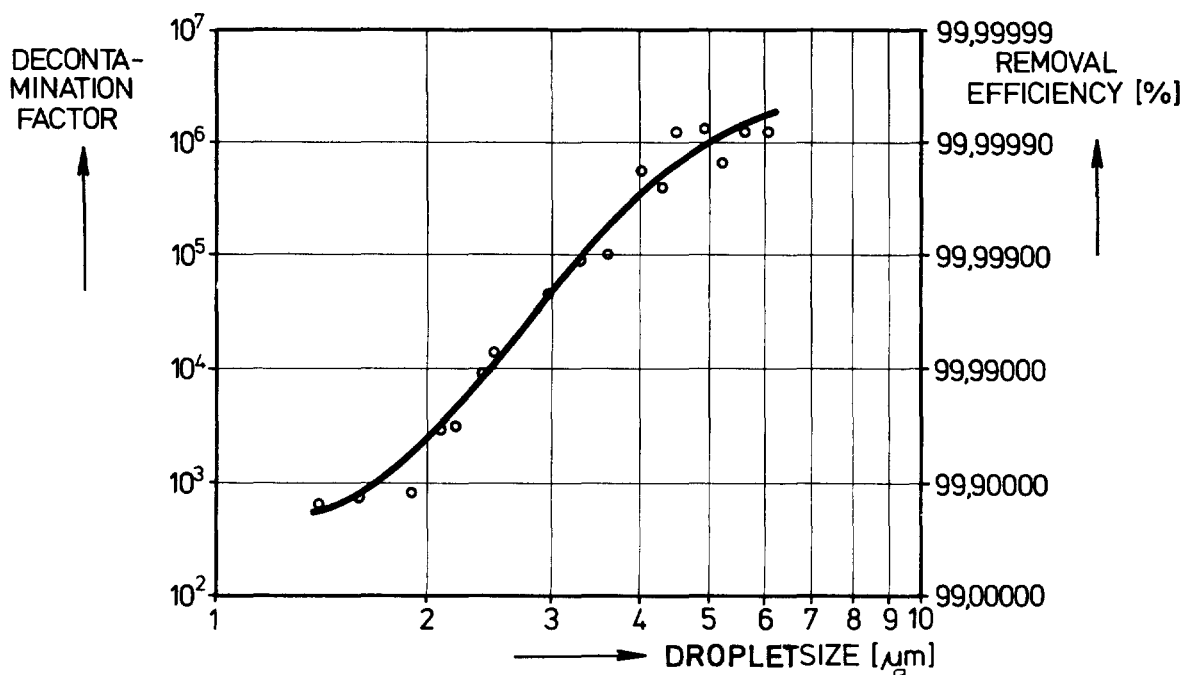
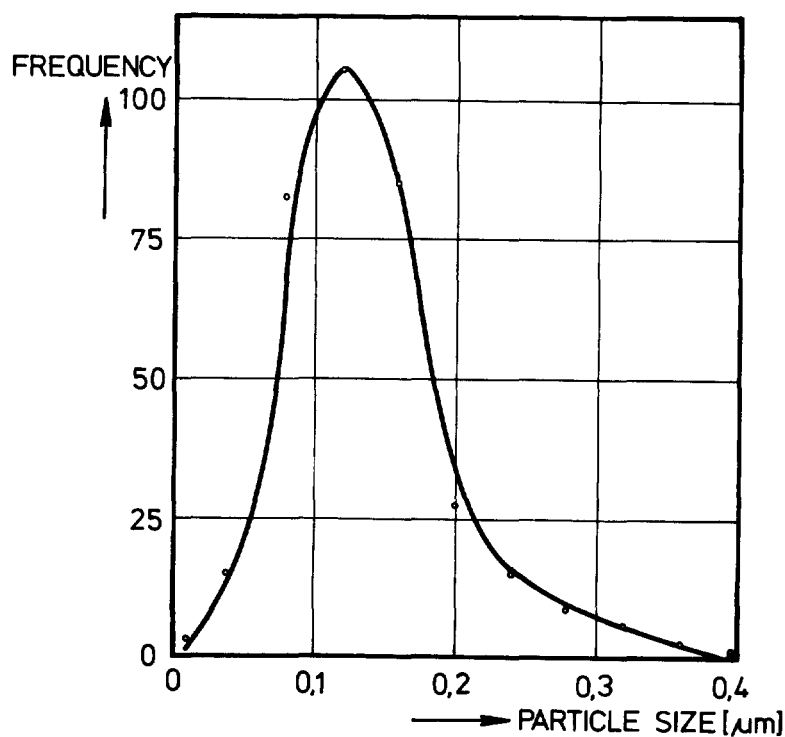


FIG.4 Droplet size distribution for the calculation of the removal efficiency (PFME/5cm)



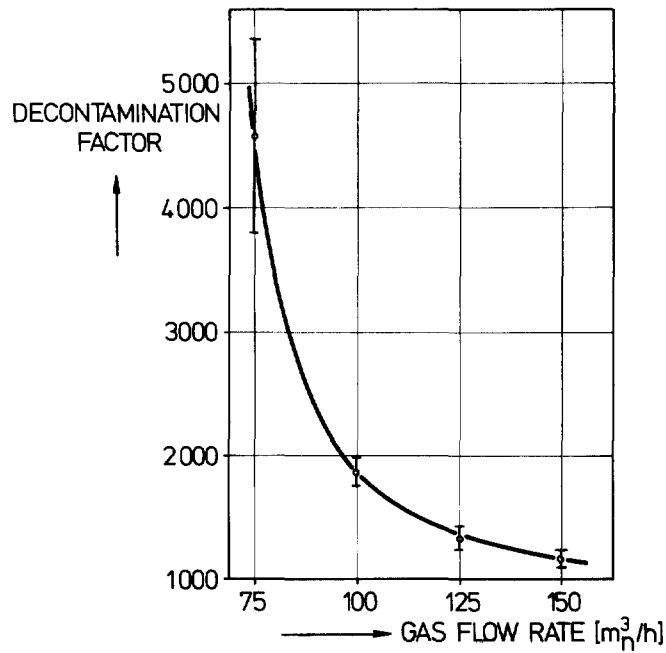
KfK LAF/80

FIG.5 Decontamination factor as a function of droplet size (PFME / 5cm)



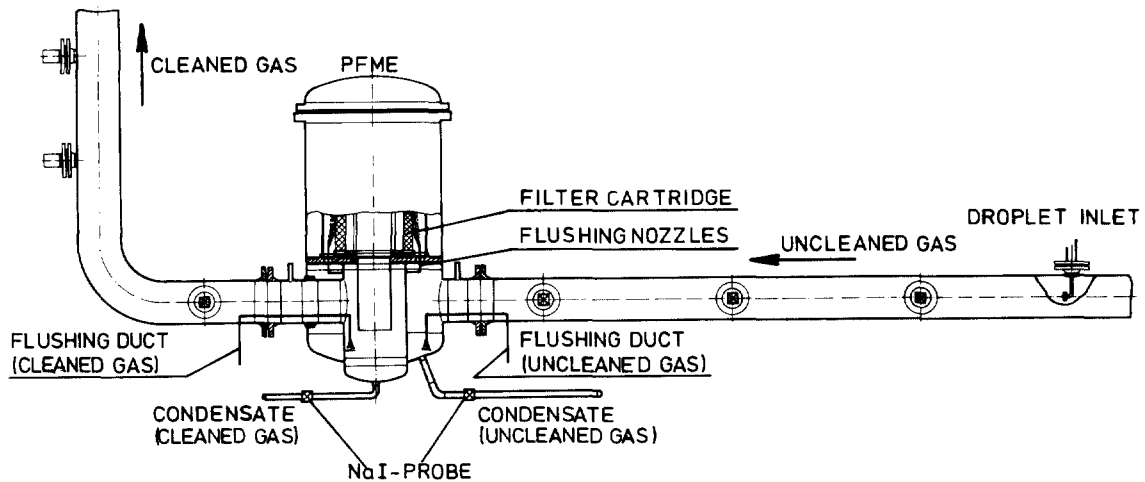
KfK LAF/80

FIG.6 Uranin particle size distribution (SEM - interpretation)



KfK LAF/80

FIG.7 Decontamination factor as a function of flowrate at PFME (5cm)



KfK LAF/80

FIG.8 : Test procedure for the investigation of loading and cleaning

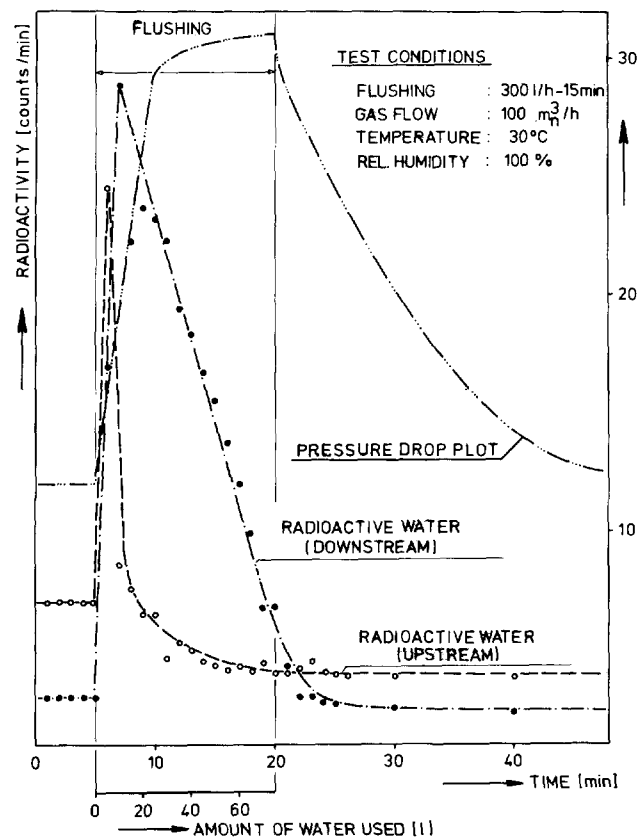


FIG. 9

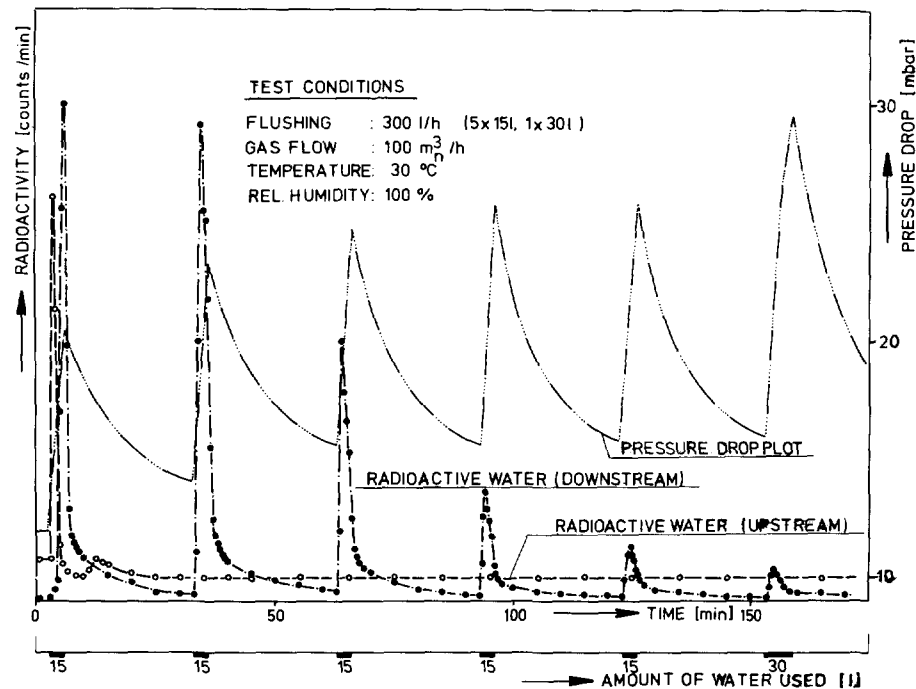
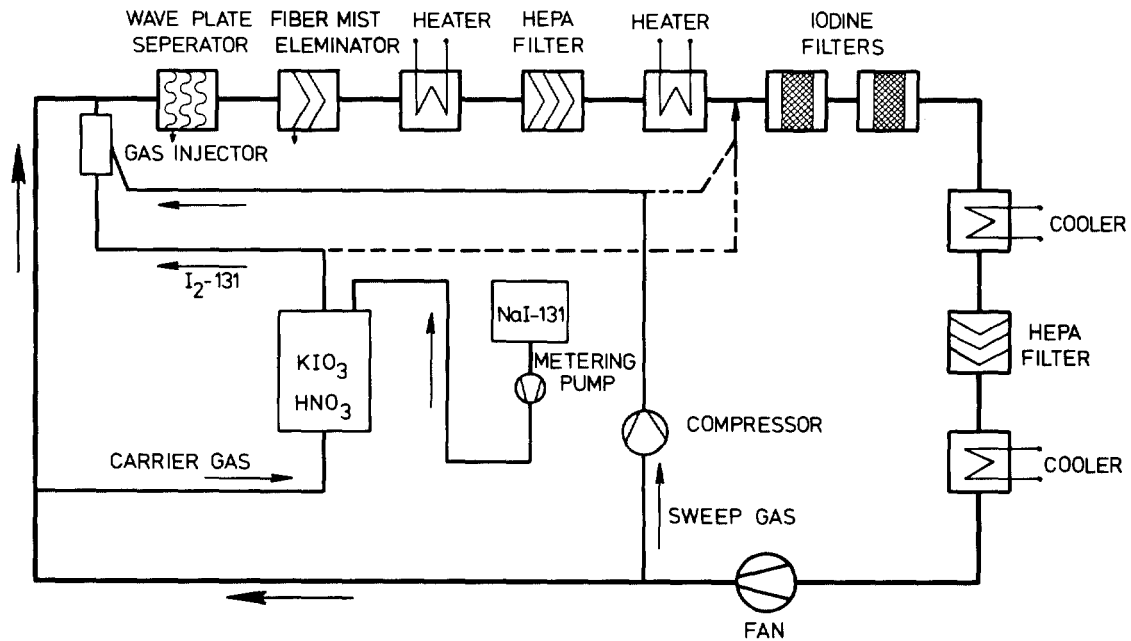


FIG. 10

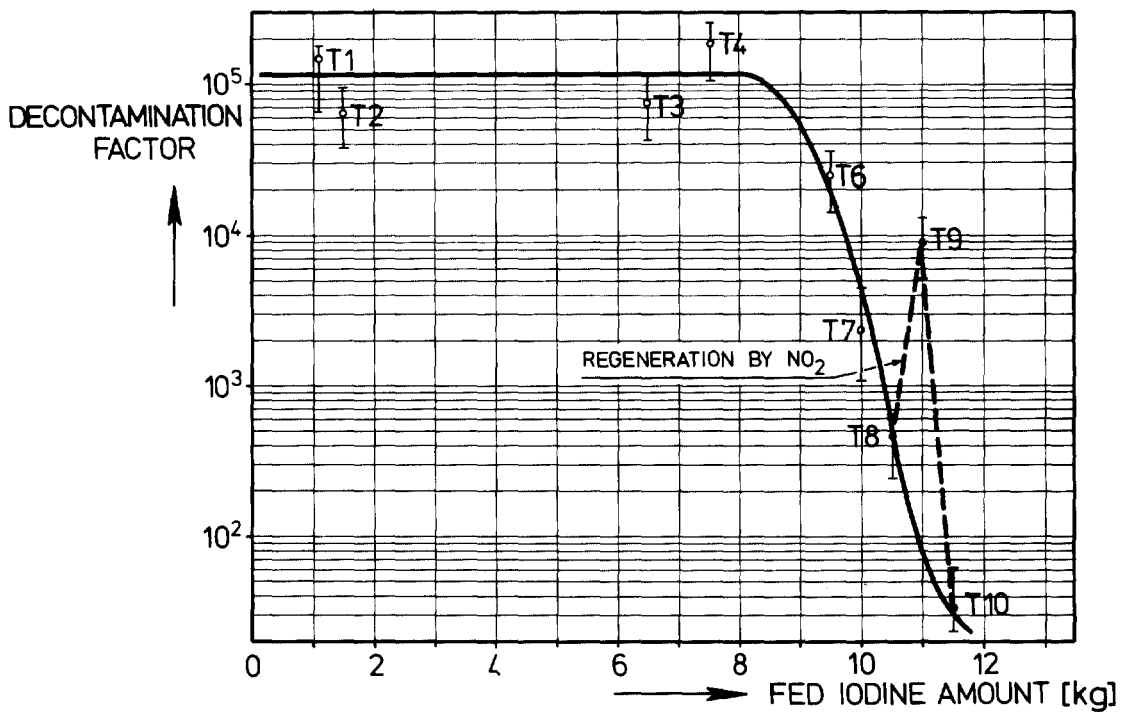
KIK LAF/80

Cleaning characteristics of the PFME loaded with Ba-139(NO<sub>3</sub>)<sub>2</sub> aerosols.



KfK LAF/80

FIG.11 Block diagram of iodine generation and supply



KfK LAF/80

FIG.12 Decontamination factor as a function of fed elementary iodine amount at the first iodine filter cartridge

## DISCUSSION

LILLYMAN: Were you using all radioactive iodine in your tests?

FURRER: No, we traced it with 39 millicuries of iodine 131. We injected all the iodine into the test loop. We always used a simulated dissolver offgas; not a real dissolver offgas. We had tested this filter system in a test rig in the WAK, and we obtained the same results. We found the same removal efficiencies in the WAK because we had a removal efficiency for iodine-129 of about 99.9 percent for a filter loading of 92 percent with iodine. We also want to have a pre-cleaning system so that we have longer stay-times for HEPA filters. We expect the droplets and the particles to deposit on the first filter.

LILLYMAN: I would hope your dissolver design itself and its condenser would eliminate any major carryover of droplets into the system, anyway.

FURRER: Because of the absorption columns?

LILLYMAN: Well, not really. It is a question of how much boiling you have on your surface and all sorts of other things like that which could affect it. I understand that if you have a massive air flow through your dissolver, you could then get some entrainment, but one of the points about a good dissolver design is to make sure you do not get an inert gas flow through it which will act as a carrier.

WILHELM: The first iodine filters were tested in WAK. They were loaded with the iodine from 20 tons of uranium. The WAK is a plant which is designed for a throughput of 200 kg of heavy metal per day. It was not run with 200 kg per day; it was mostly operated with 100 kg per day. But anyway, the iodine filter was used for a long time period till it was loaded to 92 percent of its total capacity. That is not so small a scale. We are testing the filter with iodine released from fuel this way because we do not have a large reprocessing plant. Additionally, we simulate the offgas in PASSAT with respect to the high concentration of iodine we can expect in a large reprocessing plant. This changes the conditions very much compared to the low concentration we have today in the WAK.

HILLIARD: Can you please describe the mist eliminator, as to the material, the flow rate, and the pressure drop?

FURRER: Normally, we have a layer thickness of 50 mm, and we have glass fibers of about 10 to 20 micrometers pressed packs. We have about 300 kilograms per cubic meter of glass fibers pressed in the layer. As regards flow rate, we have a maximum of linear air velocity of 2.6 to 5.6 cm per second. The pressure drop was about 15 m bars.



CONDITIONING OF REPROCESSING DISSOLVER OFFGAS  
PRIOR TO KR-RETENTION BY CRYOGENIC DISTILLATION

H.D. Ringel, H. Barnert-Wiemer, H. Hackfort,  
M. Heidendael

Kernforschungsanlage Jülich GmbH  
Institut für Chemische Technologie  
5170 Jülich, Germany

Abstract

The separation of Kr-85 from the dissolver off-gas by means of low temperature rectification requires a comprehensive and thorough pre-cleaning of the off-gas. In this section of the off-gas cleaning, work has been carried out which comprises the selection of a catalyst for the reduction of  $O_2$  and  $NO_x$  as well as the separating out of the xenon prior to the low temperature rectification. A ruthenium catalyst showed the best results:  $O_2$  and  $NO_x$  were removed so that the residual amounts were  $\leq 1$  ppm while at the same time the formation of  $NH_3$  was avoided. The xenon can be adequately removed in freezing traps in quantitative terms but the xenon, that is removed, always contains some 0.2 vol % Kr and/or  $N_2$ . In further experiments, the solubility of  $O_3$  in liquid Xe were measured; at 165 K and 1.16 bar overall pressure when a gas phase containing 4.4 Mol %  $O_3$  is in equilibrium with liquid Xe, 0.37 Mol %  $O_3$  dissolved in the liquid Xe.

I. Introduction

The radioactive inert gas krypton can be separated from the dissolver off-gas of a reprocessing plant by means of low temperature rectification (1). Hereby all the off-gas is liquefied and, as a rule, rectified in two rectification columns arranged in series. In the first of these the two inert gases krypton and xenon are separated from the carrier gas; the separation of the Kr from the Xe is then carried out in the second column. This technique guarantees a high decontamination factor for the separation of the Kr-85 from the stream of off-gas and has been tested on a large scale in the separation of liquid air. Figure 1 shows the basic flow path for the separation of the inert gases in accordance with this principle. The process requires however a very specific pre-treatment of the complete stream of off-gas and relatively large quantities of a liquefied radioactive gas have to be handled.

The pretreatment has to be carried out extremely carefully for two reasons:

- all trace impurities such as  $H_2O$ ,  $CO_2$ ,  $NO_2$  and  $NH_3$ , which have a significantly higher boiling point than  $N_2$ , can freeze out in the plant and in this way block parts of it. A further danger of blockages arises from the Xe itself since this inert gas has a vapour pressure of only  $5 \times 10^{-3}$  torr at 80 K but can occur in concentrations of up to 0.5 vol. %.
- the radiation of the Kr-85 can lead to dangerous radiolysis products, e.g. the transformation of  $O_2$  to  $O_3$ .

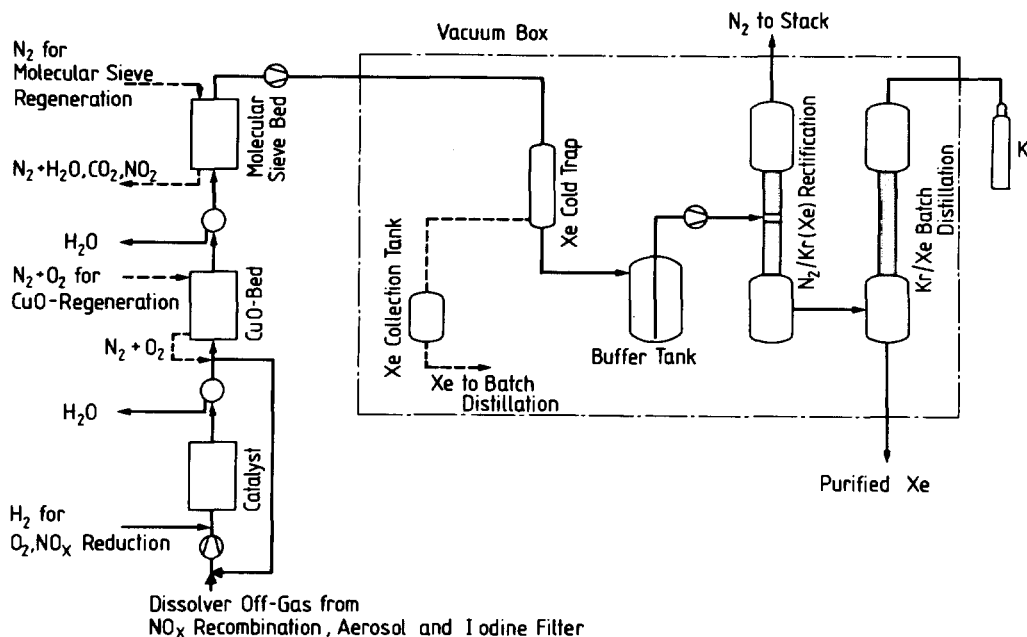


Figure 1: Simplified Flow Sheet for Off-Gas Conditioning and Cryogenic Kr-Retention

The work presented here reports on the results of experiments specially concerned with these problems. The experiments examined:

- the catalytic reduction of  $O_2$  and  $NO_x$  with  $H_2$ ,
- the pre-separation of Xe and
- the solubility of  $O_3$  in liquid xenon.

## II. $O_2$ - and $NO_x$ -Removal by Reaction with $H_2$

Since  $NO_x$  freezes out in the cryogenic facility and oxygen forms ozone in the presence of radiation both are removed before the cryogenic unit in a  $O_2/NO_x$  removal system by reaction with hydrogen in the presence of a catalyst, whereby oxygen and nitrogen oxides are converted to elemental nitrogen, water and traces of ammonia. While direct conversion results in elevated temperatures of about  $1100^\circ C$ , the same reaction takes place on precious metal catalysts in a temperature range of  $300 - 500^\circ C$ . To operate outside the explosion limits, the relatively high oxygen content is lowered by feeding the off-gas into a recycle of oxygen-free gas. Moreover, this dilution is necessary to avoid overheating of the catalyst, because each vol. %  $O_2$  induces a rise of temperature in the catalyst bed of about  $150^\circ C$ .

A flow sheet for the  $O_2/NO_x$  removal system is shown in figure 2: The dissolver off-gas ( $5\text{ m}^3/\text{h}$ ) is diluted by nitrogen which is recycled by a blower (K1) with a throughput of  $50\text{ m}^3/\text{h}$ . In this way, the oxygen content of the gas stream is decreased from 20 vol. % to about 2 vol. %  $O_2$  and the  $NO_x$  concentration from 0.5 vol. %  $NO_x$  to about 0.05 vol. %. The  $O_2$  concentration measured by a paramagnetic  $O_2$  analyser, and the flow rate given by a flow-meter, control the hydrogen feed. Behind the catalyst bed (K.B.) the gas stream, primarily  $N_2$ , passes through a water-cooled condenser (WT1) to remove the formed water. The surplus hydrogen ( $\sim 1000\text{ ppm}$ )

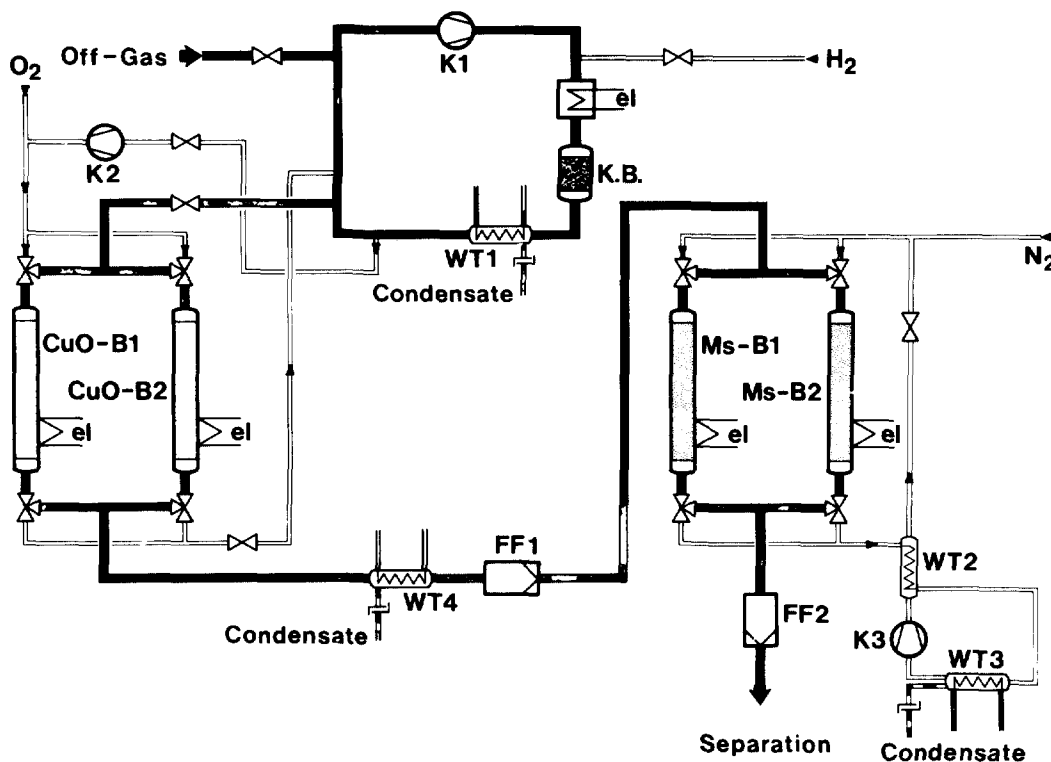


Figure 2: Flow sheet of the  $O_2/NO_x$  Removal System for Preconditioning of the Off-Gas Prior Low Temperature Rectification

is subsequently removed by reaction with activated copper oxide (CuO-B1 or CuO-B2) and the water from that reaction is removed in a water-cooled heat exchanger (WT4). Before leaving the  $O_2/NO_x$  removal system the gas is dried by molecular sieves (MS-B1 or MS-B2) which also adsorb traces of impurities like  $CO_2$ ,  $NO_2$  and  $NH_3$ .

During preliminary experiments with a platinum catalyst it was found that nearly all of the  $NO_x$  reacted with the hydrogen to form ammonia. It was then tested whether this ammonia would decompose in the CuO beds following the reduction catalyst. But only 10 % of the  $NH_3$  were decomposed in the CuO beds. Therefore laboratory tests were made to find a catalyst suitable for  $O_2$  and  $NO_x$  removal to below 1 ppm and at the same time suppression of the reaction leading to the formation of ammonia (2).

Table 1 summarizes the specific data of the three catalysts selected for  $O_2/NO_x$  removal. The main differences between the catalysts consist in the active components: the Kali-Chemie catalyst contains several noble metals; the Girdler catalyst has been specified as a 0.1 % Pt + 3 % Ni catalyst; the Doduco catalyst is a typical ruthenium catalyst.

Figure 3 shows the flow sheet of the catalyst test assembly in the laboratory. The test reactor was a tube with an inner diameter of 34 mm, the bed height was 100 mm for all catalysts. Three thermocouples measured the temperature in the bed. Test temperatures were 300°, 400°, and 500°C. The space velocity was varied according to company data between 5 and 30  $m^3/l$  h. The volumetric gas

Manufacturer	Name	Minimum Temperature °C	Maximum Temperature °C	Active Components	Shape of Catalyst	Spec. Surface m <sup>2</sup> /g	Re-commended Bed-Height	Spec. Density kg/l
Kali-Chemie, Hannover	KCO-S9	300	700	Pt Metals	Spheres, 2 – 4 mm Diameter	95	100 mm	0.8
Girdler Süd-chemie, München	G-43	200	900	0,1 % Pt 3 % Ni	Cylinders, 4 x 4 mm	210	3 : 1 Height: Diameter	0.82
Doduco, Sinsheim	Ru-Katalysator 0.3 Nr. 5110-28097	200	500	Ru	Spheres, 2 – 4 mm Diameter	10	> 20 mm	0.78

Table 1: Tested Reduction Catalysts

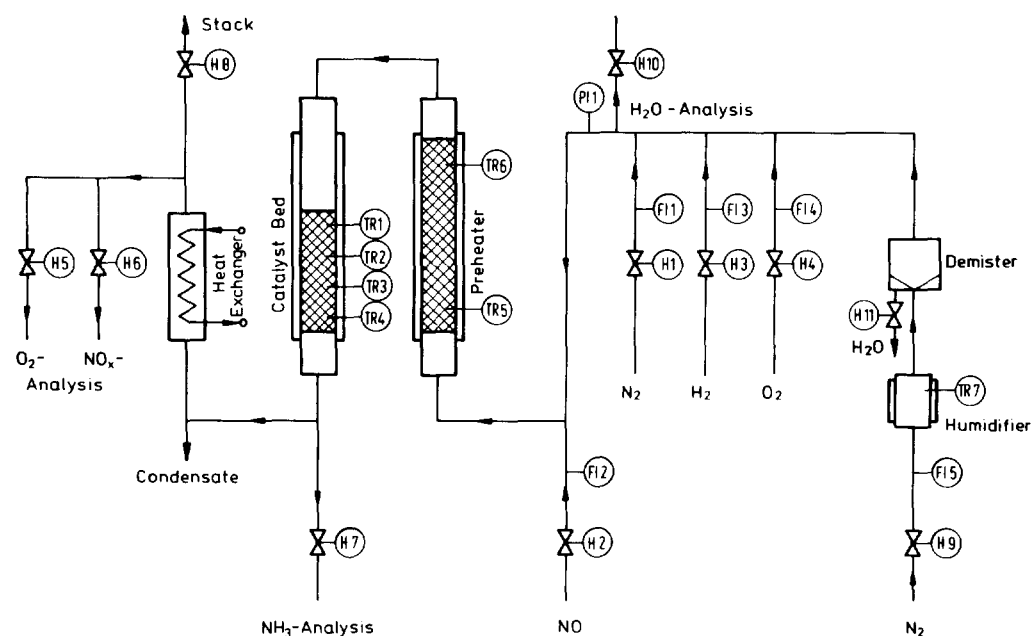


Figure 3: Flow sheet of Catalyst Test Assembly

composition was in all runs 1 %  $O_2$ , 0.5 %  $NO$ , 2.75 %  $H_2$ , and the remainder  $N_2$ . In one series 1 %  $H_2O$  was added.

For  $O_2$  analysis an electrochemical trace analyser (Elcoflux of Hartmann & Braun, Frankfurt) and for  $NO_x$  analysis a chemiluminescence analyser (Model 952 of Beckmann, Munich) were used.  $NH_3$  was absorbed in a weak acid and titrated.

The experiments proved that all three catalysts removed  $O_2$  and  $NO_x$  below a residual concentration of  $\leq 1$  ppm. The main difference

between the catalysts was found in the formation of  $\text{NH}_3$ . Figure 4 shows the  $\text{NH}_3$  formation for dry gas mixtures. For all catalysts  $\text{NH}_3$  formation decreased with increasing space velocity. For the Kali-Chemie catalyst  $\text{NH}_3$ -formation increased with increasing temperature, for the Girdler catalyst it decreased with increasing temperature.

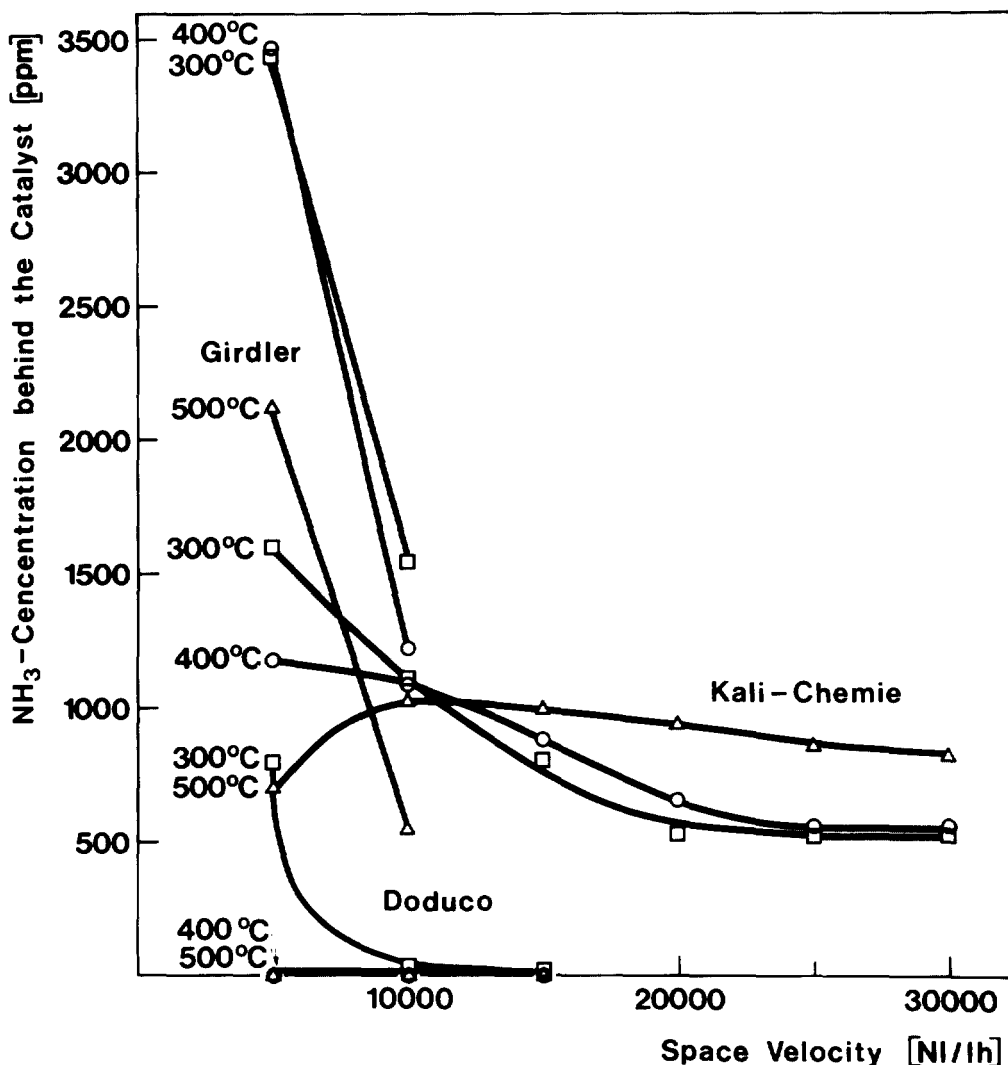
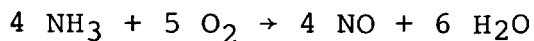


Figure 4:  $\text{NH}_3$ -Formation at Different Catalyst Temperatures and Space Velocities for Dry Gases  
Inlet Gas Composition: 1 %  $\text{O}_2$ , 0.5 %  $\text{NO}$ , 2.75 %  $\text{H}_2$ , Remainder  $\text{N}_2$

For the Ru catalyst of Doduco no  $\text{NH}_3$  was found at temperatures  $\geq 400^\circ\text{C}$ . This is possibly due to the fact that at temperatures over  $300^\circ\text{C}$   $\text{NH}_3$  reacts with  $\text{O}_2$ :



and on a ruthenium catalyst  $\text{NH}_3$  reacts with  $\text{NO}$  to form  $\text{H}_2$  and  $\text{H}_2\text{O}$ :

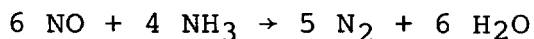


Figure 5 shows the result of alike experiments but with humidified gas mixtures. No appreciable difference was found for the behaviour of dry and humid gas mixtures. For humid gas mixtures the  $\text{NH}_3$  formation is lower for the Girdler and Doduco catalysts, but not for the Kali-Chemie catalyst.

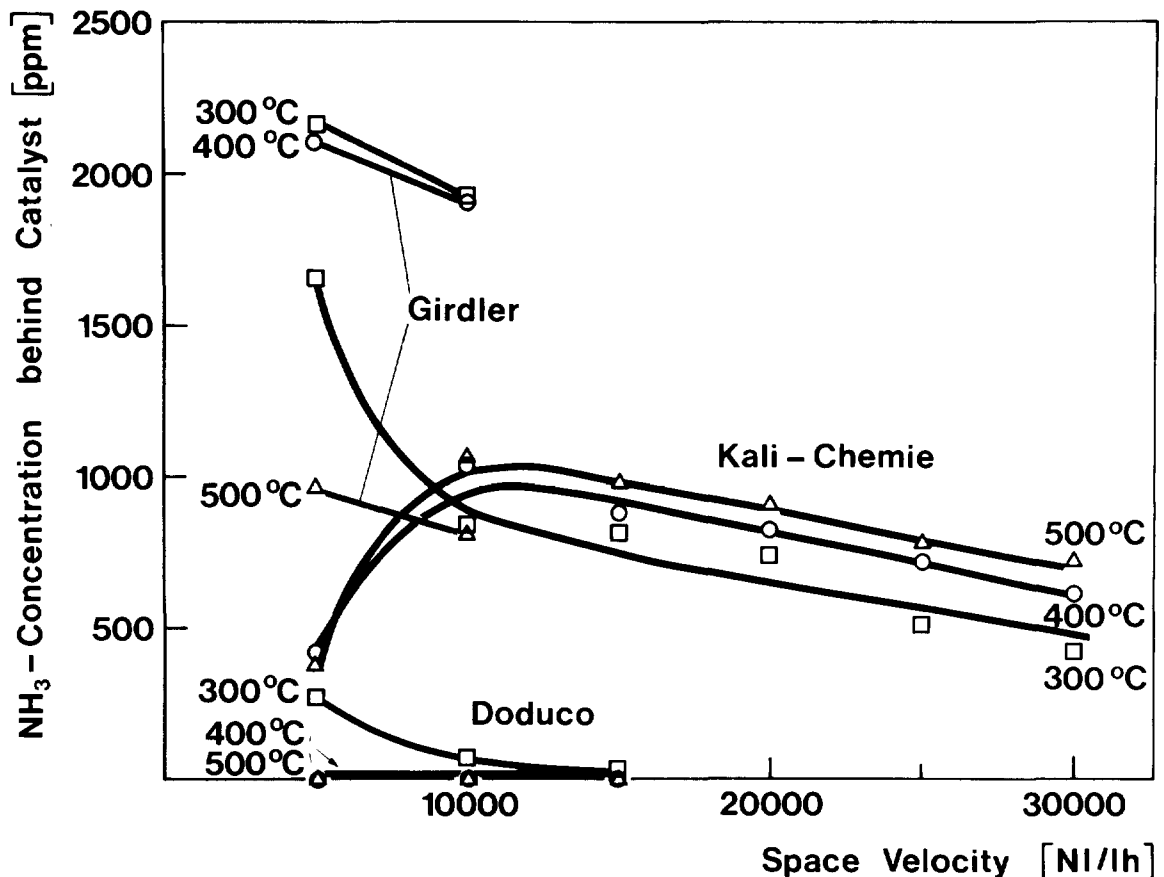


Figure 5:  $\text{NH}_3$ -Formation at Different Catalyst Temperatures and Space Velocities for Humid Gases  
Inlet Gas Composition: 1 %  $\text{O}_2$ , 0.5 %  $\text{NO}$ , 1 %  $\text{H}_2\text{O}$ , 2,75 %  $\text{H}_2$ , Remainder  $\text{N}_2$

Summing up the tests it can be said that of the tested catalysts only the Ru catalyst of Doduco is recommendable for the reduction of  $\text{NO}_x$  and  $\text{O}_2$  with  $\text{H}_2$ . Only this catalyst reliably suppressed the formation of  $\text{NH}_3$  for bed temperatures above  $400^\circ\text{C}$  at all space velocities.

### III. Pre-separation of Xenon

In the separation of liquid air by low temperature rectification no de-sublimation of xenon occurs at the entry to the column with the low concentrations of xenon (0.08 ppm by volume); in addition the small quantities of xenon in the column are dissolved by the liquid oxygen. In the purification of off-gas, on the other hand, xenon concentrations of over 5000 ppm by volume have to be reckoned with and a dissolving of the xenon in the liquid oxygen is not given. 5000 ppm by volume at a total pressure of 760 torr corresponds to a

xenon partial pressure of 3.8 torr; the sublimation pressure of xenon at 80 K is however only  $5.10^{-3}$  torr. These values together with the sublimation pressure curves of other gases, which are of significance in the case under discussion, are entered in Figure 6. The danger of

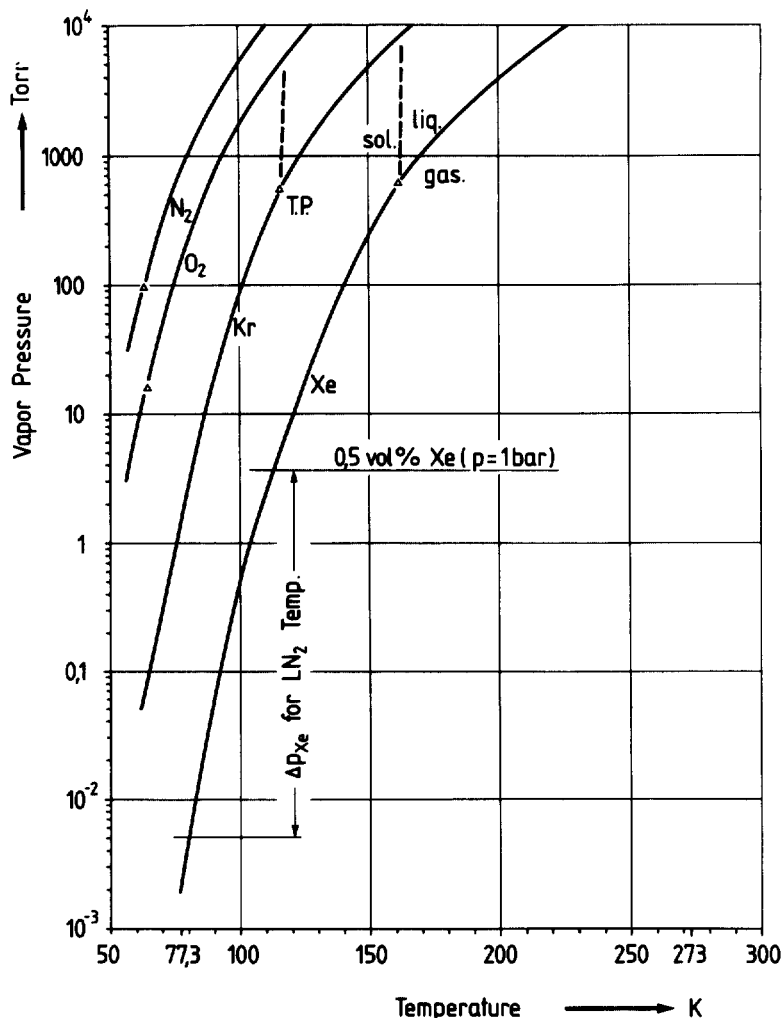


Figure 6: Vapor Pressure for  $N_2$ ,  $O_2$ , Kr and Xe

operational disturbances as a result of the plant getting blocked can be avoided by increasing the operating pressure and hence the rectification temperature as well as by other measures (3). With the objective of completely excluding the possibility of operational disturbances, the main part of the xenon is separated out prior to the liquefaction of the gas in the procedure being considered here (4). Here, the possibility of separating out the Xe at the temperature of  $LN_2$  in special freezing-out traps was investigated.

Figure 7 shows the construction of such a freezing-out trap. The trap consists in principle of two stainless steel tubes of different diameters which are put together in such a way that an annulus is formed. The inner tube is cooled from beneath with  $LN_2$

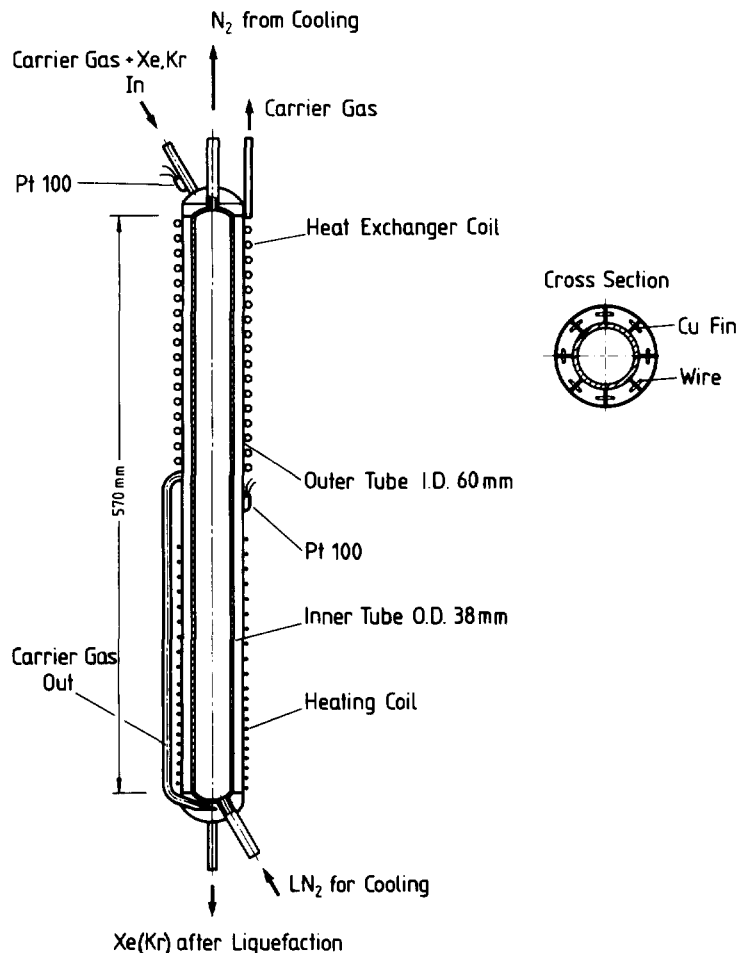


Figure 7: Cold Trap for Xe-Deposition

while in the annular space between the two tubes the Xe (or Kr respectively) is separated from the carrier gas. Hereby, the gas mixture enters the annular space from above, flows downwards while being cooled, with the inert gases being separated out and leaves the separator at the bottom of the trap. The upper part of the trap is constructed as a heat exchanger: the carrier gas, as it flows away, is led around the trap in a helical Cu tube thereby cooling down the gas mixture as it enters.

A number of longitudinal copper ribs are soldered along the annulus. These serve to significantly increase the area available for the separating out of the inert gases as well as the transportation of heat between the outer and inner tubes. Wire spirals are tensioned between the ribs in order to break up the laminar flow in the annulus. The temperature was measured at the position of entry of the gas and in the middle of the trap, in each case with a Pt 100. The lower part of the trap carries a resistance heating device in order to melt the inert gas which has frozen out. Four traps of the same construction with further auxiliary devices are mounted together in a container having a vacuum insulating system. Experiments were carried out with two different carrier gases: N<sub>2</sub> and He.



Separating out of Xe from N<sub>2</sub> as carrier gas

As a rule, the dissolver is rinsed with air, i.e. after the pre-cleaning and the separating off of the oxygen the N<sub>2</sub> carrier gas contains for example 0.5 vol. % Xe and 0.05 vol. % Kr. Hereby trace impurities in ppm range are disregarded. The experiments were carried out with a specially made-up gas mixture of this composition whereby it was attempted to remove the Xe as completely and as selectively as possible.

The experiments were generally carried out under the following operational conditions:

Overall pressure in the trap: 0.8 bar = 600 torr. At this pressure a liquefying of the N<sub>2</sub> carrier gas is avoided and thus an additional dissolving of the Xe in the liquid nitrogen prevented. Total gas throughput: 1 Nm<sup>3</sup>/h. Temperature at outer trap mantle: 89 - 90 K. This temperature is set when the cooling with LN<sub>2</sub> is at maximum. It is estimated that the inner surfaces of the trap must therefore have a temperature of 78 - 80 K at their coldest points. The consumption of LN<sub>2</sub> amounted to about 0.5 l/h.

Fundamentally the experiments confirmed that, in the case of the trap construction described, one gas component can be adequately separated out of the carrier gas but that at the same at least small quantities of the other gas component always separate out as well, even when the partial pressure of the latter lies below its sublimation pressure. When the cooling of the trap was at a maximum (temperature measured on the trap at the outer mantle = 89 K), the Xenon, which was separated out, contained some 0.2 vol. % Kr and 0.2 vol. % N<sub>2</sub>. Hereby the yield of Xe attained a value of 98 %, i.e. 2 % of the Xe was not separated out and left the trap with the carrier gas. The partial pressure of the Xe in the carrier gas sinks from 3 torr to a residual pressure of some 0.06 torr; this is still 10 times as high as the sublimation pressure of Xe at 80 K.

The above results are average values obtained during continuous operation which was free of disturbances. However blockages of the trap occurred frequently. In these cases, the pressure in the trap rose rapidly from 0.8 bar to, for example, 0.9 bar while, at the same time, the gas throughput fell. Once a maximum pressure was reached, the pressure then fell equally rapidly to the original value again. Such pressure peaks occurred to an extent periodically at intervals of 10 - 20 minutes. This can probably be attributed to the nature of the xenon desublimation. Apparently the Xe froze in a very voluminous manner under the conditions pertaining in the trap, i.e. it separated out in a snow-like manner; it was possible to observe this optically in a simplified glass model of the trap. It is probable that the Xe snow grows preferentially at particular parts of the trap, or that it collects at particular parts and partially blocks the trap. When a maximum pressure difference is reached at the point of blockage, the snow is blown down and the blockage is removed. This process could be confirmed at the trap exit by means of gas analyses; some of these showed concentrations of Xe, which were more than twice as high as the Xe input concentration, shortly after a blockage. Thus this process can lead to the total Xe yield falling

rapidly from 98 % to 80 % and less. A new design of the trap would have to take this situation into account by the use of filling bodies, filter elements or simply by means of a modified exit to the trap.

It was attempted in further experiments to improve the purity of the xenon which was separated out by carrying out the separation at higher temperatures. When the temperature of the outer mantle was raised by 30 K, the content of Kr in the Xe which was separated out fell to 0.09 vol. % and less but under these conditions the Xe yield only amounted to 20 %.

#### Separating out of Xe from He as carrier gas

For the dissolving of HTR fuel, it was suggested that a closed dissolver with He rinsing be used; the separation of the inert gases can then be carried out much more easily (5). In principle two freezing traps arranged one after the other are sufficient to permit Xe and Kr to be separated out selectively from the He carrier gas flow. In the case described here, the two inert gases were frozen out separately in the two traps at the same temperature but at different overall pressures. Hereby the following example:

From a He gas containing 2 vol. % Xe and 0.2 vol % Kr the two inert gases are to be separated out as selectively as possible whereby the two traps are cooled to the same temperature of 80 K. When the overall pressure in the first trap is 0.8 bar (600 torr), the partial pressure of the Xe in it is reduced from 12 torr to a theoretical value of  $5 \cdot 10^{-3}$ . The Kr partial pressure in the trap is 1.2 torr, i.e. below the sublimation pressure of 3 torr. Thus theoretically no Kr should separate out in the trap. The partial separating out of the Kr takes place in the second trap through which the gas flows with an overall pressure of, for example, 5 bar (3750 torr). In this trap the Kr partial pressure is reduced from 7.5 torr to 3 torr; i.e. 40 % of the Kr is separated out, the remainder is recycled to the dissolver with the He carrier gas. Thereby the Kr concentration in the dissolver goes up to some 0.3 % vol. %. The Xe partial pressure in the second trap falls theoretically from  $3.2 \cdot 10^{-2}$  to  $5 \cdot 10^{-3}$  torr again, i.e. one would expect only a further 0.035 % of the total xenon to be separated out.

The experiments, which were carried out with a total gas throughput of  $1 \text{ Nm}^3/\text{h}$  and the a/m values for pressure and temperature showed the following results:

1st trap (0.8 bar, 89 K at the outer mantle):

The Xe separated out contained 0.8 vol. % Kr; 99.5 % of the Xe was the maximum separated out.

2nd trap (5 bar, 89 K at the outer mantle):

The Kr separated out contained 2 vol. % Xe. Some 40 % of the Kr was separated out.

Partial blockages of the first or Xe trap occurred too when He was the carrier gas. They were, however, noticeably different in form to those that occurred with  $\text{N}_2$  as carrier gas. After periods of operation, of from 10 to 40 minutes, the pressure rises rapidly (in

exceptional cases only relatively slowly) in the trap up to a maximum pressure of, for example, 1.2 bar and then remains constant. The maximum pressure reached was very different in the different experiments. No evidence of blowing-free could be observed. It must therefore be supposed that the Xe ice, which separates out under these circumstances, is much firmer or harder than it is when Xe is being separated out from a N<sub>2</sub> gas stream.

#### IV. Ozone Solubility in Liquid Xenon

The behaviour of trace impurities such as O<sub>2</sub>, CH<sub>4</sub>, NO or inleaking air with boiling points between those of N<sub>2</sub> and Xe is very important for the operation of the rectification column. To maintain an undisturbed rectification process it is necessary to determine the amount of impurity accumulation in dependence of their initial concentration.

Ozone formed by Kr-85 radiation of O<sub>2</sub> represents one of the most severe safety problems. An initial O<sub>2</sub>-concentration of 10 vpm already may lead to a maximum equilibrium concentration of 3 vol %-O<sub>2</sub> after 20 days /6/.

Therefore, with an experimental set up described in detail elsewhere /7/ we started low temperature investigations of liquid-vapour equilibria in the binary system Xe-O<sub>3</sub>. First results determined to an accuracy of about 20 % are listed in Table 2. All of them are found to be greater than values according to "Raoult's-Law". The liquid Xe-O<sub>3</sub>-mixture showed a blue colour throughout the whole temperature range investigated, indicating a homogeneous solution.

$p$ [mbar]	$T$ [K]	$C_L$ [mol %]	$C_G$ [mol %]
1045	165	0,12	1,68
1074	165	0,26	3,57
1160	165	0,37	4,42
1407	170	0,24	2,61
1822	175	0,24	4,2
2271	180	0,06	0,53

Table 2: Ozone-equilibrium concentrations of the liquid ( $C_L$ ) and gaseous ( $C_G$ ) phase in binary Xe-O<sub>3</sub>-mixtures at different temperatures and total pressures

From a comparison of these results with the expected O<sub>3</sub>-generation we assume that at the still bottom a sufficient quantity of ozone will dissolve in the liquid Xenon and therefore a dangerous O<sub>3</sub>-accumulation will not occur.

#### V. References

- /1/ Bendixsen, C.L., Offutt, G.F.  
Rare Gas Recovery Facility at the Idaho Chemical Processing  
Plant, IN-1221 (1969)

- /2/ Barnert-Wierner, H.; Bendick, B.  
Untersuchungen an Katalysatoren zur Reduktion von Stickoxiden  
und Sauerstoff mit Wasserstoff, JÜL-1677 (1980)
- /3/ Hutter, E. et.al., Kr-85-Abtrennung aus der Abluft von Wiederaufarbeitungsanlagen: Verfahrenstechnische Anpassung und Ergebnisse, Deutsches Atomforum, Reaktortagung 1980 p. 441 - 44
- /4/ Bohnenstingl, J., et.al., Cryogenic Separation of Krypton and Xenon from Dissolver Off-Gas, IAEA-SM 207/20 (1976)
- /5/ Bohnenstingl, J. et.al., Separation of the Fission Product Noble Gases Krypton and Xenon from Dissolver Off-Gas in Reprocessing HTGR-Fuel, 14th ERDA Air Cleaning Conference, 1002-16 (1976)
- /6/ v. Ammon, R., et.al., Die Entwicklung der Abtrennung von Kr-85 aus dem Abgas von Wiederaufarbeitungsanlagen, KfK-Nachrichten, Jahrg. 11, 3, 19 (1979)
- /7/ Hackfort, H., Chatzipetros, J., Esser, U., to be published

I-129, Kr-85, C-14 AND NO<sub>x</sub> REMOVAL  
FROM SPENT FUEL DISSOLVER OFF-GAS AT ATMOSPHERIC PRESSURE  
AND AT REDUCED OFF-GAS FLOW

E. Henrich, R. Hufner  
Kernforschungszentrum Karlsruhe,  
Institut für Heiße Chemie,  
Federal Republic of Germany

Abstract

A dissolver off-gas (DOG) system suitable for a LWR, FBR or HTR spent fuel reprocessing plant is described, incorporating the following features:

- The DOG flow is reduced to a reasonably small volume, using "fumeless" dissolution conditions. By maintaining high concentrations, the retention procedures are simplified and accompanied by an economic reduction of the equipment size.
- All process operations are conducted at atmospheric or sub-atmospheric pressure, including noble gas removal by selective absorption, without using high temperature processes.
- All processes, except HEPA filtering, are continuous and do not accumulate large amounts of waste nuclides. The DOG process sequence is mutually compatible with itself and with processing in the headend, showing on-line redundancy for the removal of the most radiotoxic nuclides.
- The DOG system only deviates slightly from proven technology.

The stage of development and relevant results are given both for a lab. scale and a pilot plant scale.

I. Introduction

The increasing use of nuclear electric power has been connected with the observance of high safety standards, taken on the basis of licensing decisions made. A higher retention of radioactive waste gases, far below ICRP limits,<sup>1</sup> has therefore been recommended for future nuclear plants. The removal of I-129, Kr-85 and eventually C-14 from the DOG of spent fuel reprocessing plants is of special importance in this connection. The many R and D efforts to produce a simple,<sup>2,3</sup> safe and reliable integration of Kr-85 removal into the DOG system are an expression of the technical complexity involved.

II. General Aspects and Principles

The purpose of the DOG system is to separate the toxic components from a non-toxic carrier gas. Most results reported use air as a carrier gas, though more expensive carrier gases have been proposed to simplify separation procedures.<sup>4</sup> Compatibility with air is important at least under accident conditions.

The components removed from the DOG are either recycled or conditioned for final disposal. I-129, Kr-85 and C-14 (as  $^{14}\text{CO}_2$ ) are carried almost completely into the DOG either with or without minor process modifications. The procedures selected to remove these nuclides should therefore facilitate their subsequent waste treatment.

The  $\text{NO}_x$  evolved during fuel dissolution, plus a very small aerosol fraction of non-volatile nuclides, are carried into the DOG, together with some tritiated water vapour and traces of  $\text{RuO}_4$ . The procedures selected for removal of these components should facilitate recycling or reuse and not produce additional waste streams.

Some special recycling may be advantageous even for iodine or krypton. Retention procedures might be simplified by first removing a large fraction in a simple procedure suitable for subsequent conditioning, followed by complete removal and recycling in a second step. Complete removal is thereby decoupled from compatibility with waste treatment while at the same time additional safety is introduced by on-line retention redundancy.

The retention of radioactive waste gases reduces radiological risks to the public. The concentration and accumulation necessary for removal and waste treatment may enhance the dose to plant personnel. Technical procedures should be designed therefore to guarantee a large net safety output at reasonable cost. High temperature and high pressure procedures are usually accompanied by other additional safety measures, thereby complicating the system and should therefore need to be compensated by other advantages.

A safety feature which involves the minimization of the free radiotoxic inventories between the storage container and the final waste form helps to reduce the risk of accidental release and the dose to unscheduled on-line maintenance personnel. Therefore, continuous removal and conditioning processes involving small residence times and inventories are preferred to the accumulating batch procedures.

Redundant on-line retention, being inherent to the system, should be preferred to parallel redundancy, at least for the most radiotoxic components. On-line redundancy means that an insufficient retention caused by changes in operating conditions, component malfunctions or operator errors, etc, will be corrected automatically in downstream process steps without any additional action.

Reducing the carrier gas flow to a reasonably low value still compatible with processing may save space and cost by reducing the equipment size. Moreover, a better removal efficiency or simpler removal procedures are possible in a "concentrated" DOG. This has been practised in the Windscale Magnox plant which uses continuous "fumeless" dissolution.<sup>5</sup> In LWR or FBR reprocessing plants using a chop and leach headend, the shear off-gas (SOG) dilutes the DOG by an amount depending on the shear type and the shearing philosophy. Reducing the SOG to a reasonably low volume still compatible with fuel chopping brings back the advantages of a "concentrated" DOG.

A separate evaluation of the isolated process steps may underestimate the importance of interactions within the total serially-connected DOG system and with processing in the headend. This may result in additional adaptation steps, thus complicating the total system. Moreover, evaluation criteria such as removal efficiency, system complexity and reliability, cost, total system compatibility including potential future release restrictions, etc. cannot be clearly separated from each other.

For the DOG system discussed below, we have tried to consider these aspects and criteria as thoroughly as possible, without deviating too much from proven technology. Firstly, a general view of the total system will be given, followed by a more detailed discussion of process operations and equipment relative to DOG sequences.

### III. General View of the Total DOG System (see Fig. 1)

The air flow within the DOG system is about  $100 \text{ Nm}^3/\text{t U}$  on the average, allowing for slow flow variations from approximately zero up to a maximum of about  $150 \text{ m}^3/\text{t U}$ . Approximately one half of the air is expected to come from the one shear in operation, the rest originating from the other dissolvers and a few other vessels. During spent oxide fuel dissolution about  $100 \text{ Nm}^3/\text{t U NO}_x$ , about  $1 \text{ Nm}^3/\text{t U Xe}$  and Kr, most of the fission product iodine and practically all the  $^{14}\text{CO}_2$  are removed into the DOG, together with some aerosols, tritiated water vapour and traces of  $\text{RuO}_4$ . Towards the end of dissolution and afterwards, the fission product iodine removal is completed by boiling under reflux, supported by  $\text{NO}_2$ -sparging and carrier iodate addition.<sup>6</sup>

Following the main DOG line, the toxic components are removed in a series of 4 scrubbers. The aerosols,  $\text{NO}_x$  and iodine are scrubbed with nitric acid in two plate columns,<sup>7</sup> each partitioned into two functional parts and also with a HEPA filter. The noble gases and C-14 are scrubbed with a fluorocarbon solvent in two packed columns, each partitioned into three functional parts. The successive removal is obtained by changing the absorbent combined with stepwise temperature decrease.

In the first nitric acid scrubber the DOG is scrubbed with larger volumes of dilute nitric acid at about normal temperature and slightly below. Oxygen is added upstream of the scrubber slightly above the stoichiometric volume needed for complete  $\text{NO}_x$  recombination. About  $45 \text{ Nm}^3/\text{t U O}_2$  are required<sup>3</sup> (without calculating  $\text{NO}_2$ -sparging of the fuel solution) and  $100 \text{ Nm}^3/\text{t U}$  carrier air contribute less than half. Using oxygen instead of air avoids dilution with large volumes of  $\text{N}_2$  and maintains a "concentrated" DOG. This is usually described as<sup>2</sup> "fumeless" dissolution. The decontamination factors (DFs)<sup>3</sup> obtained for  $\text{NO}_x$ ,  $\text{I}_2$  and  $\text{RuO}_4$  are at least  $>10^2$  but usually  $>10^3$  under normal operating conditions,<sup>7</sup> the aerosol concentration being reduced by about one order of magnitude. The used scrub acid is recycled to the dissolution acid storage tank after a more or less efficient iodine removal.

Aerosol decontamination is obtained within the column using a packing and glass fibre filter in the column top, followed by a HEPA filter.

In the second nitric acid scrubber the DOG is scrubbed with small volumes of about 90 weight-% nitric acid at temperatures down to about  $-50^{\circ}\text{C}$ . The  $\text{NO}_2$ , iodine and water vapour decontamination is due not only to the considerable reduction of the corresponding vapour pressures; as oxidative absorption also reduces the total  $\text{NO}_x$  concentration to the ppm region and the iodine DFs are usually  $10^4$ .

The basis of the following noble gas and  $^{14}\text{CO}_2$  removal is the single column version of the selective absorption process using the non-toxic fluorocarbon solvent R-12, which has been developed by ORGDP during the past decade.<sup>3</sup> There are two major differences:

- The separation is performed at or slightly below atmospheric pressure, with correspondingly lower temperatures. Because the DOG is "concentrated", it is possible to use equipment of reasonable and economic size.
- The separation of Xe and Kr is carried out in a two column system. The higher boiling Xe,  $^{14}\text{CO}_2$  and  $\text{N}_2\text{O}$  are removed together in the first Xe scrubber. After  $^{14}\text{CO}_2$  removal the Xe raw product is cleaned for commercial use.<sup>2</sup> The last decontamination step is the Kr removal in the second noble gas scrubber. Most, but not necessarily all, of the reactive impurities should be removed from the Kr raw product prior to continuous conditioning by ion implantation, as the latter is insensitive enough.

The decontaminated DOG is vented to the stack without further treatment, the R-12 partial pressure being below permissible concentrations.

#### IV. Operating and Equipment Relative to DOG Sequence

##### 1. Points Relative to the Shear and the SOG

There are two basic types of mechanical shears, the bundle shear and the pin shear, either with or without fuel element disassembly prior to shearing. The SOG flow and the variations with time depend on the shear type and details of construction. A fumeless dissolution requires approximately  $\leq 1$  NL SOG per cut piece of fuel containing about 20 g U. This should be possible for both shear types using a closed fuel magazine. Flow constancy for variable throughputs will be somewhat better in a pin shear, due to the variable number of pins in the magazine and the shorter cutting periods of only a few seconds. The fuel inventory in the shear is reduced in proportion to the number of pins in the magazine.

##### 2. Iodine Removal from the Fuel Solution<sup>6</sup>

An example for the iodine desorption from simulated fuel solution by boiling under reflux is given in Fig. 2. The iodine concentrations were determined using 13h-I-123 tracer. With  $\text{NO}_2$ -sparging and carrier iodate addition to the boiling solution, shown on the same time scale, fission product iodine concentrations below the required  $10^{-6}$  mol/l  $\text{I}_2$  have been obtained. Experience with a comparable procedure in the



Karlsruhe reprocessing plant (WAK) has shown that even without chemical treatment the fission product iodine concentration in the fuel solution was frequently, although not routinely, less than  $10^{-6}$  mol/l  $I_2$ . More details are reported in reference 6.

### 3. Nitric Acid Scrub with Dilute Nitric Acid at Approximately Room Temperature<sup>7</sup>

Fig. 3 indicates why the column is divided into a lower cocurrent and an upper countercurrent part. In an  $NO_x$  absorption tower having countercurrent flow and cooled plates, the temperature decreases towards the gas exit. The high temperatures at the feed point are caused by the high off-gas temperature and release of recombination heat. With a small off-gas flow, iodine will be desorbed in the hot lower part and absorbed in the cold upper part. It will accumulate in the zone where the temperature-dependent distribution coefficient equals the gas-to-liquid flow ratio. To avoid plugging, the column is "cut" sufficiently high above the accumulation zone and the lower part turned around, with the liquid still flowing one way under gravity.

Fig. 4 is a schematic view of the pilot scale test column having 21 plates. At a gas-to-liquid flow ratio of about 50, a DOG temperature decrease from  $\geq 60^\circ C$  to  $< 15^\circ C$  and a gas residence time within the column of about  $10^3$  sec,  $NO_x$ ,  $I_2$  and  $RuO_4$  have DFs at least  $> 10^2$  but usually  $> 10^3$  have been found.

The good  $NO_x$  decontamination, corresponding to residual concentrations of  $< 500$  vpm is partially due to the long residence time. However, it can also be shown by titration of nitric and nitrous acid that no appreciable nitrous acid decomposition occurs in the colder countercurrent part, where only 2-3% of total  $NO_x$  are absorbed. Decomposition and NO reformation occurs mostly after the scrub acid has entered the cocurrent part joining the incoming  $NO_x$  and not near the gas exit.

In reasonable accord with theory, the  $NO_x$  decontamination factor decreased with approximately the third power of the DOG dilution, showing clearly the advantages of a "concentrated" DOG. The behaviour of iodine can be adequately described using iodine solubility and vapour pressure data, gas and acid flow rates and column temperature.

Fig. 5 shows a schematic view of the special column plates,<sup>8</sup> which have a good absorption efficiency, permitting short plate distances and reduced column heights. The DOG is distributed beyond the stainless steel sheet at the liquid surfaces, moving radially in good contact with the liquid. The moving gas induces a liquid circulation around the coiling coils; the SS sheet in the liquid separates countercurrent flows.

### 4. Iodine Steam Strip of Scrub Acid<sup>7</sup>

Almost all of the iodine is removed by the first scrubber under normal conditions. Some nitrous acid still present in the scrub acid serves to stabilize the absorbed iodine in the volatile elementary form. Steam stripping the iodine has been selected from among

different alternatives since either none or a negligible volume of desorption gas is necessary. The principle of the iodine steam strip performed outside the main DOG line is shown in Fig. 6.

After heat exchange and additional heating to near the boiling point, the iodine was steam stripped from the downflowing acid using a boil-up rate of 10%. The reflux condenser removes the water vapour in countercurrent multistage contact with the condensate. At higher exit temperatures the NO formed by nitrous acid decomposition is sufficient to carry the iodine, while at lower temperatures some additional  $N_2$  must be used to prevent  $I_2$  condensation. The iodine can be removed in a number of different ways, by freezing or absorption in high boiling silicones or NaOH-solution, etc. and will be converted to  $Ba(IO_3)_2$  for final disposal. Neither removal from the scrub acid nor recovery from the gas phase needs to be complete since the stripped acid is recycled to the dissolver and the stripper is connected to the DOG upstream from the first nitric acid scrubber. Partial or total recycle of the scrub to the first nitric acid scrubber is possible to maintain or enhance acid flow during standby or increased off-gas flow.

Iodine DFs ranging from  $10^2$  -  $10^3$  have been obtained, the residual iodine concentration being caused mainly by iodate formation after nitrous acid decomposition in the hot acid.

#### 5. Nitric Acid Scrub Using 90% Nitric Acid at Low Temperatures

Downstream from the HEPA filter the DOG will be fairly free from  $NO_x$ ,  $I_2$ ,  $RuO_4$  and aerosols but will still contain the fission product noble gases and  $^{14}CO_2$ . The low temperature nitric acid scrub prepares the DOG for the noble gas removal without having to introduce new chemicals. The vapour pressure of the high boiling components is reduced considerably by the low temperature; residual  $NO_x$  and iodine are additionally removed down to trace level by oxidation and absorption; even serious malfunction of the first scrubber can be corrected.

Fig. 7 shows the  $HNO_3$ - $H_2O$  phase diagram<sup>9</sup>, explaining the basis of the process. The freezing points are as low as  $-66^\circ C$  for about 90 weight % nitric acid. The darkened area corresponds to hyperazeotropic acid concentrations and shows the situation during scrubbing. At higher temperatures NO and  $I_2$  are oxidised to less volatile  $NO_2$  and iodate.  $NO_2$  absorption in the highly concentrated acid is comparable to  $NH_3$  absorption in water, and is excellent at low temperatures.<sup>10</sup>

A schematic view of the experimental set-up is shown in Fig. 8. At a gas-to-liquid flow ratio of about  $10^3$ , and using a small acid flow,  $NO_2$  accumulation is prevented by partitioning the column in a cocurrent and a countercurrent part in the same way as was done for the  $I_2$  in the first scrubber.

In the first cocurrent part the DOG was cooled from about room temperature down to  $-20$  or  $-30^\circ C$ , NO and  $I_2$  were oxidized sufficiently fast to  $NO_2$  and iodate and were dissolved in the acid. In the countercurrent part at about  $-50^\circ C$ ,  $NO_2$  and  $I_2$  trace amounts are very efficiently scrubbed. Even at  $NO_x$  and  $I_2$  concentration corresponding

to about 5% of the volume present upstream of the first nitric acid scrubber, this being about 100 times more than usual,  $\text{NO}_x$  was removed to about 1 vpm and the iodine DF was at least  $>10^3$  but usually less than the detection limit of  $>10^4$ .

Good  $\text{NO}_x$  decontamination depends mainly on a careful removal of dissolved nitric oxides from commercial acid. This could be achieved for example using a countercurrent air strip of the 90% nitric acid at  $45^\circ\text{C}$  in a 10 plate column and a gas-to-liquid flow ratio of  $10^2$ .

The volume of scrub acid used is compatible with the nitric acid balance and corresponds to about  $25 \pm 15\%$  of the acid removed as  $\text{UO}_2(\text{NO}_3)_2$  from the headend, leaving more than sufficient open space for  $\text{NO}_2$ -sparging of the fuel solution during iodine removal. Using highly concentrated nitric acid and  $\text{NO}_2$  to replace the nitrate loss reduces the water input and correspondingly the tritiated waste water output; work on acid concentration is done outside the plant.

The experiments were carried out using a lab-scale two-part stainless steel column of 0.1 m diameter and about 1 m height, the column having 2 x 8 plates. Because of the low temperature the walls showed no visible corrosion after several months. A pilot-scale scrubber will be connected to the headend facility (HET) later in the year.

## 6. The Noble Gas Scrub

Selective absorption for the removal of the noble gases was preferred to cryogenic distillation for the following reasons:

- The absorption is done at atmospheric pressure
- The accumulated steady state Kr-85 inventory is considerably lower
- Selective absorption in R-12 is less sensitive to impurities, reducing the pre-cleaning requirements and the sensitivity to malfunction of upstream equipment.

Continuous selective absorption is preferred to discontinuous adsorption on molecular sieves,<sup>11</sup> since continuous processes are more easily controlled, including their equipment and energy economy.

Fig. 9 shows the noble gas scrubbers. The defrostable input cooler reduces the DOG temperature to less than the lowest temperature in the subsequent scrubber, thus avoiding plugging by freezing components. The partial pressure of  $\text{H}_2\text{O}$  and  $\text{HNO}_3$  are reduced to negligible values  $<0.1$  vpm, but entrainment is expected to contribute more. The  $\text{N}_2\text{O}$  is the critical layout component, limiting the lowest operating temperature to about  $-125^\circ\text{C}$ . The small amount of freezing gas components permits defrost cycles of several hundred hours. Malfunction of upstream equipment can be corrected by shortening cycle time, thus giving additional on-line redundancy.

Each of the following Kr and Xe scrubbers consists of three functional packed column parts: absorber, fractionator and stripper; the R-12 flow is by gravity. The higher boiling components Xe,  $\text{N}_2\text{O}$

and  $^{14}\text{CO}_2$  are selectively absorbed in the first Xe scrubber; coabsorbed Kr is removed from the liquid R-12, together with some  $\text{O}_2$  and  $\text{N}_2$  at a fractionator boil-up rate of about 3%. The absorbed gases Xe,  $\text{N}_2\text{O}$  and  $^{14}\text{CO}_2$  (Ru) are removed completely in the stripper at a boil-up rate of about 16%. The stripper is usually separated from the fractionator at the gas side, not at the liquid one. The stripped liquid R-12 is recycled to the absorber, via a heat exchanger for energy economy. A smaller heater and cooler corrects the incomplete heat exchange.

The product cooler removes R-12 vapour to about 10 vol.%; the lowest temperature possible is given by the sublimation point of  $\text{CO}_2$  ( $-78^\circ\text{C}$ ). At room temperature the  $^{14}\text{CO}_2$  is scrubbed from the Xe raw product. Test scrubs using NaOH-solution in a packed tower showed residual  $\text{CO}_2$  concentrations well below 1 vpm. The carbonate is then precipitated using a  $\text{Ba}(\text{OH})_2$  slurry to give insoluble  $\text{BaCO}_3$  for final disposal.<sup>12</sup> The remaining Xe will be purified for commercial use, representing a value of about \$7000/tU. This should not be neglected in a cost-benefit analysis.

The same operations occur in the Kr scrubber at different flow ratios and boil-up rates and at still lower temperatures in the absorber. The R-12 concentration in the purified off-gas is below the maximum permissible concentration, therefore an additional R-12 removal system is avoided.

Operating at or slightly below atmospheric pressure gives lower temperatures compared to the ORGDP version at about 8 bar. This enhances the separation selectivity and unfortunately also sensitivity to impurities. This is believed to be compensated by the excellent on-line redundant pre-cleaning.

Radiolytic solvent degradation is proportional to the Kr inventory. With a mean residence time of Kr of  $\leq 1$  h, using the reported g-value of 4 for radiolytic degradation,<sup>13</sup> the average annual inventory of a 350 t U/a plant can be calculated to be about 400 Ci. The moderate amount of about 1 Kg/a of radiolytically degraded solvent plus some chemical degradation is expected to be sufficiently controlled to prevent corrosion, by continuous purification of a few percent bypass flow. Impurity removal will be done by pure and reactive absorption using a fixed bed.

The correct layout of the noble gas scrubbers is being presently investigated, using lab-scale equipment, including the determination of the distribution coefficients for the critical components at the lower absorber temperatures expected. Investigations of radiolytic degradation and their effects will be made at the technical university of Munich.

## 7. Ion Implantation<sup>14,15,16</sup>

Continuous Kr ion implantation into sputtered metals has been investigated on a lab scale. Neither the implantation process nor the product quality requires a high purity Kr product. Conditioning can be done continuously at low pressure ( $10^{-2}$  Torr) and about normal temperature, without accumulation of Kr in the unconditioned form, thus reducing the hazard of accidental release. The products are

thermally, mechanically and chemically stable. Comparing the alternatives, ion implantation seems to be the safest but also a somewhat more expensive method.

#### V. Conclusion

Some characteristic features of the DOG system and their relation to evaluation criteria are here summarised:

- All process operations are conducted at or below atmospheric pressure, especially during removal, fixation, transport and disposal of noble gases, thus reducing the risks of accidental release.
- High temperature processes are not used, the highest temperature being the the boiling fuel solution, thus reducing corrosion problems and their consequences.
- The temperature profile in Fig.10 is an expression of enhanced compatibility within the DOG system. The temperature decreases stepwise, without producing large jumps in the opposite direction.
- Possible flow variations between about 0 and the 1.5-fold nominal flow ensures compatibility with shearing and with DOG connections to other dissolvers and vessels.
- The water and nitric acid balance is not disturbed.
- Using a "concentrated" DOG reduces the equipment size, the energy requirements and saves space, thus reducing the cost.
- Practically all processes are continuous with reasonably small inventories reducing the risks of accidental release and personnel exposure during on-line maintenance.
- On-line redundancy is available for the retention of the most radiotoxic nuclides: (a) aerosols are removed by a series of scrubbers and filters; (b) iodine is removed in the 1st and 2nd nitric acid scrubber, the input cooler of the noble gas scrubbers and the noble gas scrubbers themselves; (c) tritiated water vapour is removed by the decreasing temperature; (d) NO<sub>x</sub> is removed in the 1st and 2nd nitric acid scrubber and in the input cooler of the noble gas scrubbers; (e) <sup>14</sup>CO<sub>2</sub> can be removed by the Xe and the Kr scrubber; (f) there is no redundant removal for Kr.

Without using "fumeless" dissolution conditions, larger DOG flows > 100Nm<sup>3</sup>/tU will also be digested in the DOG system. The circulating R-12 flow in the noble gas scrubbers has to be increased and a part of the steam stripped scrub acid has to be recycled to the first scrubber in order to maintain the gas-to-liquid flow ratios. The low temperature scrubber shows sufficient flexibility, depending on the operating temperatures.

REFERENCES

- / 1/ W. Koelzer; in "Chemie der nuklearen Entsorgung", editor F. Baumgärtner, München 1978, part I, p. 139
- / 2/ R.v. Ammon, H.W. Beaujean; in "Chemie der nuklearen Entsorgung" editor F. Baumgärtner, München 1978, part II, p. 142
- / 3/ J.R. Merriman, et al.; IAEA-SM-245/53, Vienna (February 1980)
- / 4/ H. Barnert-Wiemer et al.; Proceedings of the 15th DOE Nuclear Air Cleaning Conference, Boston, Massachusetts 7-10 August 1978, p. 477
- / 5/ G.L. Miles, Progress in Nuclear Energy, Series III, Process Chemistry, Pergamon Press Ltd., London (1956)
- / 6/ E. Henrich, R. Hufner, A. Sahm; IAEA-SM-245/16, Vienna, (February 1980)
- / 7/ E. Henrich, PWA status report, Karlsruhe (1979)
- / 8/ E. Henrich, D. Leuchtmann, W. Weinländer, R. Neuberth, K. Wegner; Boden für Absorptionskolonnen, DE-AS 2759 195 (17.04.1980)
- / 9/ Gmelins Handbuch der anorganischen Chemie; Vol. N4, p. 969
- /10/ A.Klemenc, J. Rupp; Z. anorg. allg. Chemie 194 (1930) 51
- /11/ D.T. Pence et al.; 15th DOE Nuclear Air Cleaning Conference, Boston, Massachusetts, August 7-10, 1978
- /12/ K.J. Notz, D.W. Holladay, C.W. Forsberg, G.L. Haag; IAEA-SM-245/29
- /13/ M.J. Stephenson, J.R. Merriman, D.I. Dunthorn ORGDP report, K-1780
- /14/ D.S. Whitmell, R.S. Nelson, M.J.S. Smith; IAEA-SM-245/7
- /15/ G.L. Tingey, E.D. McClanahan, M.A. Bayne, W.J. Gray; IAEA-SM-245/31
- /16/ E. Henrich, H.-J. Schmidt; Berlin, Reaktortagung (1980), p. 445

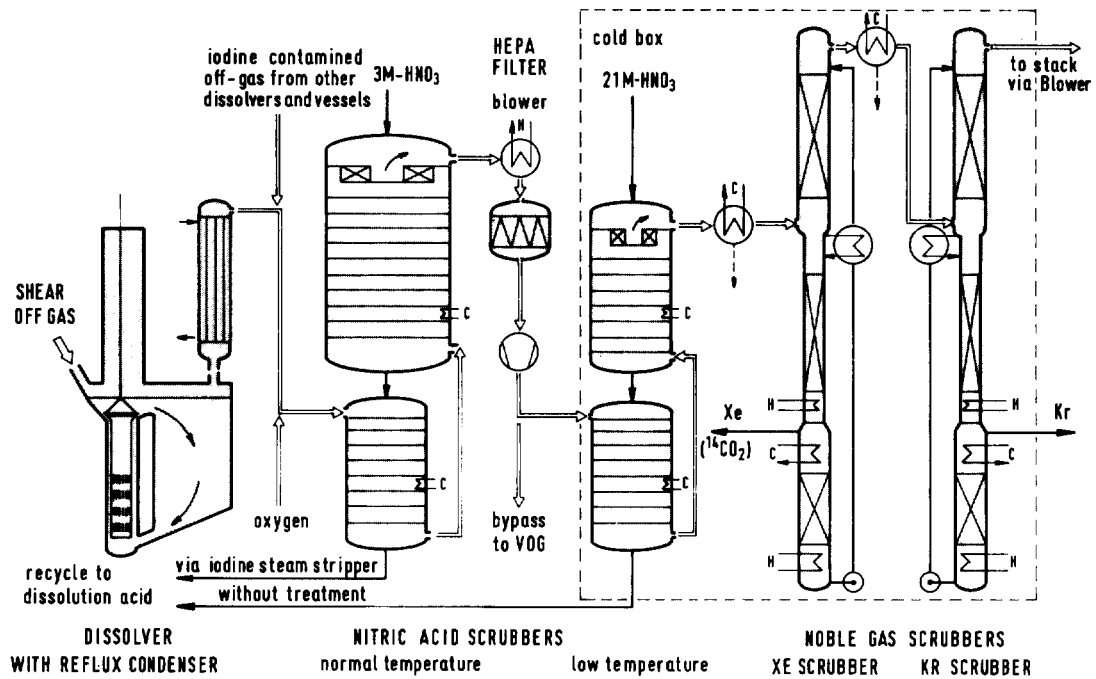


Fig. 1 Schematic DOG Flow Sheet

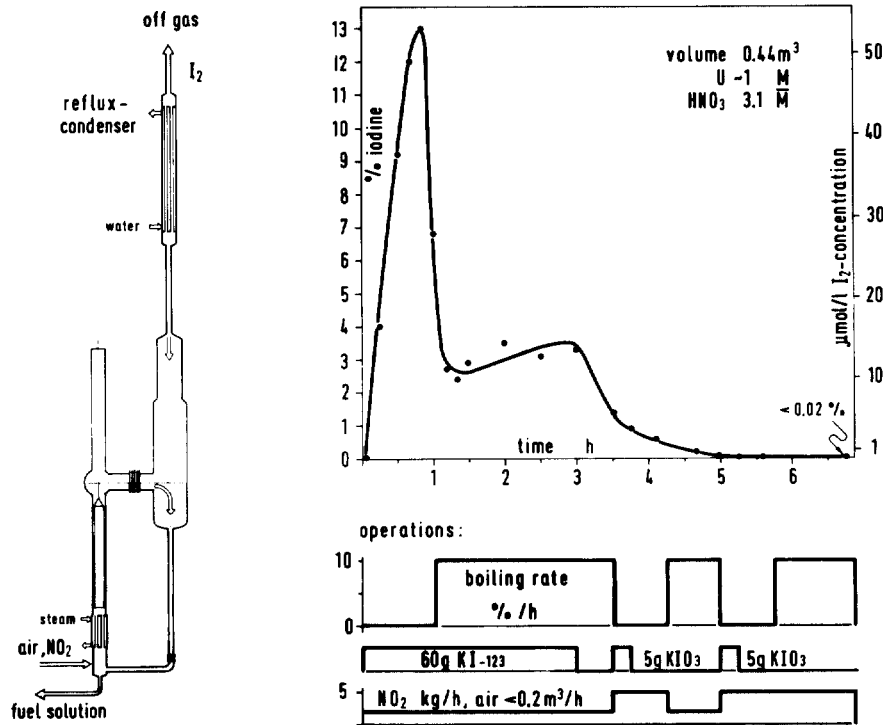


Fig. 2

Iodine desorption from fuel solution by boiling under reflux

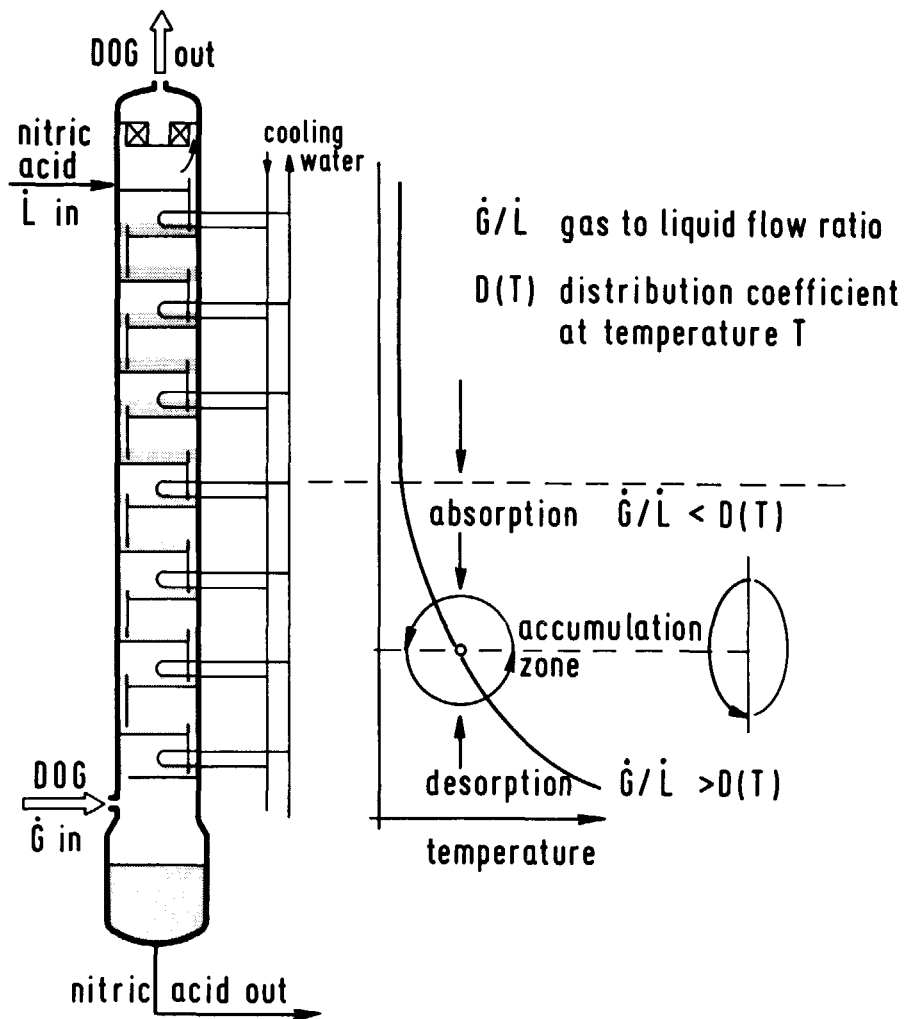


Fig. 3 Accumulation in columns

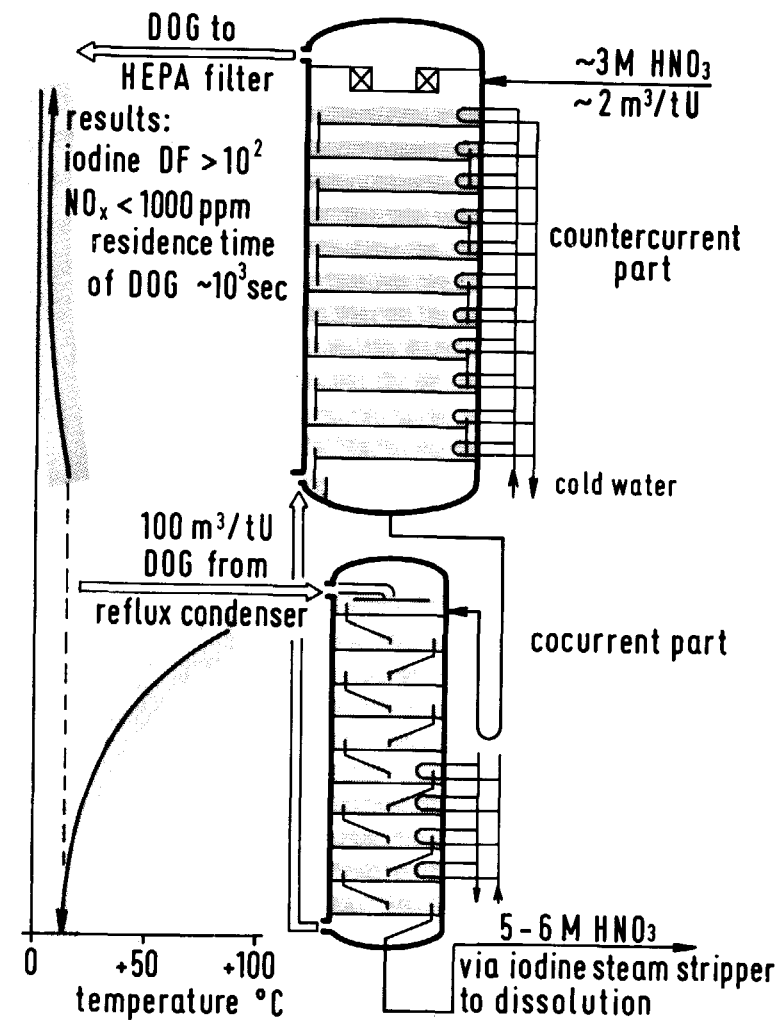


Fig. 4 Nitric acid scrubber with dilute nitric acid



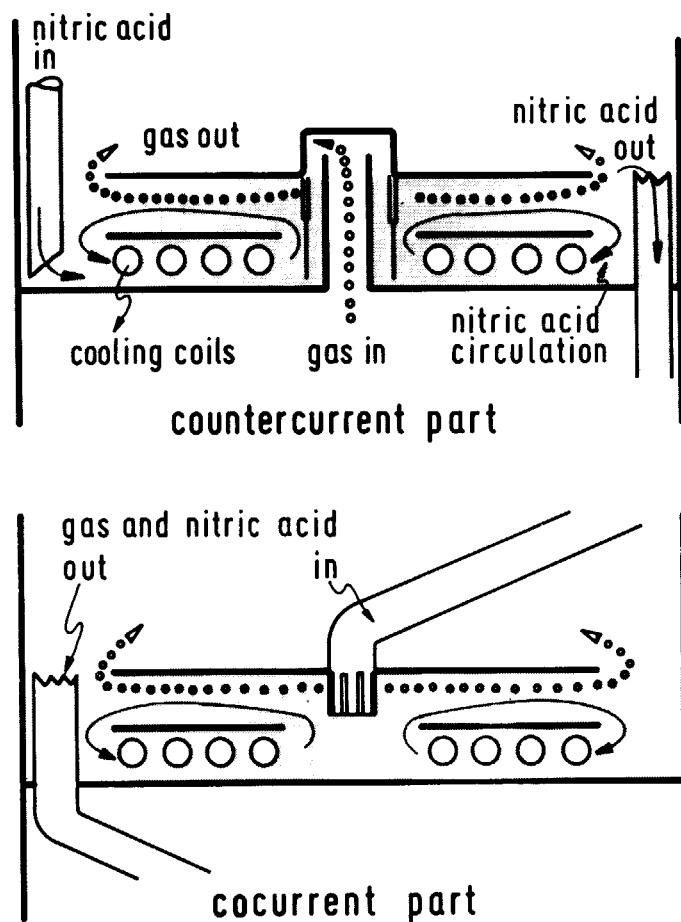


Fig. 5 Nitric acid scrubber  
plate cross-section

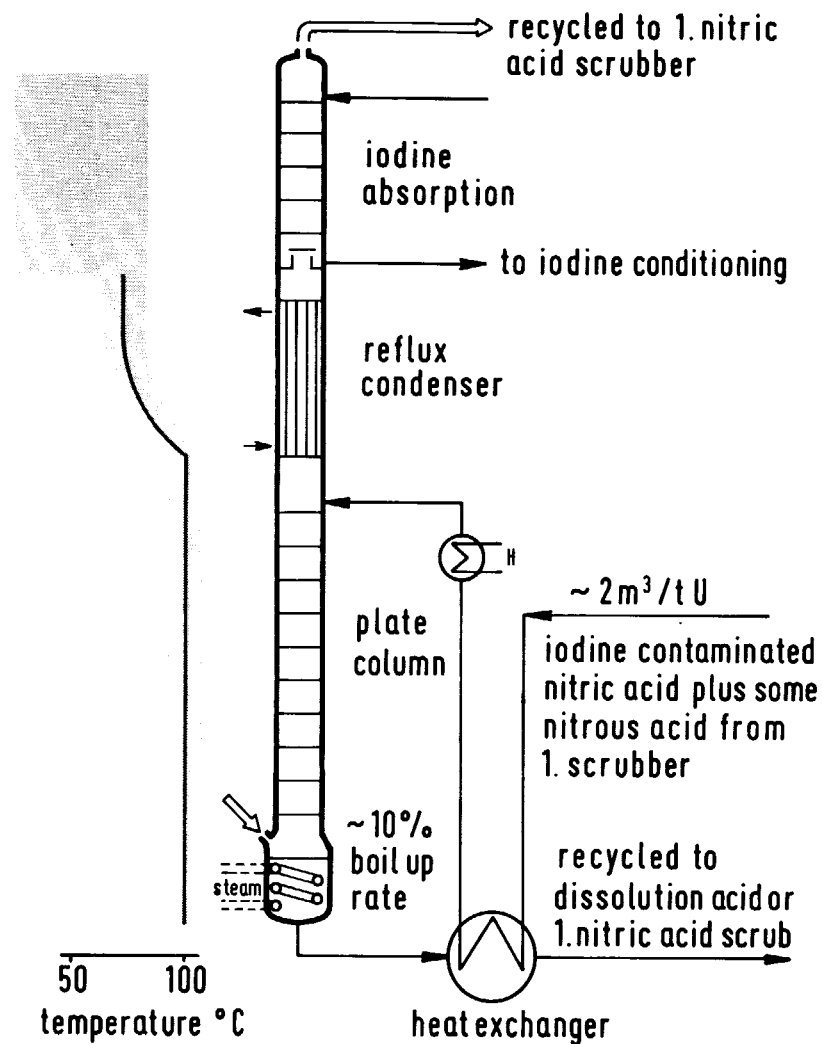


Fig. 6 iodine steam strip from scrub acid

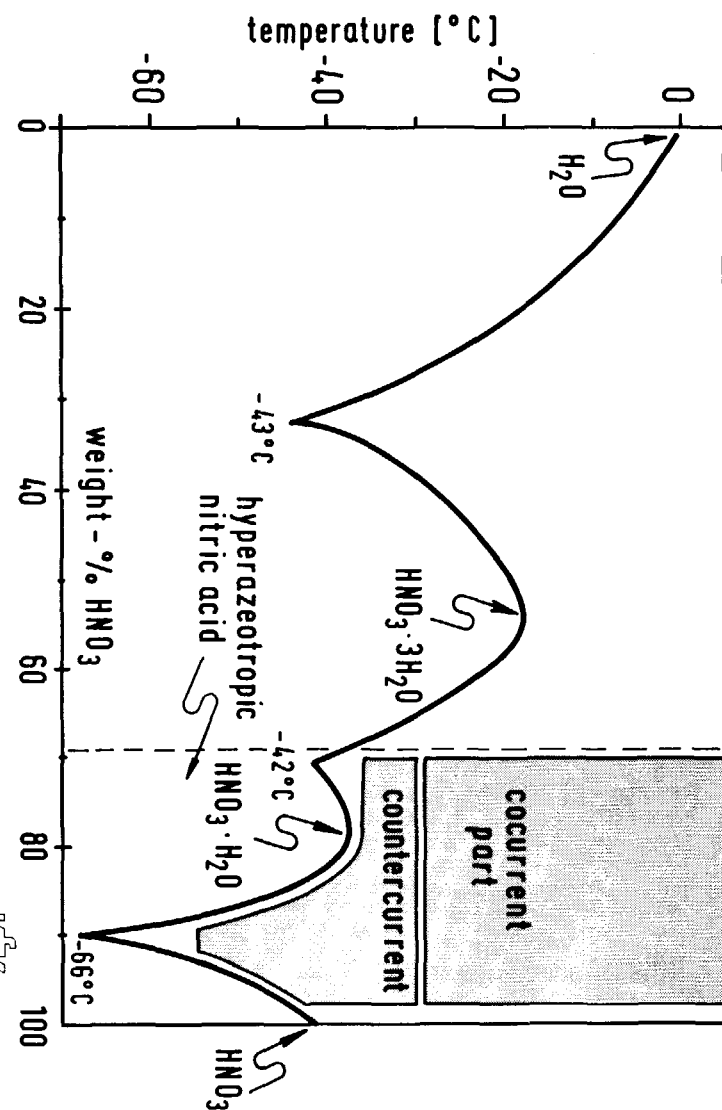


Fig. 7

 **$\text{HNO}_3\text{-H}_2\text{O}$  phase diagram**

KfK

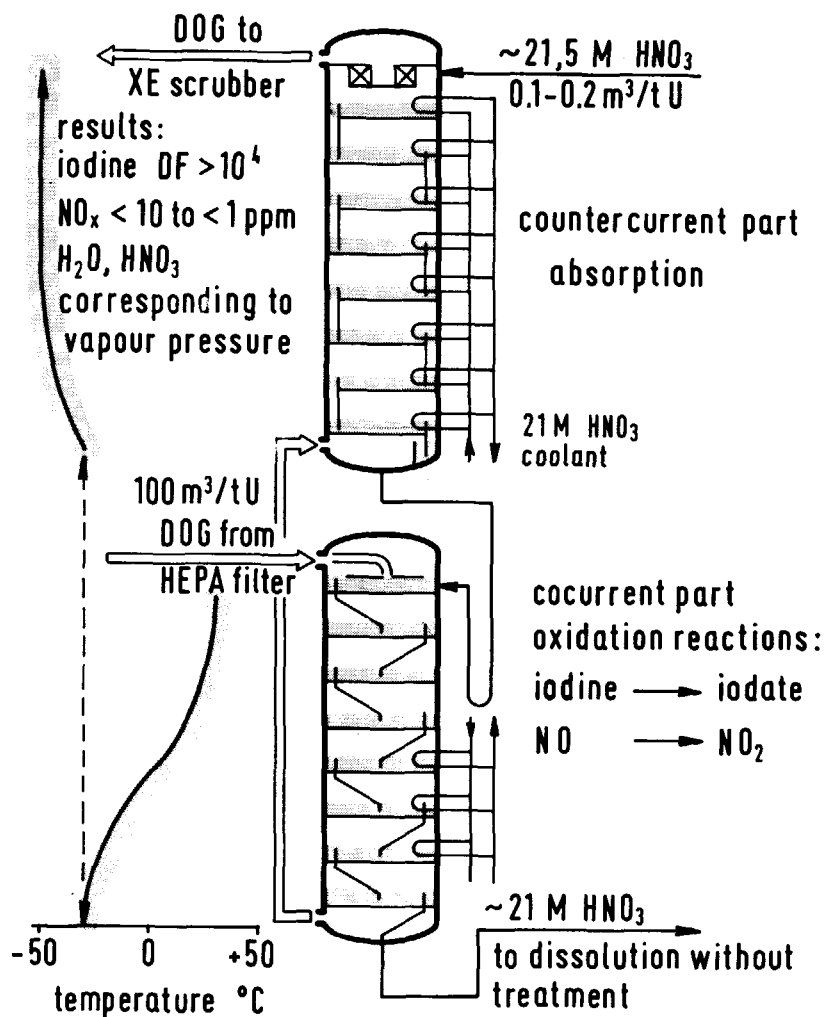
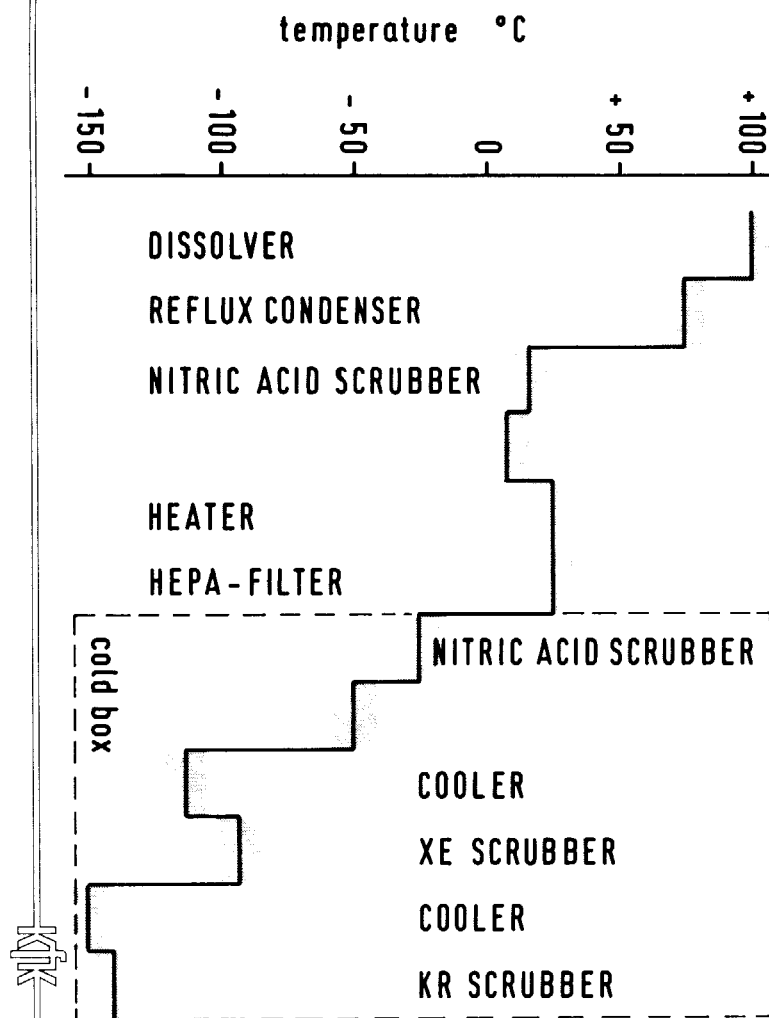


Fig. 8

**Nitric acid scrubber with hyperazeotropic acid**

KfK

Fig. 10 DOG temperature profile



611

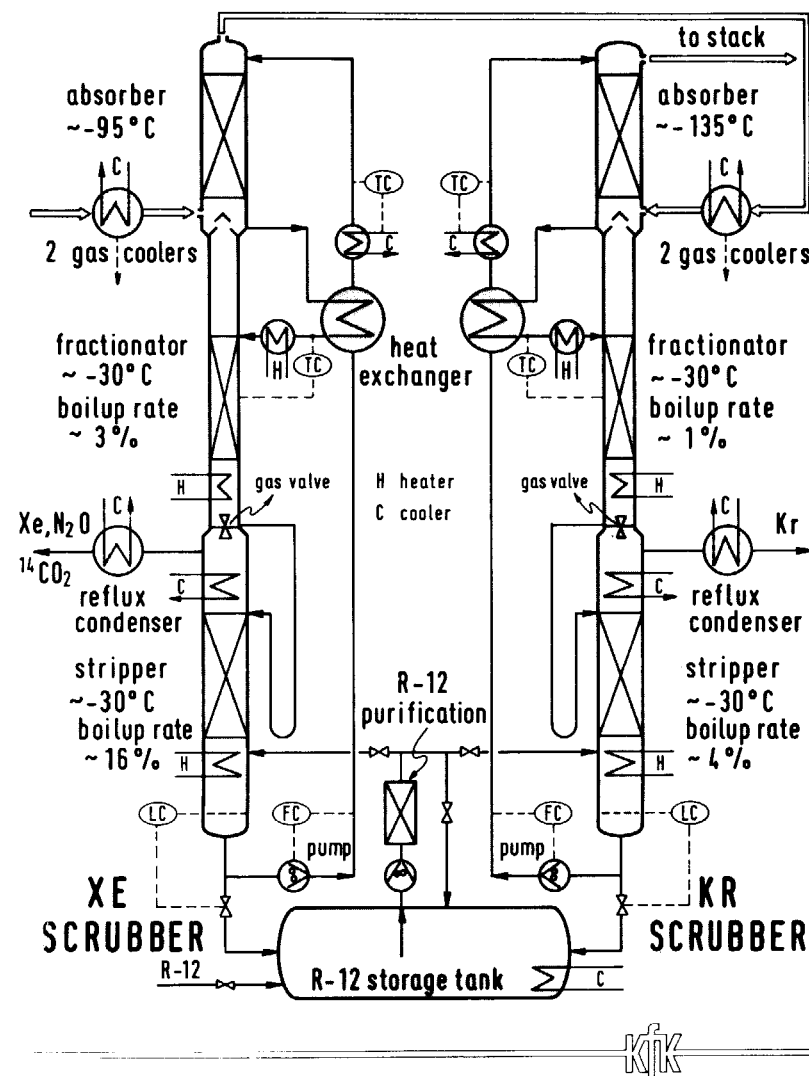


Fig. 9 Noble gas scrubbers

IMPROVED IODINE AND TRITIUM CONTROL IN REPROCESSING PLANTS

E. Henrich, H. Schmieder, W. Roesch, F. Weirich  
Kernforschungszentrum Karlsruhe, Institut für Heiße Chemie  
Federal Republic of Germany

Abstract

During spent fuel processing, iodine and tritium are distributed in many aqueous, organic and gaseous process streams, which complicates their control. Small modifications of conventional purex flow sheets, compatible with processing in the headend and the first extraction cycle are necessary to confine the iodine and the tritium to smaller plant areas. The plant area connected to the dissolver off-gas (DOG) system is suited to confine the iodine and the plant area connected to the first aqueous cycle is suited to confine the tritium. A more clear and convenient iodine and tritium control will be achieved. Relevant process steps have been studied on a lab or a pilot plant scale using I-123 and H-3 tracer.

I. Reduction of Confinement Areas and Waste Volumes

A common strategy is followed for all waste nuclides in a reprocessing plant:

1. Reduction of the confinement area: To confine the waste nuclides in a plant area as small as practicable obviates additional steps for safe control in more extended process areas. Measures must be taken already in the headend operations. The process streams leaving the confinement area must be controlled to prevent further distribution.

2. Reduction of waste classes and waste volumes: Suitable processing within the confinement area should concentrate a waste nuclide in a single, small waste stream, facilitating a simple, safe and economic transformation to the waste disposal form.

From this point of view, spent fuel reprocessing is the first step of waste treatment.

The purex process observes the two principles for the most important waste nuclides: The non-volatile fission products are removed in the first extractor to the highly active waste. In the chop and leach process the gaseous waste nuclides Xe, Kr and C-14 (as  $^{14}\text{CO}_2$ ) are removed almost completely into the small DOG volume.

The behaviour of fission product iodine and tritium is less simple, since the predominant species are the semi-volatile elementary iodine and tritiated water. They are soluble in the aqueous and organic phases and contaminate the large vessel off-gas (VOG) volumes. In a conventional purex flow sheet, they disperse throughout the process, producing large waste volumes of different quality. Slight flow sheet modifications are necessary to reduce their confinement areas and waste volumes and are expected to allow a clear, safe and more convenient economic control.

## II. Improved Iodine Control in Reprocessing Plants

For an inland reprocessing plant it has been recommended to limit the I-129 emission from a 200m high stack to  $<0.2$  Ci/a.<sup>1</sup> A decontamination factor (DF) of 300, corresponding to a 40 GWe reprocessing plant has been used as a guideline for our investigations. The iodine removal from simulated fuel solution and the iodine behaviour in a DOG system has been investigated up to pilot plant scale using I-123 tracer.

### 1. Iodine Removal from the Fuel Solution<sup>2</sup>

Two different procedures for iodine removal have been tested using 0.5 m<sup>3</sup> of simulated fuel solution. The left side of Fig. 1 shows the iodine desorption by distillation. Dilute nitric acid is distilled off and continuously replaced by fresh. The desorbed iodine disperses in the downstream condensor between the distillate and the DOG. The iodine fraction carried into the DOG increased with increasing temperature and DOG flow. Additional NO<sub>2</sub>-sparging, incorporating carrier iodate addition was found to be necessary to guarantee residual iodine concentrations well below  $10^{-6}$  mol/l I<sub>2</sub>, which corresponds to a DF of  $\geq 300$ . Distillate fractions from 20 to 50% are necessary for an effective desorption and require additional treatment in a plant; moreover, level control is necessary in the dissolver. Therefore the distillation procedure is inconvenient.

The iodine desorption by boiling under reflux does not have these disadvantages and is shown on the right in Fig. 1. Acid vapours were condensed in an up-draft condensor in multi-stage, counter-current contact with the condensate. The iodine was carried out into the DOG by unabsorbed NO<sub>x</sub> plus a small volume of additional carrier gas. At high exit temperatures only the unabsorbed NO<sub>x</sub> was sufficient to prevent iodine crystallization within the condensor. Using operating conditions comparable to those shown in Fig. 2, residual I<sub>2</sub> concentrations of  $<10^{-6}$  and frequently  $<10^{-7}$  mol/l I<sub>2</sub> were obtained.

Experience at the Karlsruhe reprocessing plant<sup>3</sup> (WAK) using recycled acid for dissolution and a similar desorption procedure, confirms these results. Even without additional NO<sub>2</sub>-sparging or carrier iodate addition, the residual iodine concentration in the fuel solution was frequently, though not routinely,  $<10^{-6}$  mol/l. For an application of iodine desorption by boiling under reflux, plus NO<sub>2</sub>-sparging incorporating carrier iodate, residual iodine concentrations below  $10^{-6}$  mol/l I<sub>2</sub> are expected routinely.

More details are given in IAEA -SM- 245/16<sup>2</sup>

### 2. Iodine Behaviour in the DOG<sup>4</sup>

#### 2.1 Iodine behaviour in nitric acid scrubbers

The acid from nitric acid scrubbers can be made to contain a fraction of less than 1 to more than 99% of the iodine carried in the off-gas; this depends on the scrubbing conditions.

For a large DOG flow of  $\geq 400$  Nm<sup>3</sup>/tU, conditions could be

selected in a plate column with one-way liquid flow, where about 99% of the nitrous fumes but only about 1% of the iodine was absorbed. Fig. 3 shows the column having 12 special plates and increasing plate distances towards the gas exit. At a DOG flow corresponding to about  $400 \text{ Nm}^3/\text{tU}$  a gas residence time of about  $4 \cdot 10^2 \text{ sec}$  and a scrub acid flow corresponding to about  $1 \text{ m}^3/\text{tU}$ , an  $\text{NO}_x$  DF of about  $10^2$  was obtained. A typical temperature and iodine concentration profile shows that about 99% of the iodine is transported with the DOG and  $\leq 1\%$  remains in the scrub acid. Selective  $\text{NO}_x$  absorption occurs at high entrance temperatures and gas-to-liquid flow ratios exceeding the iodine distribution coefficient.

A rather efficient iodine absorption, together with the  $\text{NO}_x$ , could be obtained in a two-part column shown in Fig. 4. In the first part was cocurrent flow and the DOG was cooled to about  $15^\circ\text{C}$  and in the second part was countercurrent flow. At a DOG flow corresponding to about  $100 \text{ Nm}^3/\text{tU}$ , a gas residence time of about  $10^3 \text{ sec}$  and a scrub acid flow of about  $2 \text{ m}^3/\text{tU}$ , an  $\text{NO}_x$  and  $\text{I}_2$  DF of at least  $>10^2$  but usually  $>10^3$  could be obtained simultaneously. A typical temperature and iodine concentration profile shows that the iodine is absorbed very efficiently in the countercurrent part at gas-to-liquid flow ratios less than the iodine distribution coefficient.

More details are given in the preceeding paper.<sup>5</sup>

In a packed column with recirculating scrub acid the  $\text{NO}_x$  decontamination was poor due to the slow decomposition of recirculated nitrous acid at the gas exit. Iodine fractions of more than 10 down to a few percent were absorbed, decreasing with the column temperature and the volume ratio of DOG-to-scrub acid.

## 2.2 Iodine desorption from nitric acid<sup>4</sup>

Before recycling the scrub acids, large iodine fractions have to be removed to prevent accumulation. Continuous procedures are preferred for the salt and solid-free acid, contrary to iodine removal from the fuel solution. The nitrous acid present in the scrub acid stabilizes the iodine in elementary form and is desorbed together with the iodine after decomposition to  $\text{NO}$ .

Fig. 5 shows a batch desorption in a packed column using a desorption gas. The decrease of the  $\text{I}_2$  concentration indicates that an efficient desorption requires higher temperatures and a  $\text{NO}_2$  containing desorption gas to prevent iodate formation. About  $10^3 \text{ m}^3$  of desorbing gas per  $\text{m}^3$  of scrub acid are required for batch desorption.

Fig. 6 shows that only about  $10^2 \text{ m}^3$  of desorbing gas per  $\text{m}^3$  of acid are required using countercurrent desorption in a plate column. Moreover, less iodate was formed, due to the shorter residence times of the hot acid.

Fig. 7 shows the iodine steam strip which requires only about  $1 \text{ m}^3$  of transport gas per  $\text{m}^3$  of acid, the  $\text{NO}$  produced by nitrous acid decomposition being sufficient at higher temperatures. The steam is produced from the desorbed acid, having a boil-up rate corresponding to about 10% of the acid flow.

### 3. Iodine Confinement to the DOG Area (See Fig. 8)

Some additional process adaptations are necessary to confine the iodine to the DOG area of a reprocessing plant. The most important step is an efficient iodine removal from the fuel solution; this has been proposed by ORNL more than a decade ago.<sup>6,7</sup>

The iodine removal from the dissolver by boiling under reflux, plus NO<sub>2</sub>-sparging incorporating carrier iodate seems to be a convenient procedure. But completion and control of iodine removal should be carried out in the following catch or accountancy tank, because of the following reasons: (a) possible dead volumes may not take part in the desorption (b) complete fuel dissolution without using fresh acid may increase the dissolution cycle times (c) undissolved fuel containing iodine may dissolve during transfer (d) the fuel solution is the only liquid stream discharged from the iodine confinement area. The batchwise control of the I-129, separated together with a carrier, using direct  $\gamma$ -spectroscopy, takes several hours. Iodine desorption has to be repeated in case of an insufficient desorption. Using the dissolver for these operations would considerably reduce the throughput and disturb a time programme using several dissolvers.

The iodine contaminated scrub acids originating from the DOG system must be recycled to the dissolution acid storage tank and not via the iodine-free acid and water recovery system. This is compatible with the nitric acid and water balance in the headend. For scrub acids containing larger iodine fractions a desorption step is necessary prior to dissolver recycling.

The fresh and especially the recycled acid should be sufficiently free from organics. The formation of organic iodine compounds may complicate the iodine treatment.

A large fraction of organic iodine is usually found in the VOG. Following the proposed strategy, the iodine needs to be removed only from the small DOG volume. For the large volumes of VOG additional and expensive routine iodine retention will be unnecessary.

### III. Improved Tritium Control in Reprocessing Plants

For a reprocessing plant site it has been recommended to limit the HTO emission from a 200m high stack to  $< 2 \cdot 10^5$  Ci/a, corresponding to about 20% of a 40 GWe plant throughput.<sup>1</sup> Especially at dry plant sites far more restrictive tritium release limits are expected for the liquid waste discharges.

#### 1. Tritium Behaviour During Fuel Dissolution<sup>8</sup>

The tritium behaviour during spent oxide fuel dissolution was investigated using a typical PWR fuel rod; the results are summarised in Fig. 9. More than half of the tritium was fixed in the cladding and will be discharged and stored together with the leached hulls. The tritium still contained in the oxide fuel forms tritiated water HTO and nitric acid during dissolution. Only a small fraction of less than one percent formed molecular hydrogen HT and was emitted

together with the decontaminated DOG. The fate of the tritium in the purex process can therefore be described by following the hydrogen in water and nitric acid from the fuel solution.

## 2. Tritium Behaviour in the Purex Process<sup>8,11</sup>

Fig. 10 shows a rather simplified purex flow sheet, the organic extraction cycles as well as the aqueous "cycles" being drawn separately. After an extraction-re-extraction cycle, the aqueous and organic phases are regenerated by distillation or a small volume soda scrub to minimise the waste volumes. This shows clearly that recycling is the most important principle of waste volume reduction.

The tritium from the fuel is fed to the first aqueous cycle. It must have its own tritiated acid and water recovery system in order to confine the tritium to this plant area. Tritiated waste water will be discharged from the recovery system. No aqueous phase should be transferred to the following aqueous cycles. Recycling of non-tritiated aqueous phases to the confinement area in order to reduce product losses or waste volumes should occur only in reasonably small amounts to limit the waste water output.

During extraction some of the aqueous phase is dissolved and entrained in the organic phase. The solubility of water and nitric acid depends on the temperature and the composition of both phases, the entrained fraction depends on the details of extraction. A simple method for the determination of the aqueous phase present in an organic phase has been developed. A few ml of organic phase were contacted with a few ml of heavy water. The light water phase extracted was determined spectrophotometrically in the infrared region. The aqueous phase in loaded organic solvent (HSP) from the Karlsruhe reprocessing plant was found to correspond to about 9 ml H<sub>2</sub>O per l.<sup>9</sup> In reasonable accord with reality it is assumed in the following that about 1 vol.% of the organic phase volume consists of entrained and dissolved aqueous phase.

The organic product stream HSP transports some of this tritiated aqueous phase to the following cycles. To prevent carry-over, the tritiated phase has to be replaced by a non-tritiated one in a countercurrent contactor.<sup>10</sup> This can be done either together with the usual fission product scrub HS using a large excess of non-tritiated acid or in an additional tritium scrubber HT with small excess, thus minimising the water input. A simplified flow sheet with an additional tritium scrubber is shown in Fig. 11. Mixer settlers, especially of the Holley Mott type, as well as pulsed columns have been reported to be suited for extreme organic-to-aqueous flow ratios of 25-100.<sup>11</sup>

The water input to the tritiated plant area equals the tritiated water output. Thus, the waste water volume is reduced by minimising the sources of non-tritiated water to an extent still compatible with processing in the headend. The consequence of a reduced input is an increased recycle of the tritiated aqueous phase. How frequently the tritiated aqueous phase is reused before being discarded is described by the recycle factor.

Extreme recycling is not necessarily a virtue. Tritium inventory and concentration in the confinement area increase in proportion



to the recycle factor. Even the small sinks of water will become important. The tritium scrubber HT has to be more efficient. Radiolytic tritium exchange with the organic diluent and TBP in the highly active column has been reported to be small even for large recycle factors.<sup>12</sup> Less than  $10^{-2}\%$  is expected to pass the tritium scrubber in organic form. Most of this will be removed in the alkaline solvent wash, a smaller residue will slowly accumulate in the solvent. Radiolytic leaking during re-extraction is expected to be negligible, due to the lower dose rates.

The large volumes of vessel off-gas carry some tritiated water vapour. It can be replaced by non-tritiated vapour in a counter-current scrub with a slight excess of non-tritiated water or nitric acid. Fig. 12 shows the decontamination attained in a 5 cm diameter 5 bubble cap column at different conditions.

### 3. Major Sources of Non-Tritiated Water

To get a more quantitative impression, the major sources of non-tritiated water are listed below. For simplicity, the hydrogen in nitric acid is expressed as water.

1. Scrub acid for a tritium scrubber with an organic-to-aqueous flow ratio between 100-10 corresponds to a water input of about  $\underline{0.1 - 1 \text{ m}^3/\text{tU}}$   
About  $1 \text{ m}^3/\text{tU}$  is possible without an additional tritium scrubber, using non-tritiated scrub acid in the HS contactor.
2. Two moles of nitrate per mol of U are removed as uranyl nitrate in the organic product; the nitrate has to be replaced. The higher the nitric acid concentration, the lower the water input:  

Concentrated (65%) nitric acid	$\underline{0.36 \text{ m}^3/\text{tU}}$
Fuming (100%) nitric acid	$\underline{0.08 \text{ m}^3/\text{tU}}$
Nitrogen dioxide (iodine removal)	$\underline{0 \text{ m}^3/\text{tU}}$
3. A steam jet transfer dilutes the fuel solution by about 6 vol.%. Assuming only 3 transfers with non-tritiated steam, this introduces about  $\underline{0.6 \text{ m}^3/\text{tU}}$   
This considerable amount of water generated can only be eliminated by using a separate steam generation system for tritiated water or by transfers using pumps, airlifts, etc.
4. Denitration reactions in the highly active waste concentrates, using hydrogen-containing reductants such as formol, formic acid or sugar, contribute their own reaction water:  

$$\text{eg.: } \text{CH}_2\text{O} + 2\text{HNO}_3 \rightarrow \text{CO}_2 + \text{NO} + \text{NO}_2 + 2\text{H}_2\text{O},$$

ie.  $\underline{0.15 \text{ m}^3/\text{tU}}$
5. Recycling of waste concentrates from the non-tritiated 2nd and 3rd extraction cycles may be useful in reducing the waste volumes and product losses. In principle, suitable recycled streams may also be used for the tritium scrub.

6. The large volume of vessel off-gas (VOG), including the VOG from the highly active waste storage tanks, may become an appreciable sink for tritiated water vapour, especially when using large recycle factors. Assuming a total of only  $10^3 \text{ m}^3$  VOG/tU and a dew point of  $7^\circ\text{C}$ , the calculated loss is 81/tU. Countercurrent water vapour exchange using a fourfold excess of water results in an additional 241/tU.

A very crude estimation of the possibilities for minimising these water sources: >99% of the tritium may be concentrated in about  $0.5 \text{ m}^3$ /tU tritiated waste water using an additional tritium scrubber HT. Using the HS extractor to scrub the tritium may result in a waste water volume of about 1-1.5  $\text{m}^3$ /tU. The corresponding recycle factors are about 12 or 4-6, depending on the flow sheet.

#### 4. Conclusions

An economic justification for the flow sheet modifications, or even further tritium enrichment procedures, depends on the conditioning and storage of the tritiated waste water.

1. If it will be allowed to dispose of large volumes of tritiated waste water deep under ground or in the sea without expensive conditioning, then extreme recycling in the plant or additional enrichment procedures are not necessary. The HS extractor can be used to scrub the tritium. The tritium DF should be excellent in view of the number of stages and the large excess of non-tritiated scrub acid. The tritium confinement area is maintained and a reasonable reduction of the waste water volume is possible by moderate recycling (see Fig. 13). Extreme recycling, using an additional tritium scrubber in the highly active plant area seems to be inconvenient.
2. Alternatively, if an extremely good and expensive conditioning of tritium water is necessary for transport, then storage or final disposal, recycling within the plant is important but not sufficient. As shown in Fig. 13, an additional enrichment process will be necessary. Many different enrichment processes, including  $\text{H}_2$ - $\text{H}_2\text{O}$  exchange, are being studied. The tritium will be enriched in a small volume of water suitable for conditioning and storage. The large water volume depleted in tritium will be recycled to the plant. Either the total waste water stream or only a part of it will be enriched to ensure a sufficiently low tritium inventory in the confinement area.

The tritium from reprocessing plants will probably not present a global contamination hazard for the foreseeable future. The emission of the sufficiently inert molecular hydrogen, which is produced electrolytically as an interstage product in some enrichment processes, may turn out to be an economic waste treatment procedure, avoiding possible radiation exposure of plant personnel during enrichment, conditioning, transport and storage or disposal procedures.

REFERENCES

- / 1/ Gesellschaft für Reaktorsicherheit mbH, Köln, (Oktober 20,1977)  
"Grundsätzliche sicherheitstechnische Realisierbarkeit des  
Entsorgungszentrums. Beurteilung und Empfehlungen der Reaktor-  
Sicherheitskommission (RSK) und der Strahlenschutzkommission  
(SSK)".
- / 2/ E. Henrich, R. Hufner, A. Sahm; IAEA-SM-245/16, Vienna,  
(February 1980)
- / 3/ R. Berg, H. Schüttelkopf; "Seminar on Radioactive Effluents  
from Reprocessing plants", Karlsruhe, November 1977, p.189
- / 4/ E. Henrich; PWA status report, Karlsruhe (1979)
- / 5/ E. Henrich, R. Hufner; "I-129, Kr-85, C-14 and NO<sub>x</sub> removal from  
spent fuel dissolver off-gas at atmospheric pressure and at  
reduced off-gas flow", this conference
- / 6/ D.E. Ferguson et al.; Chem. Tech. Division, Annual Progress  
Report ORNL-4272 (1968)
- / 7/ G.I. Cathers, C.J. Shipman; US-patent 3.803.295, patented  
April 9, 1974
- / 8/ E. Henrich, H. Schmieder, K.H. Neeb; IAEA-SM-245/15, Vienna,  
(February 1980)
- / 9/ H.G. Burckhardt, E. Henrich, G. Knittel, D. Fang, KfK  
unpublished results (1979)
- /10/ C. Bernard; Brevet francais no. 7,318,073 (1973)
- /11/ P. Miquel, J.P. Goumondy, E. Schneider; Seminar on radioactive  
effluents from reprocessing plants", Karlsruhe,  
(November 1977) p. 497
- /12/ A. Sameh et al., KfK-Nachrichten 3 (1979) 37

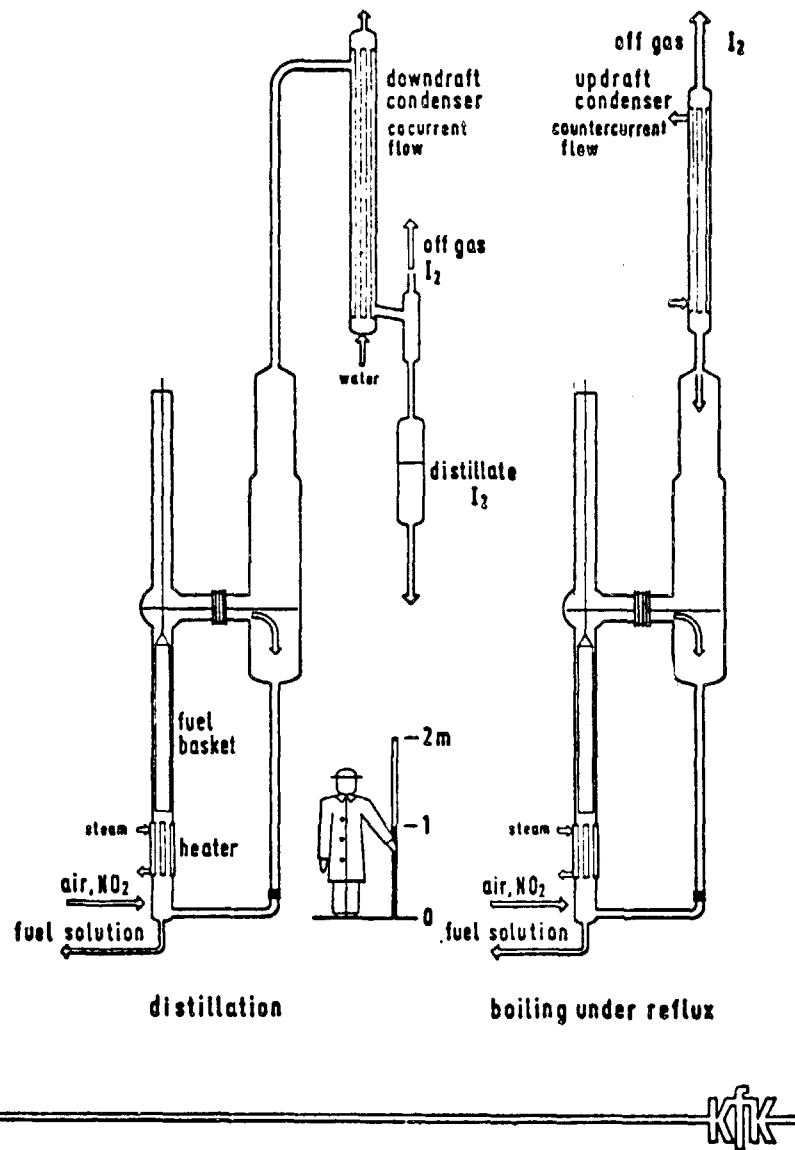


Fig. 1 Iodine desorption from fuel solution

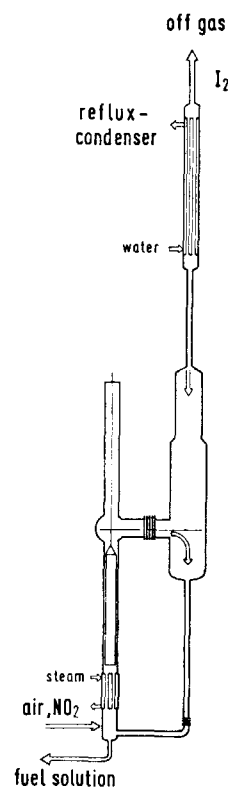
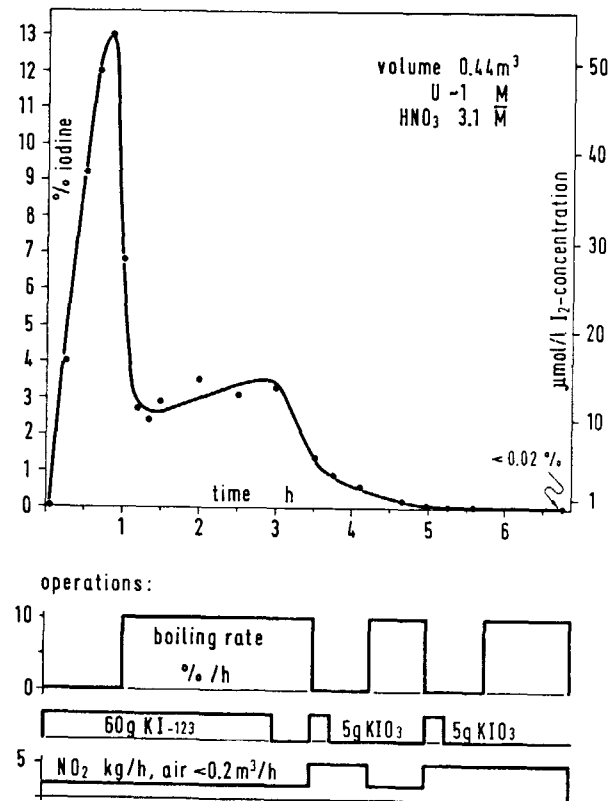


Fig. 2

Iodine desorption from fuel solution by boiling under reflux



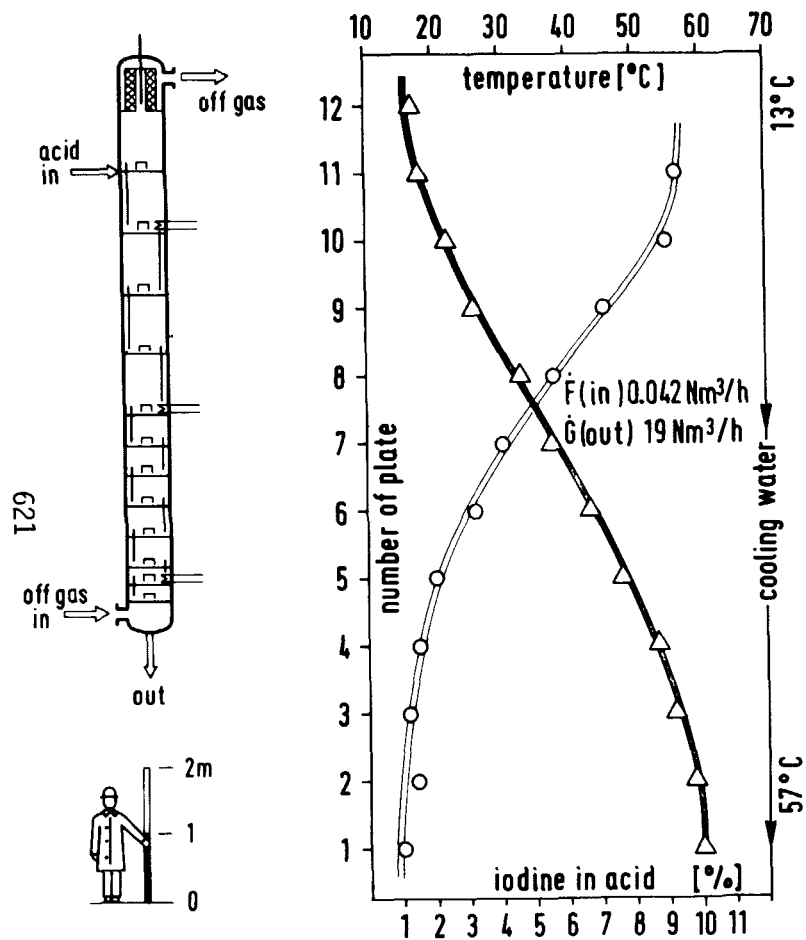


Fig. 3 nitric acid scrubber  
selective  $\text{NO}_x$  absorption

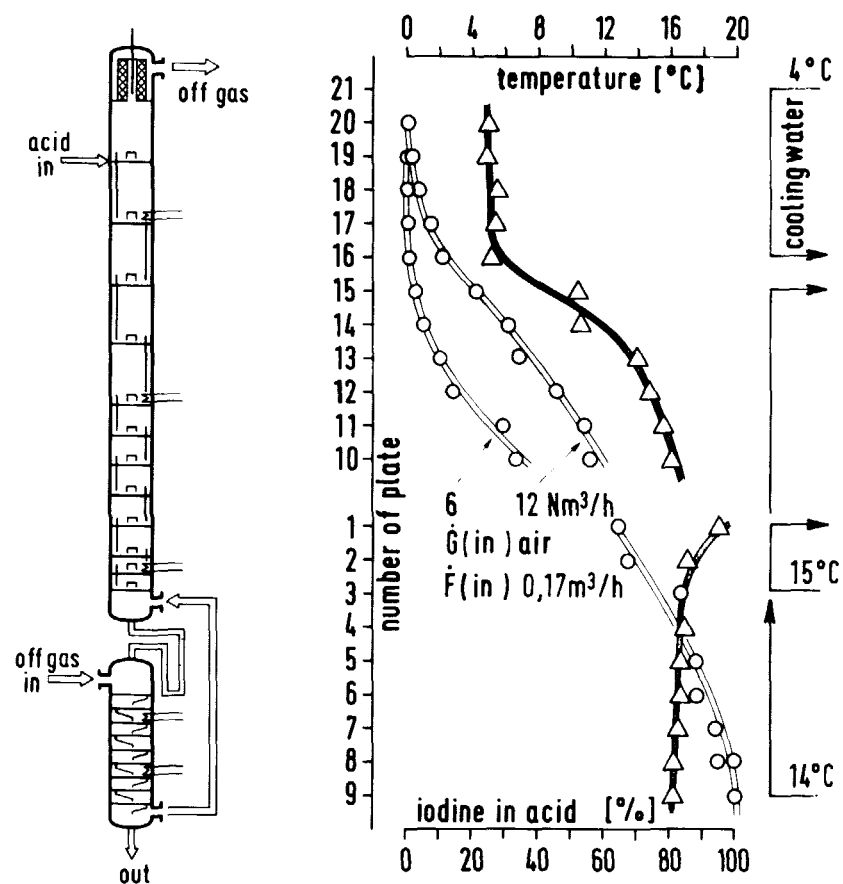


Fig. 4 nitric acid scrubber  
 $\text{NO}_x$  and  $\text{I}_2$  absorption

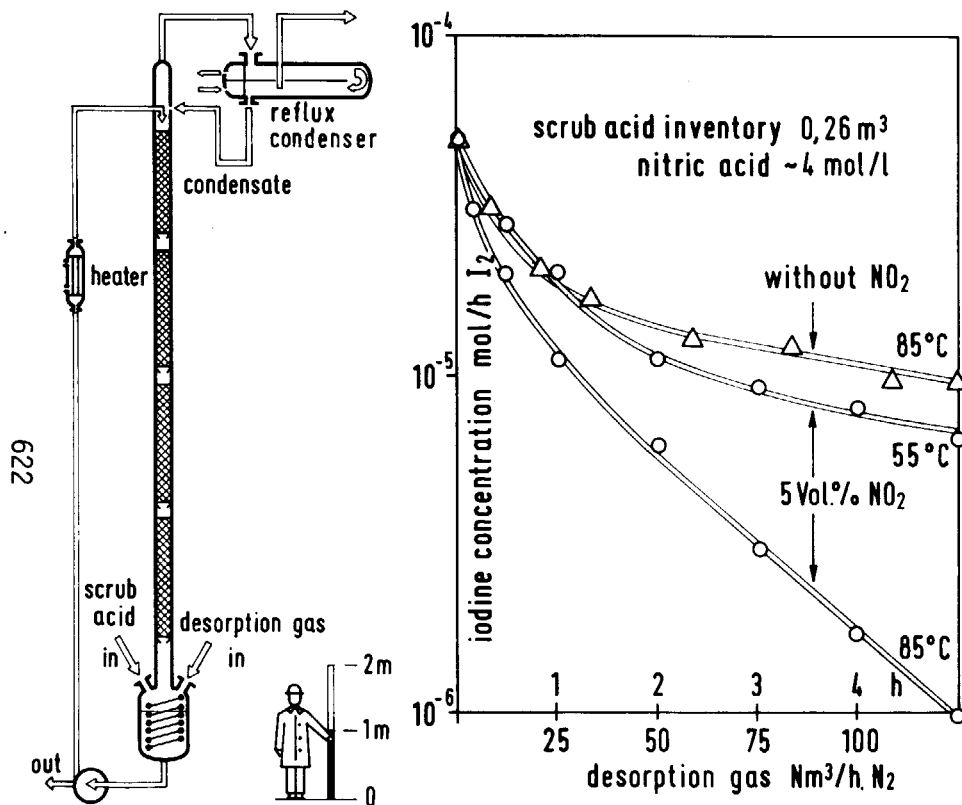


Fig. 5 Batch Desorption of Iodine in a Packed column

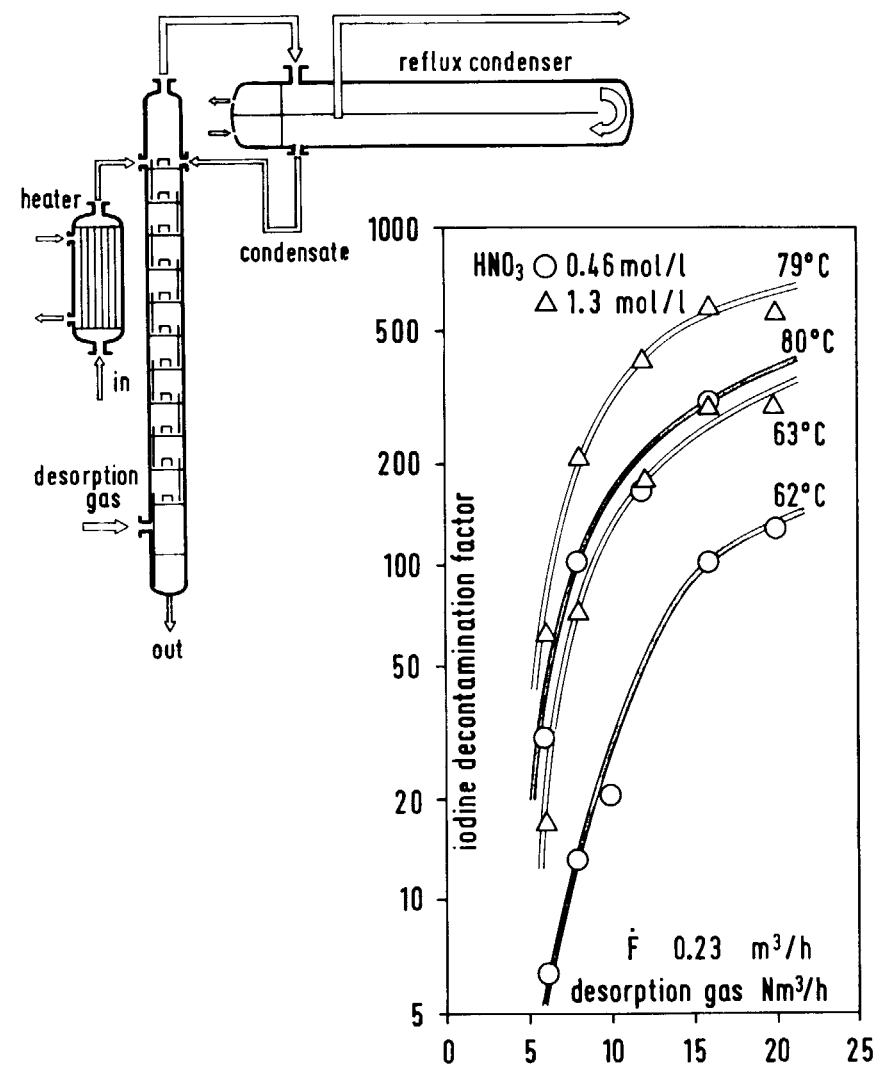


Fig. 6 Countercurrent desorption of iodine using air as desorption gas

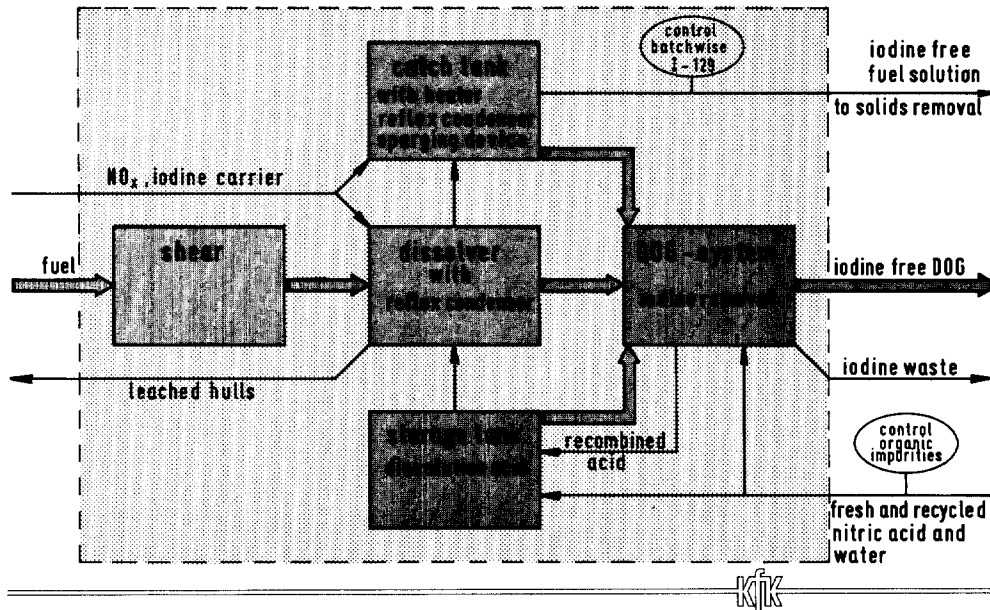


Fig. 7 Iodine contaminated plant area

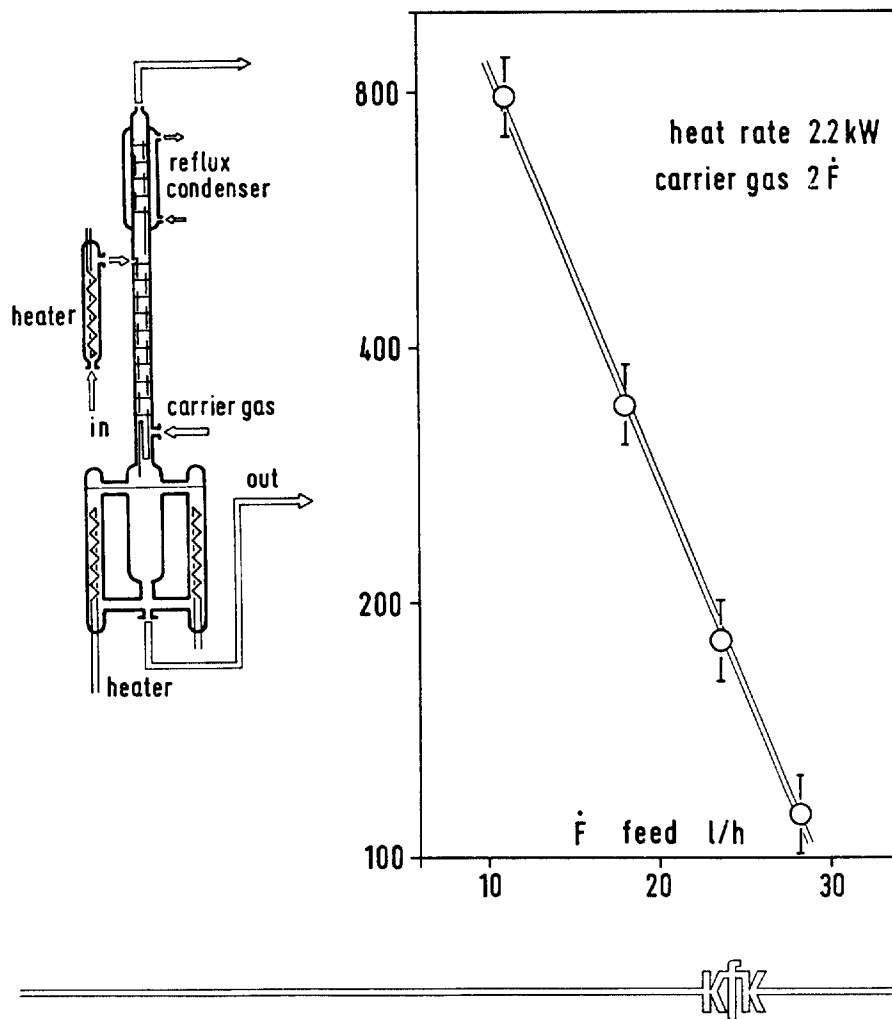


Fig. 8 Iodine steam strip

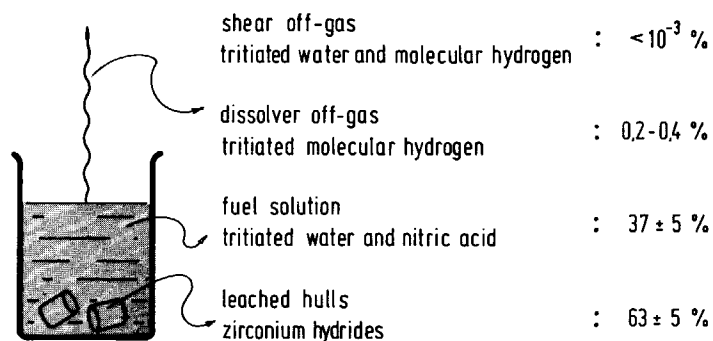


Fig. 9 Tritium behavior during dissolution of PWR fuel

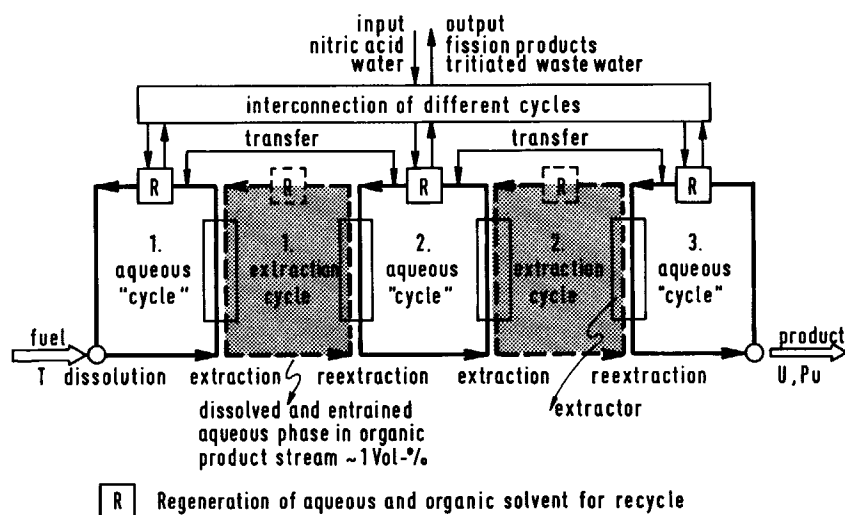


Fig. 10 Simplified purex flowsheet

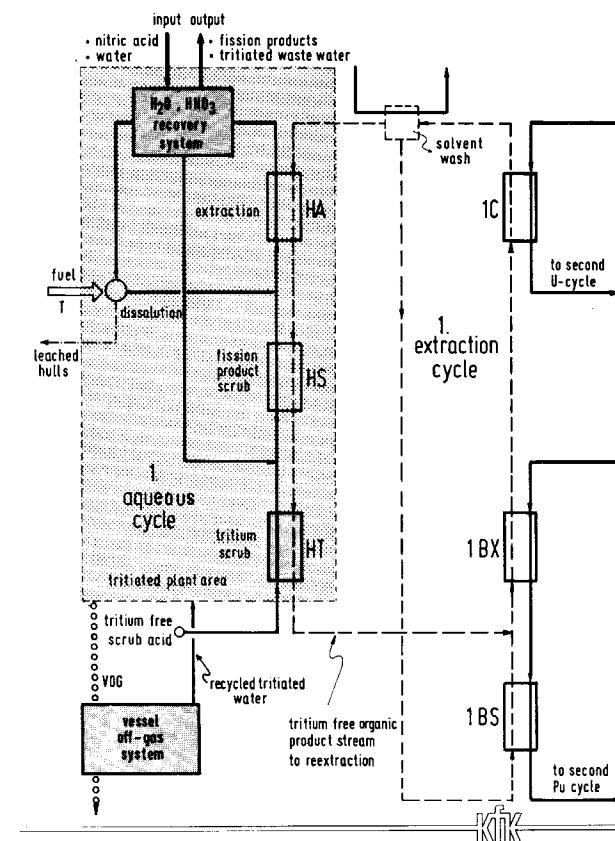


Fig. 11 Simplified purex flowsheet adapted to confinement of tritium



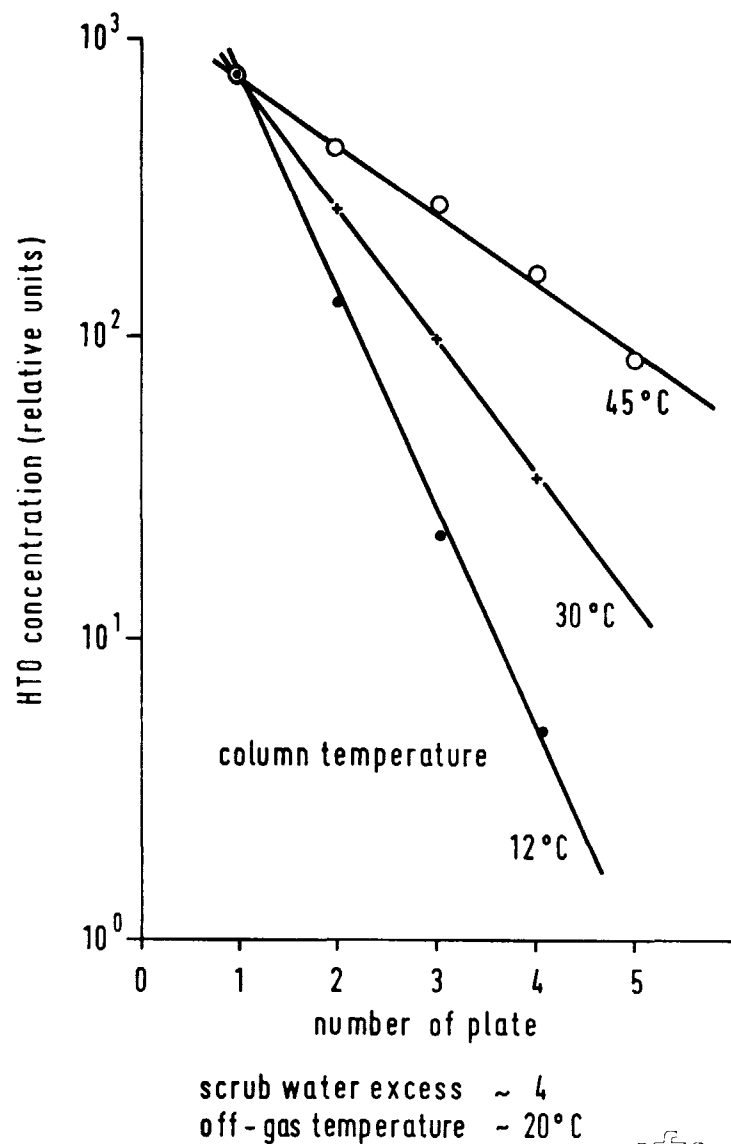


Fig. 12

HTO exchange in the off-gas

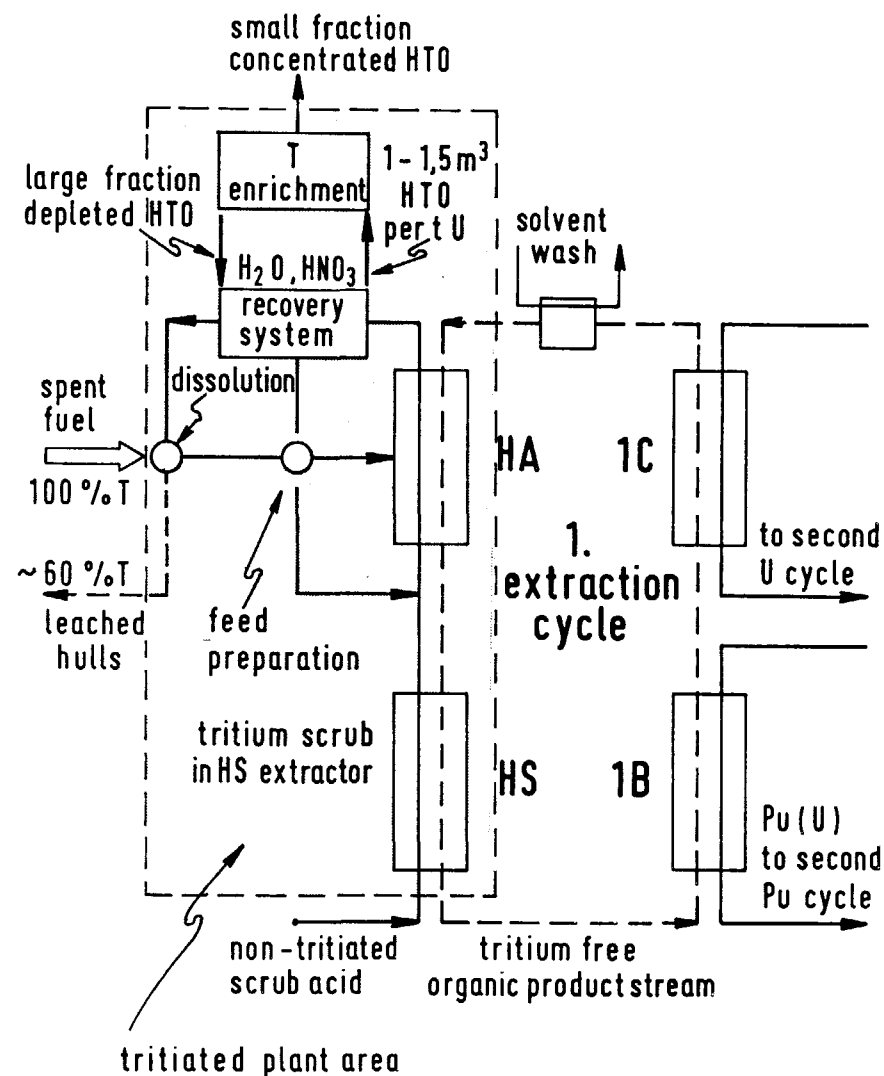


Fig. 13

confinement and concentration of tritium

## DISCUSSION

RIMSHAW: I was wondering if you have some data on iodine concentration factors? I know you are preoccupied with removing iodine, but I am also interested in the concentration of iodine as it is possible to concentrate iodine by a factor of, say, 10,000. You mentioned that you get about 100 altogether. Do you know the concentration of iodine at various places, such as in the distillate, compared to the concentration in the starting dissolver? I am a little confused as to the final fate of iodine. Do you have some sort of a let-down stream where you process the iodine and actually remove it in some non-volatile form?

HENRICH: Iodine enters the process in a predetermined volume of fuel solution and it leaves the process almost completely in a predetermined volume of iodine waste. The waste volume determines the iodine concentration factor. During processing in the dissolver offgas system, the iodine is handled mainly in the volatile elementary form by suitable chemical treatment. Therefore, in reasonable agreement with the experimental results, the iodine concentrations at various places within the dissolver offgas system can be calculated using the  $I_2$ -distribution coefficients.

RIMSHAW: My point is that when you distill an acid solution of iodine, you concentrate iodine by a factor of 10. I think you mentioned that. Do you get this result each time you carry out the distillation?

HENRICH: The proposed iodine removal from the fuel solution by boiling under reflux does not produce a distillate; the iodine is carried directly to the first nitric acid scrubber.

RIMSHAW: The next question is, how do you remove the iodine? In what form? I think iodine in the elementary form would be a volatility hazard in itself. Did you consider having a caustic solution, or a mixture of caustic and sodium iodide, or ceric iodate, or some such inorganic compound, which is relatively nonvolatile for the ultimate removal and handling of iodine? Radioactive iodine would be a hazard if you tried to move it outside your plant limits. What did you have in mind for actual transport of iodine outside your processing plant once you had it isolated? What are you going to do with it? Put it in concrete?

HENRICH: There are a lot of possible waste forms, where the iodine is fixed in nonvolatile form. We take into consideration up to 10% barium iodate in concrete, after iodine absorption, oxidation, and precipitation in NaOH-solution. This corresponds to an iodine concentration factor of approximately  $10^4$ .

WILLIAMS: You say at one point on the reprint that at high exit temperatures, only the unabsorbed  $NO_x$  was sufficient to prevent iodine crystallization. Are you saying there is no problem with iodine crystallization? In your paper, it says, "At high exit temperatures, only the unabsorbed  $NO_x$  was sufficient to prevent iodine crystallization within the condenser."

HENRICH: You have a certain iodine transport capacity for your carrier gas. It does not matter if it is water vapor, or air, or unabsorbed NO<sub>x</sub>; transport capacity refers to the amount of gas and the temperature of gas. From the vapor pressure of iodine, you can calculate how much gas you need to transport a certain amount of iodine.

WILLIAMS: Thank you. That clears it up. We are getting very worried by iodine corrosion in the setup.

SOME ASPECTS OF AEROSOL PRODUCTION AND REMOVAL  
DURING SPENT FUEL PROCESSING STEPS

F.J. Herrmann, E. Lang, J. Furrer<sup>1)</sup>, E. Henrich<sup>1)</sup>  
Gesellschaft zur Wiederaufarbeitung von Kernbrennstoffen  
Karlsruhe

<sup>1)</sup> Kernforschungszentrum Karlsruhe (KFK)  
Fed. Rep. Germany

Abstract

Modern requirements for a very high DF of the order of approx.  $10^9$  for off-gas radioactive emissions are not easily achieved with the usual off-gas purification treatments.

Control and minimization of activity-loaded aerosols must be initiated at the source. To help the reprocessing plant designer, a systems analysis has been made in which aerosol sources are recorded, and measures for reducing the discharge of radioactivity are illustrated.

The aerosol discharge has been simulated and demonstrated in test rigs.

Results from one such dissolver test rig are shown, in which  $10^{-8}$  -  $10^{-9}$  of the total dissolver activity goes to the filters. Tests show that the off-gas has an aerosol loading of 10 mg/m<sup>3</sup> gas. The values quoted are specific for the apparatus used.

It was found that the air introduced for stirring purposes into the vessel off-gas system of the extraction cycles, was also a most important source of aerosol production, giving a similar aerosol loading.

I. Introduction

An efficient aerosol removal is necessary for all off-gas from reprocessing and waste treatment plants. Apart from an efficient retention procedure excessive aerosol production must be avoided in order to limit emission of radioactivity. Both, production and retention are largely dependent on design details, layout and operation of process equipment.

Apart from the gaseous radioactive fission products I-129, Kr-85, C-14, H-3, which are present in the dissolver off-gas, aerosols occur throughout the entire process area; these can entrain toxic fission products such as Ce-144, Cs-134, Cs-137, Sr-90, Ru-106, Sb-124 and also the transuranic elements Np, Pu, Am and Cm.

Because of the radiotoxicity of these elements, much higher retention levels are required for nuclear plants than for conventional plants.

# 16th DOE NUCLEAR AIR CLEANING CONFERENCE

Table I shows in particular that minimum decontamination factors of  $5 \cdot 10^8 - 5 \cdot 10^9$  must be maintained for  $\beta$  and  $\alpha$  aerosols<sup>1)</sup>.

Table I Activity yield, recommended maximum emission levels and necessary minimum plant decontamination factors for a reprocessing plant

Nuclide	Annual yield of activity CI/A	Recomm. emission levels (exhaust air) (CI/A)	Minimum decontam. factor
H-3	$1.0 \cdot 10^6$	$2 \cdot 10^5$	5
C-14	1000	1000	1
Kr-85	$1.6 \cdot 10^7$	$1 \cdot 10^6$	16
I-129	57	0,2	285
$\beta$ -Aerosols	$2.5 \cdot 10^9$	5	$5 \cdot 10^8$
$\alpha$ -Aerosols	$2.5 \cdot 10^8$	0,05	$5 \cdot 10^9$

Assumed heavy metal throughput	1400 t/a
Fuel element specification:	
Burn-up	36000 MWd/t Uranium
Cooling time	365 d
Initial enrichment	3,5 %

The major part of the off-gas of a reprocessing plant arises not from the reaction gas evolved in the process, but the air which is used for stirring, transferring, pulsing and scavenging, etc.

The discharged activity is obtained from the quantity of air arising, from its aerosol loading and from the specific activity at source. This is illustrated by the following equation:

## Activity Discharge A

$$A = \sum_i c_i q_i M_i \left( \frac{Ci}{l} \cdot \frac{ml}{m^3} \cdot m^3 = Ci \right)$$

$c$  = specific activity

$q$  = loading

$M$  = off-gas quantity

$\sum_i$  = sum of aerosol sources

Figure 1

The specific activity, aerosol loading and the quantity of air present in a process step are used in order to estimate the radio-activity discharge from a particular process step.

A short survey of the sources with their aerosol loading and the quantities of air used now follows. Using the example of the dissolver unit and based on experimental results, an estimation is made of the aerosol discharge from the most important process section of a reprocessing plant.

An analysis of the system shows how measures can be taken within the organisation and the layout of the apparatus to reduce the aerosol discharge.

## II. Aerosol Sources and Aerosol Loading

Apart from the mechanical chopping of the fuel elements, process steps which can be considered as aerosol production sources are those in which either boiling takes place or where air is introduced into the process. These are, for instance, dissolution, evaporation, extraction (pulsed columns), stirring, transferring and scavenging.

Aerosols may be generated in two different ways:

- a) Aerosols are formed on the surface of the liquid when air and steam bubbles travel through the liquid and burst; the aerosols are carried along with the stream of gas. The aerosol droplets contain the same specific activity as the agitated solution. It will be shown later that an aerosol content of  $10 \text{ mg/m}^3$  gas can be assumed. This applies for processes of dissolution, evaporation, stirring and transferring with air.
- b) It is assumed that there is an aerosol content of  $0,1 - 1 \text{ mg/m}^3$  gas in processes where the gas does not flow through but flows over or where the surface of the liquid is only moved slightly, e.g. in the case of scavenging air and of pulsing.

## III. Quantities of Air used in Transferring, Stirring, Scavenging and Pulsing

The activity discharged is proportional to the quantity of off-gas. An analysis of the air used in the process both quantity and method is important in determining the spread of radioactivity and should be considered first in minimization measures.

In a reprocessing plant the ratios of the dissolver off-gas to vessel off-gas and cell off-gas are approximately

$$1 : 10 : 100$$

The cell off-gas will not be further discussed as it is normally practically free of contamination.

The following table shows, using the example of the 1<sup>st</sup> extraction cycle, the proportions of air in the vessel off-gas (VOG)

which are used for stirring, transferring, pulsing and scavenging operations. The estimates are based on a plant with an assumed annual throughput of 1400 t Uranium.

Table II Contribution of Stirring, Transferring, Scavenging Processes and Pulse Air to the Total Quantity of Off-Gas from Vessels in the 1<sup>st</sup> Extraction Cycle

Aerosol Sources	Air m <sup>3</sup> /h	Aerosol Loading (mg/m <sup>3</sup> air)
Stirring Air	440 - 3000	10
Transfer Air (Airlift)	160 - 200	10
Pulse Air	600	0,1
Scavenging Air	150	0,1 - 1

It should be recognised that the proportion of air from these individual operations produces a total vessel off-gas of max. 4000 m<sup>3</sup>/h.

It can be seen that the pulse air predominates in absolute quantity; however, the discharge of aerosols caused by stirring and by transfer air is distinctly higher because the aerosol loading here is up to a factor of 100 higher. It would therefore be reasonable to minimize the aerosol discharge by reducing the proportion of stirring air.

#### IV. Aerosol or Radioactive Discharge

A good example of aerosol discharge is shown here at the point where the total activity of the spent fuel element is released: namely in the dissolver. The following diagram (Fig. 2) shows the dissolver with condenser, scrub column and Hepa-filter.

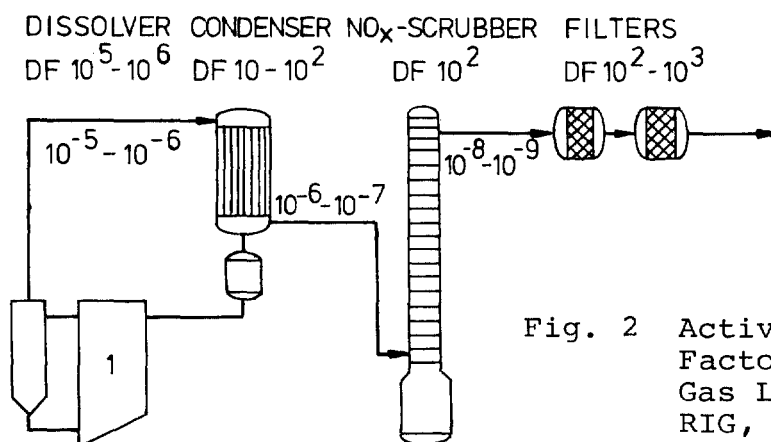


Fig. 2 Activity and Decontamination Factors in Dissolver Off-Gas Line (Head End Test RIG, KfK)

Tests have been carried out in the KfK-IHCh to investigate the problem of aerosol discharge, Uranium and Lithium salts being used as tracer materials, (Fig. 3).

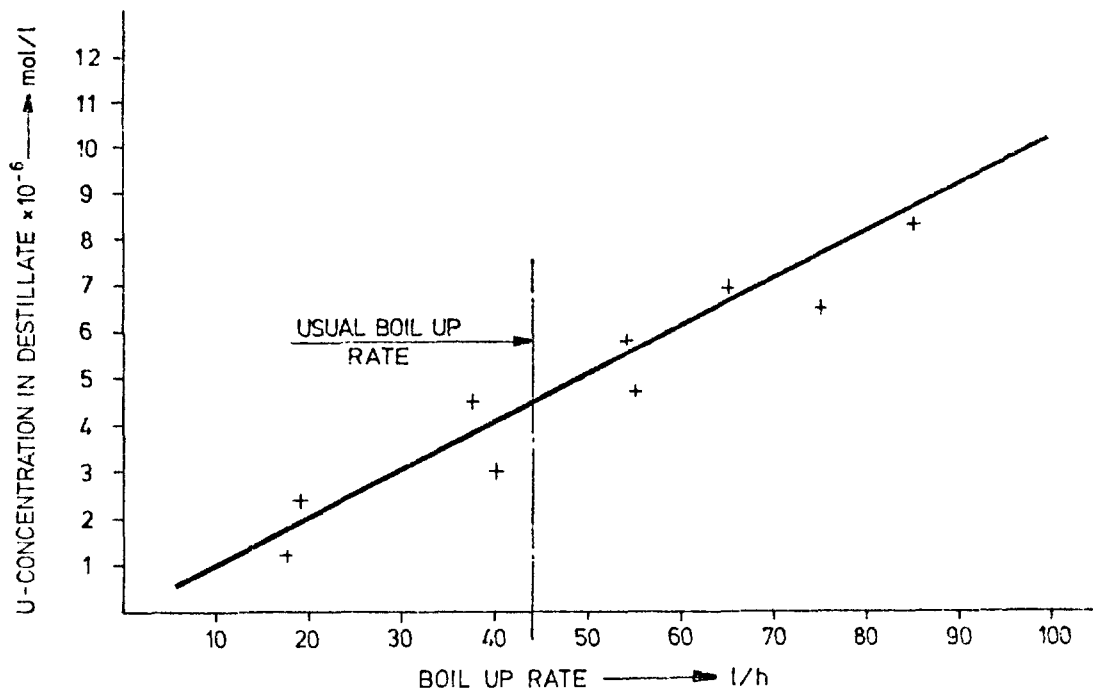


FIGURE 3 URANIUM CONCENTRATION IN DESTILLATE  
vs. BOIL UP RATE.  
(INITIAL U-CONCENTRATION 0,9 mol/l)

The results show that  $10^{-5}$  -  $10^{-6}$  of the initial activity from the dissolver is carried over into the off-gas system. After passing through the condenser and recombination columns, there is still  $10^{-8}$  -  $10^{-9}$  of the initial activity reaching the filter (Fig. 2).

In these tests 10 % of the dissolver solution was distilled. Because of this and the discharged activity, the aerosol loading can be calculated to be 10 mg/m<sup>3</sup> gas.

An estimation of the maximum aerosol droplet size has been carried out for this case. This value of 11  $\mu$ m occurs when the sedimentation speed of the particle (using Stokes' Law)<sup>2)</sup> is the same as that of the off-gas (0.07 m/s).

The value of 10 mg/m<sup>3</sup> gas is consistent with the experimental determination of aerosol loading established by ORNL<sup>3)</sup> using a gas velocity of 0.07 m/s.

An aerosol loading of some 10 mg/m<sup>3</sup> was also found during experimental tests at KfK. This value was obtained by stirring in vessels with a gas loading of 1-50 m<sup>3</sup>/h and m<sup>2</sup> of liquid surface,



Figure 4 (Conversion factor 10 from dry to wet).

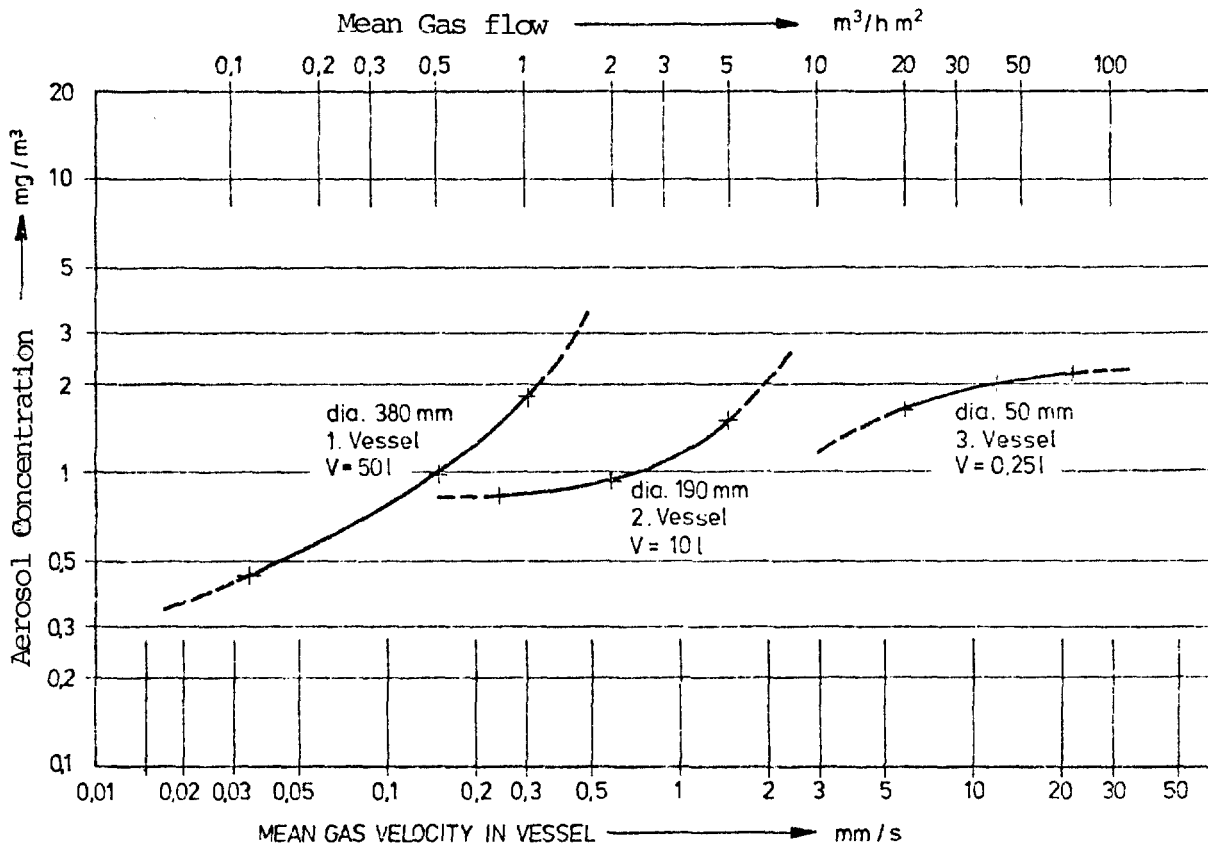


FIGURE 4 AEROSOL MASS CONCENTRATION (DRY) IN DEPENDENCE ON SIZE OF VESSEL. GAS VELOCITY AND GAS LOAD FOR 10 W%  $\text{NaNO}_3$  - SOLUTION.

Information relative to handling of solid aerosol discharge arising from shearing, which is also a part of the dissolver off-gas, is not as detailed as that given for liquid aerosol discharge arising from the dissolution.

Recent results on grain-size distribution of the shearing dust (which mainly consists of burned-up fuel particles) show that 2 % of the Uranium is present as fine particles, 50 % of which are under  $150 \mu\text{m}$  <sup>4)</sup>.

If one assumes a linear grain-size distribution of under  $150 \mu\text{m}$  and a maximum discharged particle size of  $10 \mu\text{m}$  when passing through the dissolver, then out of 1 t Uranium approx. 7 g Uranium is discharged during shearing. This corresponds to a loading of  $13 \text{ mg/m}^3$  and a DF of  $10^5$  for the dissolver relative to the dust from shearing.

The maximum particle size is governed by the linear gas speed and further also by the dissolver geometry and the quantity of off-gas. These last parameters must be correspondingly taken into consideration in plant design and construction.

#### V. Minimization of Activity Discharge

The volume of stirring air with its high aerosol loading ( $10 \text{ mg/m}^3$  gas) is immediately obvious in the analysis of the aerosol sources and their discharge.

Pulsators operated by pulsed air should be used as an alternative to stirring the vessel contents with air.

On average, approx.  $20 \text{ Nm}^3/\text{h}$  per  $\text{m}^2$  liquid surface is used for stirring a vessel. Usually, the vessel is stirred occasionally for about 20 minutes for homogenisation purposes, for example prior to sampling.

From tests on the use of pulsators carried out by the KfK<sup>5)</sup> for the same liquid surface area only 3 mins are required to achieve a homogeneous mixing with a pulse amplitude of 13 mm, a pulse frequency of 17/min and an excess pressure of 0,5 bar.

A comparison of the two processes shows that in total the same exhaust air quantity is produced as with air stirring. However, the activity discharge is reduced by a factor of 100 corresponding to a  $10^{-2}$  lower loading.

The following further measures are suggested to minimize activity discharge:

- Replacement of the airlift by developing suitable pumps.
- Minimization of aerosol discharge during airlift operations by increasing the volumes of the de-gassing pot and suitable installations before the exit of the off-gases into the vessel off-gas tract.
- Investigations of the conditions in which the pulsator and pulsed column exhaust air can be recycled.

To minimize aerosol discharge from the dissolver, a corresponding increased volume above the dissolver must be included in the planning in order to reduce carry-over of the accumulated liquid aerosols and shearing dust.

Furthermore, piping diameters and air or gas velocities must be layed out to minimize aerosol discharge.

## VI. Improvement of Activity Retention

### VI.1 Off-gas Routes

There are principally two concepts for the layout of off-gas routes:

- a) Joint channelling of all off-gas pipes from dissolver and vessels to a common off-gas purification, with the exception of the highly active intermediate storage.
- b) Separate treatment for dissolver and vessel off-gases; as already described, but note that the vessel off-gases are divided according to areas of activity.

Separate off-gas treatment has the following advantages:

- In case of immediate or later necessity for retention of noble gases from the dissolver off-gas this route should be separated from the VOG to maintain a small gas flow with high Kr-85 concentrations.
- In case of separate routing of VOG no cross contamination between high and low activity areas can take place.

So individual routes can be adapted to the respective condition of the off-gas:

### VI.2 Aerosol Trapping - Liquid Aerosols

Because small deviations in the process can lead to an increase in wet aerosol generation, highly effective droplet and mist traps are necessary. They must be installed after the last off-gas scrubber since ordinary droplet traps on top of the scrubber are not very effective.

The efficiency of the mist trap relates to the degree of contamination and loading of the plant sections following the heater and Hepa-filter.

A suitable mist trap, in the form of a remotely-operated, cylindrical fibre packet, has been designed and constructed in the KfK<sup>6)</sup> and tested under simulated off-gas conditions.

A DF of  $> 100$  has been achieved for droplets of  $1-6 \mu\text{m}$  diameter and a DF of  $10^3$  <sup>6)</sup> for solid aerosols having a critical diameter of  $0,12 \mu\text{m}$ . This means a considerable increase in the operating life time of the Hepa-filters downstreams.

Literature

- 1) Radioaktive Ableitungen aus der geplanten Wiederaufarbeitungsanlage in der Bundesrepublik Deutschland und die Strahlenexposition in der Umgebung  
G. Schwarz, T.D. Urbas; KEWA, Karlsruhe  
H. Geiss und K.J. Vogt; KFA, Jülich  
  
Seminar on RADIOACTIVE EFFLUENTS FROM NUCLEAR FUEL REPROCESSING PLANTS  
Karlsruhe (F.R. Germany), 22-25 November 1977
- 2) Beschleunigung eines kugelförmigen Feststoffteilchens im Strömungsfeld konstanter Geschwindigkeit  
J. Kürten, J. Raasch, H. Rumpf  
Chemie Ingenieur Technik 38 (1966) 9, 941-948
- 3) Evalution of radioactive releases from chemical plants  
E.D. Arnold. A.T. Gresky, J.P. Nichols  
ORNL-TM-19
- 4) Mechanical Processing of spent power reactor fuel at Oak Ridge National Laboratory  
Watson et.al.: TiD-7583
- 5) Radionuklidtechnische Untersuchungen zur Homogenisierung einer Suspension in einem Pulsationsmischer  
A. Merz, G. Hardock, R. Walter; KfK, Karlsruhe  
Vortrag: Fachausschuß "Mischvorgänge" VDI-GVC  
16.2.77 Königstein (Taunus)
- 6) Contribution to this Conference  
J. Furrer et.al., KfK-LAF II, Karlsruhe